9-20-2013 12:00 AM

Effect of Instantaneous Load Eccentricities on the Inelastic Torsional Responses Under Bi-Directional Seismic Excitations

Xiaojing Cui
The University of Western Ontario

Supervisor
Hanping Hong
The University of Western Ontario

Graduate Program in Civil and Environmental Engineering
A thesis submitted in partial fulfillment of the requirements for the degree in Master of Engineering Science

EFFECT OF INSTANTANEOUS LOAD ECCENTRICITIES ON THE INELASTIC TORSIONAL RESPONSES UNDER BI-DIRECTIONAL SEISMIC EXCITATIONS

(Thesis format: Integrated Article)

by

Xiaojing Cui

Graduate Program in Engineering Science
Department of Civil and Environmental Engineering

A thesis submitted in partial fulfillment
of the requirements for the degree of
Master of Engineering Science

The School of Graduate and Postdoctoral Studies
The University of Western Ontario
London, Ontario, Canada

ABSTRACT

This study evaluated the inelastic torsional response due to instantaneous load eccentricities. The load eccentricities, which caused by the motion of the center of mass are time-dependent, even exist for two-way symmetric structures under seismic excitations. The eccentricities and bi-directional horizontal excitations can lead to the torsional motion. The study of the impacts of such a second-order effect (called A-Δ effect) on structural systems and, this effect in combination with the P-Δ effect on structural systems has not been reported in the literature.

This study is focused on the investigation of the structural responses under the A-Δ and/or P-Δ effects. For the assessment of inelastic seismic displacement demand and inelastic torsional response of buildings, the structure is represented using idealized one-story model and each lateral load resisting element is modeled using the Bouc-Wen hysteretic model. The governing equations of motion were developed by considering these effects and the structures that are subjected to biaxial excitations. The numerical analyses were carried out by implementing the governing equations in MATLAB®. Since the ground motion is uncertain and varies from record-to-record, 123 ground motion records from 11 California seismic events were considered to take into account this record-to-record variability.

The results indicate that a slight underestimation of seismic displacement demand is observed, if the instantaneous load eccentricities are ignored, especially for two-way symmetrical systems. On the other hand, when considering both the instantaneous load eccentricities and P-Δ effect, the instantaneous load eccentricities can introduce significant changes on both lateral and torsional displacements, if the stability factor θ is large.

Key words: Inelastic seismic analysis; Instantaneous load eccentricities; Ground motion; Second-order effect; Torsional effect.

ACKNOWLEDGMENTS

I have found the preparation of this thesis an enjoyable and rewarding experience. Thanks are due to several people for their involvement during my research.

I am deeply indebted to my supervisor, Dr. Hanping Hong, for his continuous guidance and encouragement during my studies, for his patience, motivation, enthusiasm, and immense knowledge. His guidance helped me in all the time of research and writing of this thesis. No words can sufficiently express my thanks for his invaluable assistance, comments, and suggestions which were very inspiring. I am honored by working with him. I could not have imagined having a better advisor and mentor for my study.

I also would like to thank my colleagues and friends Taojun Liu, Enyang Wang, Wei Ye, Sihan Li, Huamei Mo, Guigui Zu, Shucheng Yang, and Thomas G. Mara, for their great help and support.

Special thanks go to my parents Yujie Cui and Fengying Yu, and my husband, Xi Liu, for their support, patience, understanding and inspiration.

TABLE OF CONTENTS

LIST OF TABLES

LIST OF FIGURES

LIST OF SYMBOLS AND ABBREVIATIONS

Symbols

Chapter 2

a_0	Coefficient of Rayleigh damping
a_1	Coefficient of Rayleigh damping
c_θ	Rotational viscous damping coefficient
c_x	Viscous damping coefficient along the *X*-axis
c_y	Viscous damping coefficient along the *Y*-axis
D	Closest horizontal distance to projected faults on the Earth
e_x	Stiffness eccentricity along the *X*-axis
e_{px}	The plastic center along the *X*-axis
e_y	Stiffness eccentricity along the *Y*-axis
e_{py}	The plastic center along the *Y*-axis
E_{xi}	Normalized dissipated hysteretic energy of the *i*-th lateral load resisting element along the *X*-axis
d_{ox}	Peak linear elastic response of the corresponding linear elastic SDOF system for the considered first record component
d_{0y}	Peak linear elastic response of the corresponding linear elastic SDOF system for the considered second record component
f_{xi}	Resisting force along the *X*-axis for the *i*-th lateral load resisting element
f_{yi}	Resisting force along the *Y*-axis for the *i*-th lateral load resisting element
$\boldsymbol{K}$	The stiffness matrix
k_{xi}	Elastic lateral stiffness of the *i*-th lateral load resisting element along the *X*-axis

L	Dimension of plan along the X-axis
m	Mass of system
M	Earthquake magnitude
n_{xi}	Shape parameter of Bouc-Wen model of the i-th lateral load resisting element along the X-axis
p	Pinching parameter of Bouc-Wen model
q	Pinching parameter of Bouc-Wen model
Q_{xi}	Initial yield force of the i-th lateral load resisting element along the X-axis
r	radius of gyration of the slab with respect to the center of mass
R_{xi}	The ratio of $\max(\lvert u_{xi}(t)\rvert)/\max(\lvert u_x(t)\rvert)$
R_{xiT}	The ratio of the maximum displacements of the lateral load resisting elements $\max(\lvert u_{x1T}(t)\rvert,\lvert u_{x2T}(t)\rvert)/\max(\lvert u_{x1}(t)\rvert,\lvert u_{x2}(t)\rvert)$ along the X-axis
R_{yi}	The ratio of $\max(\lvert u_{yi}(t)\rvert)/\max(\lvert u_y(t)\rvert)$
R_{yiT}	The ratio of the maximum displacements of the lateral load resisting elements $\max(\lvert u_{y1T}(t)\rvert,\lvert u_{y2T}(t)\rvert)/\max(\lvert u_{y1}(t)\rvert,\lvert u_{y2}(t)\rvert)$ along the Y-axis
S_x	Pseudospectral acceleration for the first record component
S_y	Pseudospectral acceleration for the second record
T_{x}	Uncoupled translational natural vibration period along the X-axis
T_{y}	Uncoupled translational natural vibration period along the Y-axis
W	Dimension of plan along the Y-axis
u_x	Displacement along X-axis of the rigid slab with respect to the center of mass
u_y	Displacement along Y-axis of the rigid slab with respect to the center of mass
u_{xi}	Displacement of the i-th lateral load resisting element along the X-axis

u_{xiT}	Displacement of the *i*-th lateral load resisting element along the *X*-axis considering the *A*-Δ effect
u_{yi}	Displacement of the *i*-th lateral load resisting element along the *Y*-axis
u_{yiT}	Displacement of the *i*-th lateral load resisting element along the *Y*-axis considering the *A*-Δ effect
V_{s30}	Shear wave velocity in the uppermost 30 m
z_{xi}	Hysteretic displacement of the *i*-th lateral load resisting element along the *X*-axis
θ	Rotation of the rigid slab with respect to the center of mass
θ_T	Rotation of the rigid slab with respect to the center of mass considering the *A*-Δ effect
$\dot{u}_x$	Translational velocity along the *X*-axis
$\ddot{u}_x$	Translational acceleration along the *X*-axis
$\ddot{u}_{gx}$	Ground acceleration along the *X*-axis
$\dot{u}_y$	Translational velocity along the *Y*-axis
$\ddot{u}_y$	Translational acceleration along the *Y*-axis
$\ddot{u}_{gy}$	Ground acceleration along the *Y*-axis
α_{xi}	Ratio of the post-yield to initial stiffness of the *i*-th lateral load resisting element along the *X*-axis
β_{xi}	Shape parameter of Bouc-Wen model of the *i*-th lateral load resisting element along the *X*-axis
χ	Ratio of $\lvert x_i \rvert / L$ or $\lvert y_i \rvert / W$
γ_{xi}	Shape parameter of Bouc-Wen model of the *i*-th lateral load resisting element along the *X*-axis
δ_{xi}	Ratio of Δ_{xi} to Δ_x
δ_{yi}	Ratio of Δ_{yi} to Δ_y

ϕ_x	Normalized yield strength along the *X*-axis
$\dot{\theta}$	Rotational velocity
$\ddot{\theta}$	Rotational acceleration
ζ	Damping ratio
δ_η	Stiffness degradation parameter of Bouc-Wen model
δ_ν	Strength degradation parameter of Bouc-Wen model
ζ_s	Pinching parameter of Bouc-Wen model
ψ	Pinching parameter of Bouc-Wen model
δ_ψ	Pinching parameter of Bouc-Wen model
λ	Pinching parameter of Bouc-Wen model
Δ_x	Initial yield displacement (capacity) of the structure along *X*-axis
Δ_y	Initial yield displacement (capacity) of the structure along *Y*-axis
Δ_{xi}	Initial yield displacement of the *i*-th lateral load resisting element along the *X*-axis
Δ_{yi}	Initial yield displacement of the *i*-th lateral load resisting element along the *Y*-axis
ω_x	Uncoupled translational natural vibration frequency along the *X*-axis
ω_y	Uncoupled translational natural vibration frequency along the *Y*-axis
ω_θ	Uncoupled rational natural vibration frequency
Ω_y	Ratio of uncoupled translational natural vibration frequency along the *Y*-axis to that along the *X*-axis
Ω_θ	Ratio of uncoupled rational natural vibration frequency to uncoupled translational natural vibration frequency along the *X*-axis
μ_x	Ratio of u_x to Δ_x
$\tilde{\mu}_y$	Ratio of u_y to Δ_x
μ_θ	Ratio of $r\theta$ to Δ_x

μ_{xi}	Ratio of u_{xi} to Δ_{xi}
μ_{zxi}	Ratio of z_{xi} to Δ_{xi}
μ_{zyi}	Ratio of z_{yi} to Δ_{yi}
μ_y	Ratio of $\tilde{\mu}_y \Delta_x$ to Δ_y
τ_x	Contribution of the frames that are parallel to the *Y* axis to the torsional capacity
τ_y	Contribution of the frames that are parallel to the *X* axis to the torsional capacity

Chapter 3

a_0	Coefficient of Rayleigh damping
a_1	Coefficient of Rayleigh damping
c_θ	Rotational viscous damping coefficient
c_x	Viscous damping coefficient along the *X*-axis
c_y	Viscous damping coefficient along the *Y*-axis
D	Closest horizontal distance to projected faults on the Earth
e_x	Stiffness eccentricity along the *X*-axis
e_y	Stiffness eccentricity along the *Y*-axis
E_{xi}	Normalized dissipated hysteretic energy of the *i*-th lateral load resisting element along the *X*-axis
d_x	Peak linear elastic response of the corresponding linear elastic SDOF system for the considered first record component
dy	Peak linear elastic response of the corresponding linear elastic SDOF system for the considered second record component
f_{xi}	Resisting force along the *X*-axis for the *i*-th lateral load resisting element
f_{yi}	Resisting force along the *Y*-axis for the *i*-th lateral load resisting element

F_i	Seismic design shear force at the level under consideration
k_{xi}	Elastic lateral stiffness of the *i*-th lateral load resisting element along the *X*-axis
L	Dimension of plan along the *X*-axis
m	Mass of system
M	Earthquake magnitude
n_{xi}	Shape parameter of Bouc-Wen model of the *i*-th lateral load resisting element along the *X*-axis
Q_{xi}	Initial yield force of the *i*-th lateral load resisting element along the *X*-axis
r	radius of gyration of the slab with respect to the center of mass
R_o	The overstrength-related force modification factor
R_{xi}	The ratio of $\max(\lvert u_{xi}(t)\rvert)/\max(\lvert u_x(t)\rvert)$
R_{xiT}	The ratio of the maximum displacements of the lateral load resisting elements $\max(\lvert u_{x1T}(t)\rvert,\lvert u_{x2T}(t)\rvert)/\max(\lvert u_{x1}(t)\rvert,\lvert u_{x2}(t)\rvert)$ along the *X*-axis
R_{yi}	The ratio of $\max(\lvert u_{yi}(t)\rvert)/\max(\lvert u_y(t)\rvert)$
R_{yiT}	The ratio of the maximum displacements of the lateral load resisting elements $\max(\lvert u_{y1T}(t)\rvert,\lvert u_{y2T}(t)\rvert)/\max(\lvert u_{y1}(t)\rvert,\lvert u_{y2}(t)\rvert)$ along the *Y*-axis
S_x	Pseudospectral acceleration for the first record component
S_y	Pseudospectral acceleration for the second record
T_{x}	Uncoupled translational natural vibration period along the *X*-axis
T_{y}	Uncoupled translational natural vibration period along the *Y*-axis
W	Dimension of plan along the *Y*-axis
u_x	Displacement along *X*-axis of the rigid slab with respect to the center of mass
u_y	Displacement along *Y*-axis of the rigid slab with respect to the center of mass

u_{xi}	Displacement of the *i*-th lateral load resisting element along the *X*-axis
u_{xiT}	Displacement of the *i*-th lateral load resisting element along the *X*-axis considering the *A*-Δ effect
u_{yi}	Displacement of the *i*-th lateral load resisting element along the *Y*-axis
u_{yiT}	Displacement of the *i*-th lateral load resisting element along the *Y*-axis considering the *A*-Δ effect
V_{s30}	Shear wave velocity in the uppermost 30 m
z_{xi}	Hysteretic displacement of the *i*-th lateral load resisting element along the *X*-axis
θ	Rotation of the rigid slab with respect to the center of mass
$\dot{u}_x$	Translational velocity along the *X*-axis
$\ddot{u}_x$	Translational acceleration along the *X*-axis
$\ddot{u}_{gx}$	Ground acceleration along the *X*-axis
$\dot{u}_y$	Translational velocity along the *Y*-axis
$\ddot{u}_y$	Translational acceleration along the *Y*-axis
$\ddot{u}_{gy}$	Ground acceleration along the *Y*-axis
α_{xi}	Ratio of the post-yield to initial stiffness of the *i*-th lateral load resisting element along the *X*-axis
β_{xi}	Shape parameter of Bouc-Wen model of the *i*-th lateral load resisting element along the *X*-axis
χ	Ratio of $\lvert x_i \rvert / L$ or $\lvert y_i \rvert / W$
γ_{xi}	Shape parameter of Bouc-Wen model of the *i*-th lateral load resisting element along the *X*-axis
δ_{xi}	Ratio of Δ_{xi} to Δ_x
δ_{yi}	Ratio of Δ_{yi} to Δ_y

ϕ_x	Normalized yield strength along the *X*-axis
θ_x	Stability factor along the *X*-axis
θ_y	Stability factor along the *Y*-axis
θ_{NBCC}	Stability factor defined in NBCC
$\dot{\theta}$	Rotational velocity
$\ddot{\theta}$	Rotational acceleration
ζ	Damping ratio
δ_η	Stiffness degradation parameter of Bouc-Wen model
δ_ν	Strength degradation parameter of Bouc-Wen model
Δ_{mx}	The maximum inelastic interstory deflection
Δ_x	Initial yield displacement (capacity) of the structure along *X*-axis
Δ_y	Initial yield displacement (capacity) of the structure along *Y*-axis
Δ_{xi}	Initial yield displacement of the *i*-th lateral load resisting element along the *X*-axis
Δ_{yi}	Initial yield displacement of the *i*-th lateral load resisting element along the *Y*-axis
ω_x	Uncoupled translational natural vibration frequency along the *X*-axis
ω_y	Uncoupled translational natural vibration frequency along the *Y*-axis
ω_θ	Uncoupled rational natural vibration frequency
Ω_y	Ratio of uncoupled translational natural vibration frequency along the *Y*-axis to that along the *X*-axis
Ω_θ	Ratio of uncoupled rational natural vibration frequency to uncoupled translational natural vibration frequency along the *X*-axis
μ_x	Ratio of u_x to Δ_x
$\tilde{\mu}_y$	Ratio of u_y to Δ_x
μ_θ	Ratio of $r\theta$ to Δ_x

μ_{xi}	Ratio of u_{xi} to Δ_{xi}
μ_{zxi}	Ratio of z_{xi} to Δ_{xi}
μ_{zyi}	Ratio of z_{yi} to Δ_{yi}
μ_y	Ratio of $\tilde{\mu}_y \Delta_x$ to Δ_y

Abbreviations

COV	Coefficient of variation
CS	Center of stiffness
CP	Center of strength
MDOF	Multi degree of freedom
NBCC	National Building Code of Canada
PEER	Pacific Earthquake Engineering Research
NGA	Next Generation Attenuation (database)
SDOF	Single degree of freedom

CHAPTER 1. INTRODUCTION

1.1 Background

A significant torsional response under seismic load, which lead to the structural collapse, has been observed in major earthquakes (Esteva 1987). Seismic induced torsional responses often result in the non-uniform ductility demand on the structural frames. To this end, the study of torsional behavior is critical to evaluating the seismic risk.

The estimation of torsional responses was reviewed by Rutenberg (2002) and De Stefano and Pintucchi (2008). It is seen that great efforts have been made on investigating the torsional response, and there are still pronounced attentions have been drawn in developing general and consistent conclusions. That is because a large number of parameters are needed to characterize accurately to the linear elastic and nonlinear inelastic torsional responses. Perus and Fajfar (2005) and De Stefano and Pintucchi (2010) evaluated the general trend in the seismic responses of plan-asymmetric structures.

It is well-known that the torsional response for the linear elastic system depends on the distance between the center of mass/stiffness (CM/CS) and ratio between the uncoupled lateral and torsional vibration periods. In addition to these three factors, the inelastic torsional response is also affected by the degree of the torsional restraint, which is defined using the ratio of torsional stiffness contributed by the lateral load resisting elements parallel to one of the axes to the overall torsional stiffness due to all elements (Paulay 1997), and center of strength (or plastic center (CP)). To reduce the torsional

response under seismic excitations, design codes consider an accidental design load eccentricity that is mainly attributed to two factors: the first one considers that the symmetric-plan structure is usually not perfectly symmetric because of the uncertainty in the physical property (e.g. modulus of elasticity) of the structure and/or the inaccuracy in the geometry of the structural member as compared to the design dimension; the second one is due to the ground rotational motion about the vertical axis (Chopra 2001). The adequacy of the torsional provisions in design codes were examined and reported by Chopra and Goel (1991), Tso and Smith (1999), Chopra (2001), Humar et al. (2003), and Escobar (2004).

Recently, it was indicated (Hong 2013) that when a structure responds to seismic ground motions, the CM moves with respect to its original position or supports or CS during the ground motion. This results in the instantaneous load eccentricities under seismic horizontal excitations, which is defined by the time-varying relative position of the instantaneous CM (Hong 2013). This second order effect on the torsional response was termed as the A-Δ effect. It is, so far, not clear whether this second order effect will affect the nonlinear inelastic responses of structures under bi-directional ground motions.

Moreover, there is a well-known second-order effect, known as P-Δ effect. This second order effect could affect significantly the structural responses and has significant implication in structural design. The P-Δ effect is caused by vertical loads contributed to structural lateral deformations, and can decrease the capacity of buildings to resist the seismic loading. The P-Δ effect has been widely investigated by means of simple one- and multi-story models using single- and/or multi-degree-of-freedom (SDOF and/or

MDOF) systems. The P-Δ effect of inelastic systems subjected to severe earthquakes were studied by Bernal (1987), MacRae (1994), Tremblay et al. (1999), Gupta and Krawinkler (2000), Vian and Bruneau (2003). It is also noticed that there is no commonly accepted method to estimate P-Δ effect for inelastic responses for structures under seismic excitations. The major details of these studies will be reviewed in Chapter 3. Furthermore, the P-Δ effect in combination with the A-Δ effect, which may present significant uncertainties in studying the inelastic response of buildings subjected to earthquakes, has not been investigated.

1.2 Objectives and thesis organization

The main objectives of this study are to investigate the effect of instantaneous load eccentricities on nonlinear inelastic responses under bi-directional seismic excitations, and to evaluate the torsional responses under combined A-Δ and the P-Δ effects. For the assessment of inelastic seismic displacement demand and inelastic torsional response of buildings, the structural is represented using idealized one-story model and each lateral load resisting element is modeled using the Bouc-Wen hysteretic model. The governing equations of motion were developed by considering these effects and the structures that are subjected to biaxial excitations. The numerical analyses were carried out by implementing the governing equations in MATLAB®. Since the ground motion is uncertain and varies from record-to-record, 123 ground motion records from 11 California seismic events were considered to take into account this record-to-record variability.

The structure of this thesis is as follows. Chapter 2 investigates the A-Δ effect on the inelastic torsional behavior due to biaxial (or bi-directional) excitations considering the record-to-record variability. Parametric studies are carried out for the idealized one-story model with each lateral load resisting element modeled by the Bouc-Wen model.

Chapter 3 studies the statistical characterizations of the nonlinear inelastic responses under bidirectional seismic excitations by considering the A-Δ and P-Δ effects. The influences of the lateral uncoupled frequency ratio, stability factor, load eccentricities and record-to-record variability on the inelastic torsional responses for symmetric, one-way and two-way asymmetric systems are investigated and discussed.

Finally, the conclusion remarks are summarized, and the future research are recommended in Chapter 4.

1.3 Format of the thesis

This thesis is prepared in a manuscript format as specified by the School of Graduate and Postdoctoral Studies at the University of Western Ontario. Chapter 2 and Chapter 4 are prepared in a manuscript format with its own list of notations and references.

References

Bernal D. (1987). Amplification factors for inelastic dynamic P-Δ effects in earthquake analysis. Earthquake Engineering and Structural Dynamics; 15:635–651.

Chopra, A.K. (2001). Dynamics of structures: Theory and applications to earthquake engineering (2nd ed.). Prentice Hall, N.J.

De Stefano, M. and Pintucchi, B. (2008). A review of research on seismic behavior of irregular building structures since 2002. Bull. Earthquake Eng.; 6:285–308.

De Stefano, M. and Pintucchi, B. (2010). Predicting torsion-induced lateral displacements for pushover analysis: Influence of torsional system characteristics Earthquake Engineering and Structural Dynamics; DOI: 10.1002/eqe.1002.

Escobar, J. A., Mendoza, A., and Gomez, R. (2004). Diseno simplificado por torsión sismica estatica. Ingenieria Sismica; 70 (January-June): 77-107.

Esteva, L. (1987). Earthquake engineering research and practice in Mexico after the 1985 earthquake. Bulletin of the New Zealand National Society for Earthquake Engineering; 20: 159-200.

Goel, R. K. and A. K. Chopra. (1991). Inelastic seismic response of one-story, asymmetric-plan systems: Effects of system parameters and yielding. Earthquake Engineering & Structural Dynamics; 20(3): 201-222.

Gupta, A., and Krawinkler, H. (2000). Dynamic *P*-Δ effects for flexible inelastic steel structures. ASCE Journal of Structural Engineering; 126: 145–154.

Hong, H. P. (2013). Torsional Responses under Bidirectional Seismic Excitations: Effect of Instantaneous Load Eccentricities. Journal of Structural engineering; 139(1): 133-143.

Humar, J., Yavari, S., and Saatcioglu, M. A. (2003). Design for forces induced by seismic torsion. Can. J. Civ. Eng; 30(2): 328-337.

MacRae GA. (1994). *P*-Δ effects on single-degree-of-freedom structures in earthquakes. Earthquake Spectra; 10:539–568.

Paulay, T. (1997). Are existing seismic torsion provisions achieving the design aims? Earthquake spectra; 13(2):259–279.

Pacific Earthquake Engineering Research (PEER) Center Next Generation Attenuation database. http://peer.berkeley.edu/nga/index.html. (last accessed April 4th, 2006).

Peruš I., Fajfar P. (2005). On the inelastic torsional response of single-storey structures under bi-axial excitation. Earthquake Engineering and Structural Dynamics; 34(8):931–941.

Rutenberg A. AEE Task Group (TG) 8. (2002) Behaviour and irregular and complex structures—Progress since 1998. Proc., 12th European Conf. on Earthquake Engineering, Elsevier, Oxford, U.K.

Tremblay, R., Cote, B. and Leger, P. (1999). An Evaluation of *P*-Δ Amplification Factors in Multistorey Steel Moment Resisting Frames. Canadian Journal of Civil Engineering; 26: 535-548.

Tso, W. K., and Smith, R. S. (1999). Re-evaluation of seismic torsional provisions. Earthquake Eng. Struct. Dynam.; 28(8): 899-917.

Vian D, Bruneau M. (2003). Tests to structural collapse of single degree of freedom frames subjected to earthquake excitation. Journal of Structural Engineering; 129:1676 1685.

CHAPTER 2. EFFECT OF INSTANTANEOUS LOAD ECCENTRICITIES ON THE INELASTIC TORSIONAL RESPONSE UNDER BI-DIRECTIONAL HORIZONTAL SEISMIC EXCITATIONS

2.1 Introduction

Torsional response under seismic load is of importance because they could result in structural collapse during earthquake (Esteva 1987). The assessment of seismic torsional responses can be important for seismic reliability and risk evaluation due to the non-uniform ductility demand on the structural frames induced by torsional effects. The estimation of torsional responses was reviewed by Rutenberg (2002) and by De Stefano and Pintucchi (2008), showing that although extensive research has been reported on torsional response, general and consistent conclusions are still of interest because a large number of parameters are needed to accurately characterize inelastic torsional responses. Attempts to explore the general trends in the seismic response of plan-asymmetric structures were presented by Perus and Fajfar (2005) and De Stefano and Pintucchi (2010). Furthermore, since the time-frequency energy distribution for different ground motion records could differ significantly, the observations from a few records could not be generalized; the use of a large number of records for the parametric investigation of the inelastic torsional responses and ductility demand characteristics under bidirectional excitations is desirable.

The torsional responses for linear elastic systems depend on the distance between the center of mass (CM) and the center of stiffness (CS) and the ratio between the uncoupled

lateral and torsional vibration periods. Furthermore, when a three dimensional structure is simplified as two dimensional model, it was indicated that during ground motion excitations, the CM moves with respect to its original position or to the supports or to the CS (Hong 2013). This resulted in the instantaneous load eccentricities under seismic horizontal excitations, defined by the time-varying relative position of the instantaneous CM. This second order effect on the torsional response was termed A-Δ effect. The analysis results indicate that A-Δ effect is not significant for linear elastic systems under biaxial ground motions. However, whether it influences the nonlinear inelastic responses is unknown.

The inelastic torsional response is controlled by the degree of torsional restraint, defined using the ratio of torsional stiffness contributed by the lateral load resisting elements parallel to one of the axes to the overall torsional stiffness due to all elements (Paulay 1997). It is also influenced by center of strength (or plastic center) (CP) needs to be considered. Discussion of torsional provisions in design codes can be found in (Chopra 2001, Chopra and Goel 1991, Tso and Smith 1999, Humar et al. 2003, and Escobar 2004).

The objective of this chapter is to investigate the A-Δ effect on nonlinear inelastic responses due to bi-directional horizontal excitations. For the analysis, idealized one-story model is considered, and each lateral load resisting element is modeled using the Bouc-Wen hysteretic model. The equation of motion under biaxial excitations with the A-Δ effect is presented in the following section. Numerical analysis is carried out by considering more than 100 ground motion records.

2.2 Equation of motion considering the instantaneous load eccentricities

The idealized one-story model adopted in this study is shown in Figure 2.1. The system has a rigid deck with uniformly distributed mass. The positions of the four frames with respect to the center of mass (CM) are shown in the figure. Two elements along the direction of earthquake excitation are sufficient because the system responses are not sensitive to the number of elements (Goel and Chopra 1990). Each lateral load resisting elements is modeled using Bouc-Wen hysteretic model (Wen 1976; Foliente 1995; Ma, Zhang et al. 2004; Lee and Hong 2010). The center of the stiffness (CS) defines the point where applied lateral forces will result only in translation of the deck is located at (e_x, e_y); while the plastic center (or center of strength) (CP) is defined as the location of the resultant of yield forces of the load resisting elements (Goel and Chopra 1990) located at (e_{px}, e_{py}). For the current study, the CP coincides with the center of stiffness (CS); the results of investigation of CP do not coincide with the CS is listed in appendix A. For this single-story structure (i.e. Figure 2.1), although it is idealized in form, it incorporates the important properties and dynamic characteristics of actual buildings, and as such it can provides valuable information on torsional effects of buildings to withstand severe earthquakes.

Let u_x, u_y and θ denote the displacement along the *X*-axis, displacement along the *Y*-axis and rotation of the rigid slab with respect to the CM. The equation of motion of this system can be written as (Chopra 2001),

$$m\ddot{u}_x + c_x\dot{u}_x + \sum f_{xi} = -m\ddot{u}_{gx} \tag{2.1a}$$

$$m\ddot{u}_y + c_y\dot{u}_y + \sum f_{yi} = -m\ddot{u}_{gy} \tag{2.1b}$$

$$mr^2\ddot{\theta} + c_\theta\dot{\theta} + \sum(-f_{xi}y_i + f_{yi}x_i) = 0 \tag{2.1c}$$

where m is the mass; r is the radius of gyration of the slab about the CM; c denotes the damping coefficient; $\ddot{u}_g$ is the ground acceleration; f denotes the resisting force of the element, an overdot on a variable denotes its temporal derivative, and the summation Σ is over applicable lateral load resisting elements. Symbols c and $\ddot{u}_g$ with an additional subscript x, y and θ are used to denote the quantities associated with the X-axis, Y-axis and rotation, respectively. f with subscript xi and yi denotes the resisting force along the X-axis and Y-axis for the i-th lateral loading resisting element, respectively.

The displacement of the i-th element placed parallel to X-axis, u_{xi}, and the displacement of the i-th element placed parallel to Y-axis, u_{yi}, are given by

$$u_{xi}(t) = u_x(t) - y_i\theta(t) \tag{2.2a}$$

and

$$u_{yi}(t) = u_y(t) + x_i\theta(t) \tag{2.2b}$$

where x_i and y_i denote the distances from the CM to the elements as shown in Figure 2.1. The notation $u_{xi}(t)$, $u_x(t)$, $u_{yi}(t)$, $u_y(t)$ and $\theta(t)$ is used to emphasize that u_{xi}, u_x, u_{yi}, u_y and θ are time dependent.

If each lateral load resisting element is modeled as linear elastic system, the stiffness matrix **K** of the system is given by

$$\mathbf{K} = \begin{bmatrix} K_{XX} & 0 & K_{\theta X} \\ 0 & K_{YY} & K_{\theta Y} \\ K_{\theta X} & K_{\theta Y} & K_{\theta\theta} \end{bmatrix} \tag{2.3}$$

where K_{XX}, K_{YY}, $K_{\theta\theta}$, $K_{\theta X}$ and $K_{\theta Y}$ denote the elements of the stiffness matrix **K**. The stiffness can be used to define the dynamic characteristic of the system. For example, $\omega_x = \sqrt{K_{XX}/m}$, represents the natural vibration frequency along the *X*-axis, $\omega_y = \sqrt{K_{YY}/m}$ represents the natural vibration frequency along the *Y*-axis, and $\omega_\theta = \sqrt{K_{\theta\theta}/mr^2}$ represents the rotational natural vibration frequency.

By incorporating the mass and stiffness proportional damping (i.e., Rayleigh damping), for linear systems, Eqs. (2.1) and (2.2) leads to (Chopra 2001),

$$\begin{Bmatrix} \ddot{u}_x \\ \ddot{u}_y \\ \ddot{u}_\theta \end{Bmatrix} + a_1\omega_x^2 \begin{bmatrix} a_0/(a_1\omega_x^2)+1 & 0 & -e_y/r \\ 0 & a_0/(a_1\omega_x^2) + \Omega_y^2 & e_x\Omega_y^2/r \\ -e_y/r & e_x\Omega_y^2/r & a_0/(a_1\omega_x^2) + \Omega_\theta^2 \end{bmatrix} \begin{Bmatrix} \dot{u}_x \\ \dot{u}_y \\ \dot{u}_\theta \end{Bmatrix}$$
$$+\omega_x^2 \begin{bmatrix} 1 & 0 & -e_y/r \\ 0 & \Omega_y^2 & e_x\Omega_y^2/r \\ -e_y/r & e_x\Omega_y^2/r & \Omega_\theta^2 \end{bmatrix} \begin{Bmatrix} u_x \\ u_y \\ u_\theta \end{Bmatrix} = \begin{Bmatrix} -\ddot{u}_{gx} \\ -\ddot{u}_{gy} \\ 0 \end{Bmatrix} \tag{2.4a}$$

The equations of motion for nonlinear systems can be written as,

$$\begin{Bmatrix} \ddot{u}_x \\ \ddot{u}_y \\ r\ddot{\theta} \end{Bmatrix} + a_1\omega_x^2 \begin{bmatrix} a_0/(a_1\omega_x^2)+1 & 0 & -e_y/r \\ 0 & a_0/(a_1\omega_x^2) + \Omega_y^2 & e_x\Omega_y^2/r \\ -e_y/r & e_x\Omega_y^2/r & a_0/(a_1\omega_x^2) + \Omega_\theta^2 \end{bmatrix} \begin{Bmatrix} \dot{u}_x \\ \dot{u}_y \\ r\dot{\theta} \end{Bmatrix}$$

$$+\alpha\omega_x^2 \begin{bmatrix} 1 & 0 & -e_y/r \\ 0 & \Omega_y^2 & e_x\Omega_y^2/r \\ -e_y/r & e_x\Omega_y^2/r & \Omega_\theta^2 \end{bmatrix} \begin{Bmatrix} u_x \\ u_y \\ r\theta \end{Bmatrix} \qquad (2.4b)$$

$$+(1-\alpha)\omega_x^2 \begin{Bmatrix} \sum \kappa_{xi} z_{xi} \\ \sum \Omega_y^2 \kappa_{yi} z_{yi} \\ \frac{1}{r}\sum\left(-y_i\kappa_{xi}z_{xi} + \Omega_y^2 x_i \kappa_{yi} z_{yi}\right) \end{Bmatrix} = \begin{Bmatrix} -\ddot{u}_{gx} \\ -\ddot{u}_{gy} \\ 0 \end{Bmatrix}$$

where $u_\theta = r\theta$, $\Omega_\theta = \omega_\theta/\omega_x$; $\Omega_y = \omega_y/\omega_x$; $K_{XX} = \sum_i k_{xi}$; $K_{YY} = \sum_i k_{yi}$; $e_x = K_{\theta Y}/K_{YY} = \sum k_{yi}x_i / \sum_i k_{yi}$ and $e_y = K_{\theta X}/K_{XX} = \sum k_{xi}y_i / \sum_i k_{xi}$ are known as eccentricities along the *X*-axis and *Y*-axis, respectively; $K_\theta = \sum\left(k_{xi}y_i^2 + k_{yi}x_i^2\right)$; $\kappa_{xi} = k_{xi}/K_{XX}$, $\kappa_{yi} = k_{yi}/K_{YY}$; $a_0 = 2\zeta\omega_x\omega_y/\left(\omega_x+\omega_y\right)$; $a_1 = 2\zeta/\left(\omega_x+\omega_y\right)$and z_{xi} and z_{yi} are the hysteretic displacements which will be discussed in detail in the subsequent sections. The damping ratio ζ is considered to be equal to 5% throughout this study. The expressions for a_0 and a_1 are obtained by assuming that the damping ratios for the two translational modes are identical and equal to ζ.

The components of a selected ground motion record (COALINGA 05/02/83, PARKFIELD - GOLD HILL), which are scaled by the same factor such that the PSA at *Tx* = 1.0 (s) (for the first record component) equals 0.25 (g) is illustrated in Figure 2.2. For this record, the time history responses of u_x and u_y for a defined two-way symmetric system (i.e., for the analysis the uncoupled lateral frequencies ω_x and ω_y are assumed to be the same and equal to 2π; the normalized yield strengths ϕ_x and ϕ_y are both considered

equal to 0.5; and the value of Ω_θ that equals 1.0.), are calculated and are also shown in the same figure. The figure shows that at t equal to 9.02 s, $\ddot{u}_{gx} = 0.474$ m/s^2 and $\ddot{u}_{gy} = 0.384$ m/s^2, and the position of CM is located at u_x = 0.062 m and u_y = -0.0124 m. This indicates that the instantaneous CM does not coincide with the position of CS, and a torsion moment about the CS will be induced due to ground motions. Since the CM moves with respect to its original position or to the supports or to the CS when a structure responds to seismic ground motions (see Figure 2.3), this resulted in the instantaneous load eccentricities under seismic horizontal excitations that are functions of the time-varying relative position of the instantaneous CM (Hong 2013). By taking into account this second order effect on the torsional response, which was termed A-Δ effect, Eq. (2.1c) becomes,

$$mr^2\ddot{\theta} + c_\theta\dot{\theta} + \sum\left(-f_{xi}\left(y_i - u_y\right) + f_{yi}\left(x_i - u_x\right)\right) = 0 \tag{2.5}$$

and Eq. (2.2) becomes

$$u_{xi}(t) = u_x(t) - \left(y_i - u_y(t)\right)\theta(t) \tag{2.6a}$$

and

$$u_{yi}(t) = u_y(t) + \left(x_i - u_x(t)\right)\theta(t) \tag{2.6b}$$

This resulting (time-dependent) in the stiffness matrix $\mathbf{K}$ becomes (Hong 2013),

$$\mathbf{K}=\begin{bmatrix} K_{XX} & 0 & K_{\theta X}+K_{XX}u_y \\ 0 & K_{YY} & K_{\theta Y}-K_{YY}u_x \\ K_{\theta X}+K_{XX}u_y & K_{\theta Y}-K_{YY}u_x & K_{\theta\theta}+2K_{\theta X}u_y-2K_{\theta Y}u_x+K_{XX}u_y^2+K_{YY}u_x^2 \end{bmatrix} \tag{2.7}$$

where $\mathbf{K}$ is time-dependent as the instantaneous load eccentricities vary in time. In other words, the *A*-Δ effect affects the stiffness that couples the translational and rotational displacements. Note that the (new) $K_{\theta\theta}$ in Eq. (2.7) differs from that shown in Hong (2013) as the latter contains an approximation in calculating the force (or the level arm) used to estimate the torsional moment. Based on this stiffness matrix, the governing equation shown in Eq. (2.4) becomes,

$$\begin{Bmatrix} \ddot{u}_x \\ \ddot{u}_y \\ \ddot{u}_\theta \end{Bmatrix} + a_1\omega_x^2 \begin{bmatrix} a_0/(a_1\omega_x^2)+1 & 0 & -e_y/r \\ 0 & a_0/(a_1\omega_x^2)+\Omega_y^2 & e_x\Omega_y^2/r \\ -e_y/r & e_x\Omega_y^2/r & a_0/(a_1\omega_x^2)+\Omega_\theta^2 \end{bmatrix} \begin{Bmatrix} \dot{u}_x \\ \dot{u}_y \\ \dot{u}_\theta \end{Bmatrix}$$
$$+\omega_x^2 \begin{bmatrix} 1 & 0 & -\left(e_y+u_y\right)/r \\ 0 & \Omega_y^2 & \Omega_y^2\left(e_x-u_x\right)/r \\ -\left(e_y+u_y\right)/r & \Omega_y^2\left(e_x-u_x\right)/r & \Omega_\theta^2+e_yu_y/r-e_xu_x/r \end{bmatrix} \begin{Bmatrix} u_x \\ u_y \\ u_\theta \end{Bmatrix} = \begin{Bmatrix} -\ddot{u}_{gx} \\ -\ddot{u}_{gy} \\ 0 \end{Bmatrix} \tag{2.8}$$

To more realistically represent the response of the designed structures under strong earthquake excitations, the nonlinear inelastic structural behavior needs to be considered. For this, consider that each lateral load resisting element can be modeled using Bouc-Wen hysteretic model (Wen 1976; Foliente 1995; Ma, Zhang et al. 2004; Lee and Hong 2010). The Bouc-Wen hysteretic model has 12 parameters, consisting of shape parameters {α, β, γ, n}, degradation parameters {δ_η, δ_ν} and pinching parameters {ζ_s, p, q, ψ, δ_ψ, λ} (Goda et al., 2009).

As the force-displacement relation for each load effect resisting element is modeled using the Bouc-Wen hysteretic model, f_{xi} for the i-th lateral load resisting element (frame or wall) can be expressed as,

$$f_{xi} = \alpha_{xi} k_{xi} u_{xi} + (1-\alpha_{xi}) k_{xi} z_{xi} \tag{2.9}$$

where k_{xi} is the elastic lateral stiffness. z_{xi}, is governed by (Wen 1976; Foliente 1995; Ma et al. 2004),

$$\dot{z}_{xi} = \frac{1}{\eta_{xi}} \left\{ \dot{u}_{xi} - \nu_{xi} z_{xi} \left| \dot{u}_{xi} \right| \left| z_{xi} \right|^{n_{xi}-1} \left[\beta_{xi} + \gamma_{xi} \operatorname{sgn}(\dot{u}_{xi} z_{xi}) \right] \right\} \tag{2.10a}$$

where $\eta_{xi} = 1 + \delta_{\eta xi} E_{nxi}$; the parameter $\delta_{\eta xi}$ controls the stiffness degradation; $\nu_{xi} = 1 + \delta_{\nu xi} E_{nxi}$; the parameter $\delta_{\nu xi}$ controls the strength degradation; and the normalized dissipated hysteretic energy, E_{xi}, is defined by,

$$E_{xi} = \frac{(1-\alpha_{xi})}{Q_{xi}\Delta_{xi}} \int_0^t k_{xi} z_{xi} \dot{u}_{xi} \, dt = (1-\alpha_{xi}) \int_0^t \frac{z_{xi}}{\Delta_{xi}} \frac{\dot{u}_{xi}}{\Delta_{xi}} \, dt \tag{2.10b}$$

in which $\Delta_{xi} = \left(\beta_{xi} + \gamma_{xi}\right)^{-1/n_{xi}}$ denotes initial yield displacement and $Q_{xi} = k_{xi}\Delta_{xi}$ is the initial yield force. Similarly, f_{yi} is defined by replace the subscript x with y in Eq. (2.9). Note that if α_{xi} and α_{yi} are considered to be equal to one, the material nonlinearity is neglected in the considered system and $f_{xi} = k_{xi} u_{xi}$ and $f_{yi} = k_{yi} u_{yi}$.

To illustrate the influences of Bouc-Wen model parameters on nonlinear hysteresis loops, an inelastic SDOF system subjected to four cycles of harmonic force excitations with increasing amplitude were considered. Among these parameters, α is the ratio of post-yield stiffness to initial yield stiffness. This parameter is commonly considered to

range from 0 to 1. If α equals to zero, the relationship between restoring force and displacement is ideal elastoplastic model; while if α equals to one, the relationship between restoring force and displacement is linear elastic model. Figure 2.3a indicates that shape parameter α controls the post-yield tangent stiffness of hysteresis loop. The shape parameters $\{\beta, \gamma, n\}$ define the yield displacement $\Delta_x = (\beta+\gamma)^{-1/n}$. Basically, β is within 0.5 to 1.5, γ ranges from −0.3 to 0.50 and n is suggested ranges from 0 to 3. Figure 2.3b shows that shape parameters β and γ control the loading and unloading path, while Figure 2.3c indicates that the shape parameter n changes smoothness of transition between pre-yielding and post-yielding state. Degradation parameters (i.e. δ_η and δ_ν) are functions of dissipated energy: δ_η controls the stiffness degradation and often takes a value within 0 to 0.3, while δ_ν with a value within 0 to 0.05 affects the strength degradation. Figure 2.3d reveals that the tangent stiffness of hysteresis loop decreases in each loading cycle. Moreover, figure 2.3e shows that the yield strength decreases with increase of loading and unloading cycles when $\delta_\nu = 0.03$. The range of pinching parameters ζ_s is within 0.7 to 1, and other pinching parameters (i.e. $\{p, q, \psi, \delta_\psi, \lambda\}$) considered in figure 2.3f equals to $\{2.5, 0.15, 0.1, 0.005, 0.5\}$. The figure 2.3f shows the smooth degrading hysteretic models with pinching behavior when $\zeta_s = 0.85$ has an obvious pinching effect.

Based on the considerations above, the displacements under bidirectional seismic excitations are governed by

$$\ddot{u}_x + \left(a_0 + a_1\omega_x^2\right)\dot{u}_x - a_1\omega_x^2\frac{e_y}{r}\dot{u}_\theta + \alpha_x\omega_{x1}^2\left[u_x - \frac{\left(y_1 - u_y\right)}{r}u_\theta\right] + \left(1-\alpha_x\right)\omega_{x1}^2 Z_{x1} + \alpha_x\omega_{x2}^2\left[u_x - \frac{\left(y_2 - u_y\right)}{r}u_\theta\right] + \left(1-\alpha_x\right)\omega_{x2}^2 Z_{x2} = -\ddot{u}_{gx} \tag{2.11a}$$

$$\ddot{u}_y + \left(a_0 + a_1\omega_y^2\right)\dot{u}_y + a_1\omega_y^2\frac{e_x}{r}\dot{u}_\theta + \alpha_y\omega_{y1}^2\left[u_y + \frac{\left(x_1 - u_x\right)}{r}u_\theta\right] + \left(1-\alpha_y\right)\omega_{y1}^2 Z_{y1} + \alpha_y\omega_{y2}^2\left[u_y + \frac{\left(x_2 - u_x\right)}{r}u_\theta\right] + \left(1-\alpha_y\right)\omega_{y2}^2 Z_{y2} = -\ddot{u}_{gy} \tag{2.11b}$$

$$\ddot{u}_\theta + \left(a_0 + a_1\omega_\theta^2\right)\dot{u}_\theta - a_1\omega_x^2\frac{e_y}{r}\dot{u}_x + a_1\omega_y^2\frac{e_x}{r}\dot{u}_y + \frac{\left(y_1 - u_y\right)}{r}\left[\begin{array}{l} -\alpha_x\omega_{x1}^2\left(u_x - \dfrac{\left(y_1 - u_y\right)}{r}u_\theta\right) - \\ \left(1-\alpha_x\right)\omega_{x1}^2 Z_{x1} \end{array}\right] + \frac{\left(y_2 - u_y\right)}{r}\left[-\alpha_x\omega_{x2}^2\left(u_x - \frac{\left(y_2 - u_y\right)}{r}u_\theta\right) - \left(1-\alpha_x\right)\omega_{x2}^2 Z_{x2}\right] + \frac{\left(x_1 - u_x\right)}{r}\left[\alpha_y\omega_{y1}^2\left(u_y + \frac{\left(x_1 - u_x\right)}{r}u_\theta\right) + \left(1-\alpha_y\right)\omega_{y1}^2 Z_{y1}\right] + \frac{\left(x_2 - u_x\right)}{r}\left[\alpha_y\omega_{y2}^2\left(u_y + \frac{\left(x_2 - u_x\right)}{r}u_\theta\right) + \left(1-\alpha_y\right)\omega_{y2}^2 Z_{y2}\right] = 0 \tag{2.11c}$$

where z_{xi} and z_{yi} are governed by Eq. (2.10). Eq. (2.10), Eq. (2.11) and the corresponding equation for z_{yi} needs to be solved simultaneously.

To simplify the parametric study of inelastic system, rather than estimating the displacement responses, the normalized displacements given below are considered,

$$\mu_x = \frac{u_x}{\Delta_x},\ \tilde{\mu}_y = \frac{u_y}{\Delta_x},\ \mu_\theta = \frac{u_\theta}{\Delta_x},\ \mu_{zxi} = \frac{z_{xi}}{\Delta_{xi}},\ \mu_{zyi} = \frac{z_{yi}}{\Delta_{yi}} \tag{2.12}$$

where the normalized displacements μ_x and μ_y ($\mu_y = \tilde{\mu}_y \Delta_{x/y}$ and $\Delta_{x/y} = \Delta_x / \Delta_y$) represent the "global" ductility demands along the *X*- and *Y*-axis, respectively, while μ_{xi} (or μ_{yi}) represents the ductility demand for the *i*-th lateral load resisting element.

To facilitate parametric studies of the responses of the system described above, the normalized yield strength ϕ_x and ϕ_y are introduced, which are defined by,

$$\phi_x = \Delta_x / d_{0x} \text{ and } \phi_y = \Delta_y / d_{0y} \tag{2.13}$$

where d_{0x} and d_{0y} are the peak linear elastic displacement responses along the *X*-axis and *Y*-axis. $d_{0x} = S_x/(\omega_x)^2$, $d_{0y} = S_y/(\omega_y)^2$, where S_x and S_y are the pseudo-spectral acceleration (PSA) for the ground motion component along *X*-axis and *Y*-axis, respectively.

$$\begin{Bmatrix} \ddot{u}_x \\ \ddot{u}_y \end{Bmatrix} + \begin{bmatrix} a_0 + a_1\omega_x^2 & 0 \\ 0 & a_0 + a_1\omega_y^2 \end{bmatrix} \begin{Bmatrix} \dot{u}_x \\ \dot{u}_y \end{Bmatrix} + \begin{bmatrix} \omega_x^2 & 0 \\ 0 & \omega_y^2 \end{bmatrix} \begin{Bmatrix} u_x \\ u_y \end{Bmatrix} = \begin{Bmatrix} -\ddot{u}_{gx} \\ -\ddot{u}_{gy} \end{Bmatrix} \tag{2.14}$$

By using the normalized variables defined above, Eq (2.10) and Eq (2.11) can be expressed as,

$$\begin{aligned} &\ddot{\mu}_x + \left(a_0 + a_1\omega_x^2\right)\dot{\mu}_x - a_1\omega_x^2 \frac{e_y}{r}\dot{\mu}_\theta + a_x\omega_{x1}^2\left[\mu_x - \frac{(y_1 - \tilde{\mu}_y\Delta_x)}{r}\mu_\theta\right] + \\ &\left(1-\alpha_x\right)\omega_{x1}^2\mu_{zx1} + a_x\omega_{x2}^2\left[\mu_x - \frac{(y_2 - \tilde{\mu}_y\Delta_x)}{r}\mu_\theta\right] + \left(1-\alpha_x\right)\omega_{x2}^2\mu_{zx2}\delta_x = -\frac{1}{\Delta_x}\ddot{u}_{gx} \end{aligned} \tag{2.15a}$$

$$\begin{aligned} &\ddot{\tilde{\mu}}_y + \left(a_0 + a_1\omega_y^2\right)\dot{\tilde{\mu}}_y + a_1\omega_y^2 \frac{e_x}{r}\dot{\mu}_\theta + a_y\omega_{y1}^2\left[\tilde{\mu}_y + \frac{(x_1 - \mu_x\Delta_x)}{r}\mu_\theta\right] + \\ &\left(1-\alpha_y\right)\omega_{y1}^2\mu_{zy1}\frac{\Delta_y}{\Delta_x} + a_y\omega_{y2}^2\left[\tilde{\mu}_y + \frac{(x_2 - \mu_x\Delta_x)}{r}\mu_\theta\right] + \left(1-\alpha_y\right)\omega_{y2}^2\mu_{zy2}\frac{\Delta_y}{\Delta_x}\delta_y = -\frac{1}{\Delta_x}\ddot{u}_{gy} \end{aligned} \tag{2.15b}$$

and

$$\ddot{\mu}_\theta + \left(a_0 + a_1\omega_\theta^2\right)\dot{\mu}_\theta - a_1\omega_x^2\frac{e_y}{r}\dot{\mu}_x + a_1\omega_y^2\frac{e_x}{r}\dot{\mu}_y +$$
$$\frac{(y_1 - \tilde{\mu}_y\Delta_x)}{r}\left[-\alpha_x\omega_{x1}^2\left(\mu_x - \frac{(y_1 - \tilde{\mu}_y\Delta_x)}{r}\mu_\theta\right) - \left(1-\alpha_x\right)\omega_{x1}^2\mu_{zx1}\right] +$$
$$\frac{(y_2 - \tilde{\mu}_y\Delta_x)}{r}\left[-\alpha_x\omega_{x2}^2\left(\mu_x - \frac{(y_2 - \tilde{\mu}_y\Delta_x)}{r}\mu_\theta\right) - \left(1-\alpha_x\right)\omega_{x2}^2\mu_{zx2}\delta_x\right] + \qquad (2.16a)$$
$$\frac{(x_1 - \mu_x\Delta_x)}{r}\left[\alpha_y\omega_{y1}^2\left(\tilde{\mu}_y + \frac{(x_1 - \mu_x\Delta_x)}{r}\mu_\theta\right) + \left(1-\alpha_y\right)\omega_{y1}^2\mu_{zy1}\frac{\Delta_y}{\Delta_x}\right] +$$
$$\frac{(x_1 - \mu_x\Delta_x)}{r}\left[\alpha_y\omega_{y2}^2\left(\tilde{\mu}_y + \frac{(x_2 - \mu_x\Delta_x)}{r}\mu_\theta\right) + \left(1-\alpha_y\right)\omega_{y2}^2\mu_{zy2}\frac{\Delta_y}{\Delta_x}\delta_y\right] = 0$$

$$\dot{\mu}_{zxi} = \left(\dot{\mu}_x - \left(\frac{(y_i - \tilde{\mu}_y\Delta_x)}{r}\dot{\mu}_\theta - \frac{\dot{\tilde{\mu}}_y\Delta_x}{r}\mu_\theta\right)\right) -$$
$$\mu_{zxi}\left|\dot{\mu}_x - \left(\frac{(y_i - \tilde{\mu}_y\Delta_x)}{r}\dot{\mu}_\theta - \frac{\dot{\tilde{\mu}}_y\Delta_x}{r}\mu_\theta\right)\right|\left|\dot{\mu}_{zxi}\right|^{n-1}\left[\beta + \gamma\,\mathrm{sgn}\left(\left(\dot{\mu}_x - \left(\frac{(y_i - \tilde{\mu}_y\Delta_x)}{r}\dot{\mu}_\theta - \frac{\tilde{\mu}_y\Delta_x}{r}\mu_\theta\right)\right)\mu_{zxi}\right)\right] \qquad (2.16b)$$

$$\dot{\mu}_{zyi} = \left(\dot{\mu}_y + \left(\frac{(x_i - \mu_x\Delta_x)}{r}\dot{\mu}_\theta - \frac{\dot{\mu}_x\Delta_x}{r}\mu_\theta\right)\right) -$$
$$\mu_{zyi}\left|\dot{\mu}_y + \left(\frac{(x_i - \mu_x\Delta_x)}{r}\dot{\mu}_\theta - \frac{\dot{\mu}_x\Delta_x}{r}\mu_\theta\right)\right|\left|\dot{\mu}_{zyi}\right|^{n-1}\left[\beta + \gamma\,\mathrm{sgn}\left(\left(\dot{\mu}_y + \left(\frac{(x_i - \mu_x\Delta_x)}{r}\dot{\mu}_\theta - \frac{\dot{\mu}_x\Delta_x}{r}\mu_\theta\right)\right)\mu_{zyi}\right)\right] \qquad (2.16c)$$

where $\delta_x = \Delta_{x2}/\Delta_{x1}$ and $\delta_y = \Delta_{y2}/\Delta_{y1}$ represent the ratios between yield displacements of different load resisting elements along *X*- and *Y*-axis.

Eq. (2.15) and (2.16) can be solved for $\left\{\mu_x \;\; \dot{\mu}_x \;\; \tilde{\mu}_y \;\; \dot{\tilde{\mu}}_y \;\; \mu_\theta \;\; \dot{\mu}_\theta \;\; \mu_{zx1} \;\; \mu_{zx2} \;\; \mu_{zy1} \;\; \mu_{zy2}\right\}$ using Gear's method (Shampine and Reichelt, 1997).

2.3 Statistical assessment of the normalized responses

2.3.1 Ground motion records

For the analysis, the same set of records used in Hong (2013), which is extracted from Next Generation Attenuation database (PEER 2006) is considered. This set of records consists of 123 records from 11 California earthquakes listed in Table 2.1. The record selection is based on the following criteria:

1) The low-cut filter corner frequency in processing raw data equals 0.2 Hz or less;
2) The moment magnitude of the event is greater than 6;
3) The distance D (i.e., closest horizontal distance to projected faults on the earth or the epicentral distance if the former is not available) is greater than 15 km;
4) The shear wave velocity V_{s30} in the uppermost 30m is greater than 360 (m/s), representing NEHRP's site class A, B and C (i.e., Hard rock, Rock and very dense soil and soft rock) (BSSC 2001).

2.3.2 Numerical results

The statistics of the response of inelastic systems subjected to bidirectional ground motion are evaluated. For the analysis, it is assumed that the orientation of the first record component parallels the *X*-axis, and second component parallels the *Y*-axis.

In this study, the dynamic characteristics of the structure are completely defined by ω_x, Ω_y, x_i/r, y_i/r, e_x/r and e_y/r. For a given system subjected to a given ground motion record, $\left\{\mu_x, \tilde{\mu}_y, \mu_\theta, \mu_{zx1}, \mu_{zx2}, \mu_{zy1}, \mu_{zy2}\right\}$ are solved using the following analysis steps:

1) For a given record, compute the peak linear elastic responses d_{0x} and d_{0y} for the corresponding linear elastic SDOF systems;
2) The record components are scaled with the same factor such that its first record component (X-direction) leads to the PSA at T_x=1.0 (s) equal to 0.25 (g) or 0.5(g)
3) Compute the yield displacement $\Delta_x = \phi_x d_{0x}$ and $\Delta_y = \phi_y d_{0y}$;
4) Radius of gyration r for the considered geometry is given by $r = \sqrt{\left(L^2 + W^2\right)/12}$. The aspect ratio ($L/W$) was assumed equal to be equal to 2. By the considering that the structure has the height over width ratio equal to 1 (i.e., h_n/W=1), and that the height of structure can be assigned based the following approximate relation $T_n = 0.075\left(h_n\right)^{3/4}$, where $T_n = T_x = T_y$, it is concluded that r = 10 m. This value can be used to calculate the ratio of Δ_x / r;
5) For given values of ϕ_x and ϕ_y, solve Eq. (2.16) for μ_x, μ_y and μ_θ, then calculate u_x, u_y and u_θ;
6) The normalized displacement of the resisting elements μ_{xi} and $\mu_{yi.}$ can be solved using $u_{xi}(t) = \mu_x \Delta_x - \left(\frac{y_i}{r} - \tilde{\mu}_y \frac{\Delta_x}{r}\right)\mu_\theta \Delta_x$ and $u_{yi}(t) = \tilde{\mu}_y \Delta_x + \left(\frac{x_i}{r} - \mu_x \frac{\Delta_x}{r}\right)\mu_\theta \Delta_x$. The estimated u_{xi}, u_{yi}, u_x, u_y, and u_θ are then used to assess the torsional effects;

7) Repeat Steps 1) through 6) for each of the 123 records and estimate the statistics of torsional effects.

To investigate the influence of the *A*-Δ effect on the seismic induced inelastic peak responses, symmetric, one-way asymmetric and two-way asymmetric systems are considered in the following. To simplify the parametric investigation, we do not consider the effects of degradation and pinching in the Bouc-Wen hysteretic model, therefore, the stiffness and strength degradation parameters$\{\delta_\eta, \delta_\nu\}$ and pinching parameters $\{\zeta_s, p, q, \psi, \delta_\psi, \lambda\}$ equal to zero; the shape parameters selected in this project are $\{\alpha, \beta, \gamma, n\}$ = {0.05, 0.5, 0.5, 2}. The remaining parameters for the Bouc-Wen model [α, $\beta_{\mu xi}$, $\beta_{\mu yi}$, $\gamma_{\mu xi}$, $\gamma_{\mu yi}$, n_{xi}, n_{yi}] = [0, 0.5, 0.5, 0.5, 0.5, 2, 2] are considered for each lateral load resisting element. The case defined by the above parameters is referred to as the reference case. For the numerical analysis, the aspect ratio *L/W=2* is adopted. The vibration period T_x ($2\pi/\omega_x$) is assumed to be 1 s and 2 s; T_y is assumed to be equal to T_x (i.e., $\Omega_y = 1$) for all the numerical evaluation. The uncoupled torsional-to-lateral frequency ratio Ω_θ varies from 0.8 to 2.0 (Goel and Chopra 1991). A large Ω_θ value represents torsionally stiff system with resisting elements near the perimeter of the building plan, and a small Ω_θ value indicates a torsionally flexible system with a stiff central core (De la Llera and Chopra 1995a,b).

To reduce the number of the parameters that need to be considered for the parametric investigation, it is assumed that the distances from the CM to each lateral load resisting element along each direction are equal (i.e. $|x_1| = |x_2|$ and $|y_1| = |y_2|$), and the ratio $|x_i|/L$

equals $|y_i|/W$, which is denoted using the symbol χ. Based on these assumptions, and the relation $\Omega_\theta = \sqrt{\omega_\theta / \omega_x}$ it can be shown that $\chi = \Omega_\theta \Big/ \sqrt{(W/r)^2 + K_{YY}/K_{XX}\,(L/r)^2}$. In other words, under these assumptions, the value of the ratio can be calculated based on other structural characteristics. The calculated value of χ can readily be used to define the locations of the lateral load resisting elements: two lateral load resisting elements that parallel the *X*-axis are placed at *y* equal to χW and $-\chi W$ while the two elements that parallel the *Y*-axis are placed at *x* equal to χL and $-\chi L$. For the structure systems to be analysis, the eccentricity ratios defined as e_x/r and e_y/r are considered to be equal to 0 and $0.25|y_i|/r$ for one-way asymmetric system, and $0.25|x_i|/r$ and $0.25|y_i|/r$ for two-way asymmetric systems.

2.3.2.1 Two-way symmetric system

To illustrate that the responses by considering *A*-Δ effect are not proportional to the intensity of the excitation, the record components are scaled with the same factor such that its first record component leads to a PSA at T_X =1.0*s* equal to 0.25g and 0.5g, and the obtained results for the same record shown and the structural system considered in Figure 2.3 are shown in Figure 2.5 (which is Case 2 with $\Omega_\theta = 1$ shown in Table 2.2).

To analyze the response affected by *A*-Δ effect, several ratios are defined, calculated and used. These are: the ratio of $\max(|u_{xT}(t)|)/\max(|u_x(t)|)$ denoted by R_X, the ratio $\max(|u_{yT}(t)|)/\max(|u_y(t)|)$ denoted by R_Y; and the ratios of the maximum displacements of the lateral load resisting elements R_X,

$R_{XT} = \max(|u_{x1T}(t)|, |u_{x2T}(t)|) / \max(|u_{x1}(t)|, |u_{x2}(t)|)$ and R_Y, $R_{YT} = \max(|u_{y1T}(t)|, |u_{y2T}(t)|) / \max(|u_{y1}(t)|, |u_{y2}(t)|)$,where the symbols $u_{xT}(t), u_{yT}(t), u_{xiT}(t), u_{yiT}(t),$ and $\theta_T(t)$ with an additional subscript T denote are used to denote the calculated displacements that include the *A*-Δ effect.

The obtained samples of R_X, R_Y, R_{XT}, R_{YT} and $\max(r\theta_T)$ versus M and D for the selected records listed in Table 2.2 are presented in Figure 2.6 for the system where $\Omega_\theta = 1$ which is defined in Table 2.2. For the calculation, each record is scaled such that its PSA at T_X is equal to a target value specified in Table 2.2 for the considered system. The results shown in Figure 2.6 indicate that the correlation coefficients calculated from the samples are small; therefore R_X, R_Y, R_{XT}, R_{YT}, and $\max(r\theta_T)$ are not sensitive to magnitude or distance. Therefore, it is reasonable to assume that R_X, R_Y, R_{XT}, R_{YT}, and $\max(r\theta_T)$ are independent of M and D.

Statistics summarized in Table 2.2 indicate that the means of R_X, R_Y, R_{XT} and R_{YT} are near unity and the coefficient of variation (COV) values of R_X and R_Y are small. This suggests that the influence of *A*-Δ effect on the displacements of the CM is negligible. However, due to the *A*-Δ effect, the displacements on the lateral load-resisting elements are affected to a larger degree; the COV values of R_{XT} and R_{YT} are relatively significant compared to those without considering *A*-Δ effect. For example, considering the first and last case listed in Table 2.2, the maximum values of R_{XT} and R_{YT} are 1.004 and 1.010 for the second case, 1.014 and 1.017 for the last case, respectively. For the corresponding cases without *A*-Δ effect, the maximum values of R_X and R_Y are 1.0001 and 0.9999 for the

first case, 1.0014 and 1.0013 for the last case, respectively. By considering the results for eight systems shown in Table 2.2, the torsional displacement considering *A*-Δ effect are 0.0004 and 0.0059 for second case and last case respectively; the results indicate that, there is an underestimation in seismic torsional displacement if the *A*-Δ effect is ignored, and the responses affecting by the *A*-Δ effect are sensitive to the natural vibration periods.

Another key parameter that influences the response is Ω_θ, the uncoupled torsional-to-lateral frequency ratio. The computed statistics of the inelastic responses shown in Table 2.2 for several structural systems indicate that, as Ω_θ decreases the system becomes increasingly flexible in torsion and the torsional deformation tends to increase as the structural vibration periods increase.

2.3.2.2 One-way asymmetric system

The considered one-way asymmetric system is listed in Table 2.3. For these systems, the obtained statistics of the samples of R_X, R_Y, max$(r\theta)$, R_{XT}, R_{YT} and max$(r\theta_T)$ for each considered system are summarized in the same table. An illustration of the time histories of the responses of an one-way asymmetric system ($e_x/r = 0$, $e_y/r = 0.25|y_i|/r$) subjecting to the ground motion shown in Figure 2.3 is shown Figures 2.7a and 2.7b by ignoring and considering the *A*-Δ effect, respectively. The samples of R_{XT}, R_{YT} and max$(r\theta_T)$ versus *M* and *D* for the case with $\Omega_\theta = 1$ shown in Table 2.3 are depicted in Figure 2.8.

For one-way asymmetric system considering *A*-Δ effect, the influence of this second order effect on the displacements of the CM is again negligible since the means of R_X, R_Y,

R_{XT}, R_{YT} are near unity. Comparison of results shown Table 2.2 for symmetric system and Table 2.3 for one-way asymmetric system with $e_x/r = 0$ and $e_y/r = 0.25|y_i|/r$, indicates that the stiffness eccentricity affects the torsional displacement to a large degree. Since the torsional responses are already present for unsymmetrical system, the addition of the instantaneous load eccentricities does not affect significantly the total responses (as compared to the cases for the symmetrical systems). The results presented in Figure 2.8 show that the correlation coefficients between both calculated ratios or torsional displacement and D or M are small, which indicates that R_X, R_Y, max$(r\theta)$, R_{XT}, R_{YT} and max$(r\theta_T)$ could be assumed to be independent to magnitude or distance.

Note that with the increase of the natural vibration period, the means of torsional displacements with and without *A*-Δ effect increases slightly. For example, for the last case shown in the table, the displacements for the cases with and without A-Δ effect are 0.0719 and 0.0707, an increase of about 1.8 percent. This shows that the responses affected by the *A*-Δ effect are somewhat sensitive to the natural vibration periods.

2.3.2.3 Two-way asymmetric system

For the two-way asymmetric system, a similar analysis that was carried out in the previous section is carried out. The cases for this analysis are presented in Table 2.4. The time histories of the displacements for the second case listed in the table are illustrated in Figures 2.8a and 2.8b by ignoring and considering the *A*-Δ effect. Variations of R_{XT}, R_{YT} and max$(r\theta_T)$ versus *M* and *D* for this case is presented in Figure 2.10. The figure shows the calculated correlation coefficients not significant, and there

are no pronounced trends. This is similar as two-way symmetric system and one-way asymmetric system. The statistics of the ratios of the responses are also presented in Table 2.4, and the conclusions that can be drawn from the Table are similar to those observed from Tables 2.2 and 2.3.

2.4 Discussion and Conclusions

In this study, the concept of the instantaneous load eccentricities under seismic horizontal excitations, defined by the time-varying relative position of the instantaneous CM, which causes a second order effect that is termed as the A-Δ effect, is considered. A statistical characterization of inelastic torsional response with A-Δ effect under a set of 123 California seismic records is carried out by modeling the lateral load resisting elements using the Bouc-Wen hysteretic model. The analysis is focused on the torsional response ratio for an idealized single-storey structure, which is defined as the response of lateral load resisting elements by considering the torsional effect and A-Δ effect to that by neglecting the A-Δ effect. The main conclusions that can be drawn from the numerical results are:

(1) On average, a slight underestimation of seismic displacement demand occurs if the A-Δ effect is ignored, especially for two-way symmetrical systems.

(2) The responses affecting by the A-Δ effect are sensitive to the natural vibration periods.

(3) Since the torsional responses are already present for unsymmetrical system, the addition of the instantaneous load eccentricities does not affect significantly the total responses.

The observations indicate that the consideration of the A-Δ effect is not necessary since in most considered cases, on average, the A-Δ effect does not affect the inelastic responses to a large degree

For the presented analysis results, it is considered that the CP coincides with the CS. For completeness, results for the CP that differs from the CS are also evaluated (see Appendix A). The conclusions that can be drawn from the results shown in the Appendix A are similar to those shown in this chapter.

The influence of the A-Δ effect on single story considering rotational components of ground motion (coupled tilt and Translational Ground Motion Response Spectra), that is not investigated in this study, deserves further consideration.

References

Akaike, H. (1974) A new look at the statistical model identification. IEEE Transactions on Automatic Control; 19: 716–723.

Building Seismic Safety Council (BSSC) (1995). NEHRP Recommended Provisions for Seismic Regulations for New Buildings, FEMA 222A/223A, Vol. 1 (Provisions) and Vol. 2 (Commentary), developed for the Federal Emergency Management Agency, Washington, D.C.

Chopra, A.K. (2001). Dynamics of structures: theory and applications to earthquake engineering (2nd ed.). Prentice Hall, N.J; 2001.

De La Llera J.C. and Chopra, A. K. (1995a). Understanding the inelastic seismic behaviour of asymmetric-plan buildings. Earthquake Engineering and Structural Dynamics; 24(4):549 – 572.

De la Llera, J. C. and Chopra, A. K. (1995b) Estimation of accidental torsion effects for seismic design of buildings. Journal of Structural Engineering, ASCE; 121(1):102–114.

De Stefano, M. and Pintucchi, B. (2008). A review of research on seismic behaviour of irregular building structures since 2002. Bull. Earthquake Eng.; 6:285–308

De Stefano, M. and Pintucchi, B. (2010). Predicting torsion-induced lateral displacements for pushover analysis: Influence of torsional system characteristics Earthquake Engineering and Structural Dynamics; DOI: 10.1002/eqe.1002.

De-La-Colina, J. (1999). Effects of torsion factors on simple non-linear systems using fully-bidirectional analyses. Earthquake Engineering and Structural Dynamics 1999; 28(7):691–706.

Esteva, L. (1987). Earthquake engineering research and practice in Mexico after the 1985 earthquake. Bulletin of the New Zealand National Society for Earthquake Engineering; 20: 159-200.

Foliente, G. C. (1995). Hysteresis modeling of wood joints and structural systems. Journal of Structural Engineering; 121(6):1013–1022.

Goda, K., Hong, H.P. and Lee, C.S. (2009). Probabilistic characteristics of seismic ductility demand of SDOF systems with Bouc-Wen hysteretic behavior. Journal of Earthquake Engineering; 13:600–622.

Goel, R. K. and Chopra, A. K. (1991). Inelastic seismic response of one-storey, asymmetric-plan systems: Effects of system parameters and yielding. Earthquake Engineering & Structural Dynamics;20(3): 201-222.

Hong, H. P. (2013). Torsional Responses under Bidirectional Seismic Excitations: Effect of Instantaneous Load Eccentricities. Journal of Structural engineering; 139(1): 133-143.

Hong, H. P., Goda, K. and Davenport, A. G. (2006). Seismic hazard analysis: a comparative study. Canadian J. Civil Eng; 33(9): 1156–1171.

Hong, H. P. and Hong, P. (2007). Assessment of ductility demand and reliability of bilinear single-degree-of-freedom systems under earthquake loading. Canadian J. Civil Eng; 34(12): 1606–1615.

Humar, J. L. and Kumar, P. (1998). Torsional motion of buildings during earthquakes II Inelastic response. Canadian Journal of Civil Engineering; 25(5)**:**917–934.

Lee, Chien-Shen. (2011). Inelastic seismic displacement demand of simplified equivalent nonlinear structural systems. Ph.D. diss., The University of Western Ontario(Canada).

Lee, C.S., and Hong, H.P. (2010). Inelastic Responses of Hysteretic Systems under Biaxial Seismic Excitations, Engineering Structures; Volume 32, Issue 8: 2074-2086.

Lucchini, A. Monti, G. and Kunnath, S. (2009). Seismic behavior of single-story asymmetric-plan buildings under uniaxial excitation. Earthquake Engineering and Structural Dynamics; 38:1053–1070

Ma, F., Zhang, H., Bockstedte, A., Foliente, G.C. and Paevere, P. (2004). Parameter analysis of the differential model of hysteresis. Transactions of the ASME, 71(3), 342–349.

Pacific Earthquake Engineering Research (PEER) (2006). Center Next Generation Attenuation database. http://peer.berkeley.edu/nga/index.html. (last accessed April 4th, 2006).

Paulay, T. (1997). Are existing seismic torsion provisions achieving the design aims? Earthquake spectra; 13(2):259–279.

Peruš I. and Fajfar P. (2005). On the inelastic torsional response of single-storey structures under bi-axial excitation. Earthquake Engineering and Structural Dynamics; 34(8):931–941.

Rutenberg A. (1998). AEE Task Group (TG) 8: behaviour and irregular and complex structures–progress since 1998. Proceedings of the 12th European conference on earthquake engineering, CD ROM. London; 2002.

Ryan, K.L. and Chopra, A.K. (2004). Estimation of seismic demands on isolators in asymmetric buildings using non-linear analysis. Earthquake Engineering and Structural Dynamics; 33(3):395–418.

Shampine, L. F. and Reichelt, M. W. (1997) The MATLAB ODE suite, SIAM J. Scientific Computing; 18(1), 1-22.

Tso, W.K. and Wong, C. M. (1995). Seismic displacements of torsionally unbalanced buildings. Earthquake Engineering and Structural Dynamics 1995; 24:1371–1387.

Tso, W.K. and Myslimaj, B. (2002). Effect of strength distribution on the inelastic torsional response of asymmetric structural systems. Proceedings of the 12th European Conference on Earthquake Engineering, Paper No. 081, London, U.K.

Wen Y.K. (1997). Method for random vibration of hysteretic systems. Journal of Engineering Mechanics; 102(2):249–263.

Table 2.1 Selected records from the NGA database (PEER, 2006)

Event ID	Earthquake name	Number of records	Record ID
25	Parkfield	2	28, 33
30	San Fernando	6	58, 59, 64, 81, 89, 94
50	Imperial Valley-06	2	164, 190
76	Coalinga-01	23	323, 327, 330, 335, 336, 339, 342, 344, 345, 346, 347, 350, 351, 352, 353, 354, 355, 356, 357, 358, 364, 366, 369
90	Morgan Hill	2	450,470
101	N. Palm Springs	1	531
118	Loma Prieta	29	731, 734, 735, 736, 739, 745, 747, 749, 750, 751, 762, 769, 771, 773, 776, 781, 782, 787, 788, 789, 791, 794, 795, 796, 797, 804, 807, 812, 813
123	Cape Mendocino	1	827
125	Landers	4	838, 887, 891, 897
127	Northridge-01	42	942, 945, 946, 957, 963, 965, 974, 980, 990, 991, 993, 994, 1005, 1007, 1008, 1011, 1015, 1017, 1019, 1020, 1021, 1022, 1023, 1026, 1027, 1028, 1029, 1030, 1031, 1033, 1038, 1039, 1041, 1046, 1047, 1053, 1057, 1065, 1070, 1074, 1079, 1091
158	Hector Mine	11	1763, 1767, 1768, 1786, 1794, 1795, 1812, 1824, 1831, 1832, 1836

Table 2.2 Statistics of R_X, R_Y, R_{XT} , R_{YT} , and max$(r\theta_T)$ for two-way symmetric systems considering A-Δ effect.

System and loading condition		Variable				
T_x, T_y, Ω, *PSA (g)*	Statistics	R_X	R_Y	R_{XT}	R_{YT}	max$(r\theta_T)$
Case 1	Mean	1.0000	1.0000	1.0008	1.0016	0.0004
	COV	0.0000	0.0000	0.0009	0.0018	1.1912
1.0, 1.0, 0.8, *0.25*	ρ_M	0.1233	0.1307	0.0708	-0.2013	0.1642
	ρ_D	0.0089	0.0696	0.0595	-0.1250	0.1363
	Maximum	1.0001	1.0001	1.0043	1.0080	0.0030
	Minimum	0.9999	0.9999	1.0000	1.0000	0.0000
Case 2	Mean	1.0000	1.0000	1.0008	1.0016	0.0004
	COV	0.0000	0.0000	0.0009	0.0019	1.1096
1.0, 1.0, 1.0, 0.25	ρ_M	0.0272	0.2414	0.0429	-0.2280	0.1560
	ρ_D	0.0426	0.1782	0.0091	-0.1196	0.1332
	Maximum	1.0001	1.0001	1.0041	1.0099	0.0025
	Minimum	0.9999	0.9999	1.0000	1.0000	0.0000
Case 3	Mean	1.0000	1.0000	1.0008	1.0017	0.0003
	COV	0.0000	0.0000	0.0008	0.0017	1.0275
1.0, 1.0, 1.25, 0.25	ρ_M	0.0770	0.2696	0.0521	-0.2171	0.1557
	ρ_D	-0.0090	0.1205	0.0277	-0.1814	0.1278
	Maximum	1.0001	1.0001	1.0037	1.0097	0.0017
	Minimum	0.9999	1.0000	1.0000	1.0000	0.0000
Case 4	Mean	1.0000	1.0000	1.0008	1.0016	0.0002
	COV	0.0000	0.0000	0.0008	0.0017	1.0069
1.0, 1.0, 1.6, 0.25	ρ_M	0.1764	0.1530	0.0982	-0.1451	0.1848
	ρ_D	0.0219	0.1406	0.0929	-0.1603	0.1307
	Maximum	1.0001	1.0001	1.0048	1.0095	0.0009
	Minimum	0.9999	0.9999	1.0000	1.0000	0.0000
Case 5	Mean	1.0000	1.0000	1.0007	1.0015	0.0001
	COV	0.0000	0.0000	0.0008	0.0016	1.0352
1.0, 1.0, 2.0, 0.25	ρ_M	0.0633	0.2574	0.1034	-0.0805	0.2024
	ρ_D	-0.1376	0.1759	0.1015	-0.1275	0.1454
	Maximum	1.0001	1.0001	1.0039	1.0085	0.0007
	Minimum	0.9999	0.9999	1.0000	1.0000	0.0000
Case 6	Mean	1.0000	1.0000	1.0014	1.0031	0.0014

1.0, 1.0, 1.0, 0.5	COV	0.0001	0.0001	0.0014	0.0034	1.0229
	ρ_M	0.1037	0.0151	-0.0781	-0.2666	0.1994
	ρ_D	0.0006	-0.0171	-0.0153	-0.1865	0.1422
	Maximum	1.0004	1.0005	1.0083	1.0200	0.0085
	Minimum	0.9997	0.9997	1.0000	1.0000	0.0002
Case 7	Mean	1.0000	1.0000	1.0012	1.0021	0.0021
2.0, 2.0, 1.0, 0.25	COV	0.0001	0.0001	0.0016	0.0021	1.1487
	ρ_M	0.1471	0.0535	0.3067	0.1077	0.4782
	ρ_D	0.0481	-0.0208	-0.0649	-0.0686	0.1707
	Maximum	1.0012	1.0006	1.0105	1.0157	0.0151
	Minimum	0.9998	0.9998	1.0000	1.0000	0.0001
Case 8	Mean	1.0000	1.0000	1.0018	1.0034	0.0059
2.0, 2.0, 1.0, 0.5	COV	0.0002	0.0002	0.0023	0.0033	1.1451
	ρ_M	0.2230	0.0651	0.2660	0.0691	0.5315
	ρ_D	0.0834	-0.0541	-0.0327	-0.1391	0.1402
	Maximum	1.0014	1.0013	1.0135	1.0174	0.0482
	Minimum	0.9997	0.9995	1.0000	0.9998	0.0003

Table 2.3 Statistics of R_X, R_Y, max($r\theta$), R_{XT} , R_{YT}, and max($r\theta_T$) for one-way asymmetric systems considering A-Δ effect.

System and loading condition		Variable					
T_X, T_Y, Ω, e_x, e_y, *PSA (g)*	Statistics	R_X	R_Y	max($r\theta$)	R_{XT}	R_{YT}	max($r\theta_T$)
Case 1	Mean	1.0000	0.9999	0.0099	0.9999	0.9999	0.0100
	COV	0.0007	0.0007	0.6867	0.0013	0.0024	0.6812
1.0, 1.0, 0.8,	ρ_M	-0.0700	0.0343	0.2562	-0.0860	0.0672	0.2545
0, 0.25y_1,	ρ_D	-0.0261	-0.0752	0.0770	0.0029	0.0298	0.0789
0.25	Maximum	1.0020	1.0029	0.0627	1.0038	1.0086	0.0614
	Minimum	0.9968	0.9959	0.0015	0.9955	0.9914	0.0015
Case 2	Mean	1.0001	1.0000	0.0127	1.0000	1.0000	0.0127
	COV	0.0008	0.0010	0.5976	0.0014	0.0024	0.5940
1.0, 1.0, 1.0,	ρ_M	-0.0068	-0.1229	0.2521	0.0314	-0.0551	0.2526
0, 0.25y_1,	ρ_D	0.0148	-0.1460	0.0009	-0.0245	0.0126	0.0011
0.25	Maximum	1.0028	1.0036	0.0672	1.0032	1.0104	0.0663
	Minimum	0.9959	0.9925	0.0019	0.9948	0.9920	0.0020
Case 3	Mean	1.0001	1.0000	0.0125	1.0000	1.0001	0.0126
	COV	0.0008	0.0010	0.5264	0.0012	0.0023	0.5256
1.0, 1.0, 1.25,	ρ_M	0.0133	-0.1637	0.2421	0.1437	-0.0787	0.2434
0, 0.25y_1	ρ_D	0.0283	-0.1387	0.0637	0.0899	-0.0435	0.0658
0.25	Maximum	1.0027	1.0042	0.0539	1.0039	1.0073	0.0534
	Minimum	0.9966	0.9932	0.0024	0.9957	0.9918	0.0024
Case 4	Mean	1.0001	0.9999	0.0105	1.0000	1.0002	0.0105
	COV	0.0007	0.0008	0.4956	0.0011	0.0021	0.4969
1.0, 1.0, 1.6,	ρ_M	0.0517	-0.1200	0.2303	0.0758	-0.0637	0.2326
0, 0.25y_1	ρ_D	0.0416	-0.0427	0.0988	0.0796	-0.0024	0.1031
0.25	Maximum	1.0030	1.0019	0.0376	1.0045	1.0083	0.0378
	Minimum	0.9965	0.9953	0.0028	0.9963	0.9922	0.0029
Case 5	Mean	1.0001	0.9999	0.0089	1.0001	1.0000	0.0089
	COV	0.0006	0.0007	0.5111	0.0012	0.0020	0.5140
1.0, 1.0, 2.0,	ρ_M	0.0704	-0.2466	0.3122	0.0251	-0.0146	0.3148
0, 0.25y_1	ρ_D	0.0490	-0.0565	0.2589	0.0975	0.1261	0.2634
0.25	Maximum	1.0027	1.0016	0.0299	1.0075	1.0069	0.0300
	Minimum	0.9973	0.9964	0.0038	0.9962	0.9925	0.0037
Case 6	Mean	1.0000	0.9998	0.0229	0.9998	1.0002	0.0229
	COV	0.0010	0.0023	0.9146	0.0023	0.0042	0.9133

1.0, 1.0, 1.0, 0, 0.25y_1 0.5	ρ_M	0.0343	-0.0663	0.3199	-0.0023	-0.0435	0.3226
	ρ_D	0.0616	-0.1262	0.1884	0.0145	-0.0778	0.1888
	Maximum	1.0043	1.0054	0.1552	1.0052	1.0158	0.1528
	Minimum	0.9950	0.9779	0.0042	0.9915	0.9866	0.0042
Case 7	Mean	1.0000	1.0000	0.0361	1.0001	1.0002	0.0363
	COV	0.0007	0.0011	1.1454	0.0019	0.0028	1.1324
2.0, 2.0, 1.0, 0, 0.25y_1 0.25	ρ_M	0.0733	-0.1434	0.4893	0.1176	0.1004	0.4948
	ρ_D	0.0062	-0.1348	0.3032	0.0691	0.0859	0.3034
	Maximum	1.0022	1.0046	0.2998	1.0065	1.0082	0.2884
	Minimum	0.9967	0.9912	0.0032	0.9949	0.9922	0.0031
Case 8	Mean	1.0000	0.9999	0.0707	1.0001	1.0005	0.0719
	COV	0.0009	0.0019	1.4284	0.0030	0.0050	1.3910
2.0, 2.0, 1.0, 0, 0.25y_1 0.5	ρ_M	-0.0245	-0.1155	0.4864	0.0559	-0.0023	0.4959
	ρ_D	-0.1000	-0.0680	0.3298	0.2195	0.1323	0.3245
	Maximum	1.0035	1.0072	0.6835	1.0084	1.0177	0.6464
	Minimum	0.9972	0.9824	0.0054	0.9896	0.9826	0.0058

Table 2.4 Statistics of R_X, R_Y, max($r\theta$), R_{XT}, R_{YT}, and max($r\theta_T$) for two-way asymmetric systems considering A-Δ effect.

System and loading condition		Variable					
T_x, T_y, Ω, e_x, e_y, PSA(g)	Statistics	R_X	R_Y	max($r\theta$)	R_{XT}	R_{YT}	max($r\theta_T$)
Case 1	Mean	1.0001	1.0000	0.0203	1.0000	1.0003	0.0203
1.0, 1.0, 0.8,	COV	0.0012	0.0014	0.8857	0.0015	0.0024	0.8825
0.25x_1,	ρ_M	-0.0947	-0.0617	0.2693	-0.1226	0.0310	0.2690
0.25y_1,	ρ_D	-0.1330	-0.1157	0.1668	-0.0020	0.0093	0.1671
0.25	Maximum	1.0040	1.0031	0.1249	1.0057	1.0078	0.1232
	Minimum	0.9927	0.9891	0.0036	0.9955	0.9912	0.0036
Case 2	Mean	1.0003	1.0000	0.0250	0.9998	1.0002	0.0250
1.0, 1.0, 1.0,	COV	0.0015	0.0017	0.7881	0.0018	0.0024	0.7869
0.25x_1,	ρ_M	-0.0436	-0.1113	0.2658	-0.1199	0.0622	0.2657
0.25y_1,	ρ_D	-0.0075	-0.1620	0.1451	0.0208	0.0164	0.1459
0.25	Maximum	1.0086	1.0037	0.1270	1.0065	1.0075	0.1269
	Minimum	0.9963	0.9854	0.0048	0.9888	0.9918	0.0048
Case 3	Mean	1.0001	1.0000	0.0248	0.9999	1.0001	0.0248
1.0,1.0, 1.25,	COV	0.0017	0.0015	0.7169	0.0017	0.0024	0.7157
0.25x_1,	ρ_M	0.0630	-0.0975	0.2777	-0.0574	-0.0397	0.2772
0.25y_1,	ρ_D	0.1146	-0.1047	0.1685	0.0174	0.0299	0.1684
0.25	Maximum	1.0072	1.0030	0.1167	1.0066	1.0086	0.1159
	Minimum	0.9893	0.9887	0.0055	0.9927	0.9904	0.0055
Case 4	Mean	0.9997	1.0000	0.0223	1.0000	1.0000	0.0223
1.0, 1.0, 1.6,	COV	0.0019	0.0013	0.6696	0.0016	0.0020	0.6701
0.25x_1,	ρ_M	-0.0470	-0.0437	0.2815	-0.0403	0.1784	0.2810
0.25y_1,	ρ_D	0.0227	-0.0442	0.2380	-0.0534	0.1495	0.2388
0.25	Maximum	1.0045	1.0042	0.0975	1.0079	1.0071	0.0972
	Minimum	0.9874	0.9914	0.0053	0.9937	0.9947	0.0053
Case 5	Mean	0.9999	0.9999	0.0196	1.0000	1.0000	0.0196
1.0, 1.0, 2.0,	COV	0.0013	0.0010	0.6779	0.0017	0.0019	0.6792
0.25x_1,	ρ_M	-0.0916	-0.0631	0.2280	0.0057	0.1272	0.2285
0.25y_1,	ρ_D	0.0191	-0.1715	0.1856	0.0915	0.1600	0.1862
0.25	Maximum	1.0036	1.0026	0.0777	1.0077	1.0055	0.0778
	Minimum	0.9947	0.9936	0.0031	0.9951	0.9951	0.0031
Case 6	Mean	1.0003	0.9997	0.0459	1.0002	1.0006	0.0460
1.0, 1.0, 1.0,	COV	0.0020	0.0041	1.0658	0.0028	0.0048	1.0639

$0.25x_1$,	ρ_M	0.1331	-0.0667	0.3531	-0.0816	-0.0359	0.3500
$0.25y_1$,	ρ_D	0.1204	-0.1237	0.2300	0.0091	-0.0220	0.2280
0.5	Maximum	1.0127	1.0165	0.3036	1.0093	1.0170	0.2985
	Minimum	0.9922	0.9636	0.0095	0.9882	0.9847	0.0096
Case 7	Mean	0.9998	0.9998	0.0701	0.9997	1.0002	0.0707
2.0, 2.0, 1.0,	COV	0.0023	0.0017	1.3495	0.0028	0.0040	1.3555
$0.25x_1$,	ρ_M	-0.0574	-0.1591	0.4091	0.0182	0.1643	0.4111
$0.25y_1$,	ρ_D	0.0823	-0.1616	0.3200	0.0286	0.2066	0.3201
0.25	Maximum	1.0196	1.0048	0.7576	1.0145	1.0250	0.7676
	Minimum	0.9923	0.9905	0.0094	0.9863	0.9914	0.0095
Case 8	Mean	1.0001	1.0001	0.1380	1.0001	1.0014	0.1393
2.0, 2.0, 1.0,	COV	0.0020	0.0020	1.6755	0.0048	0.0074	1.6621
$0.25x_1$,	ρ_M	0.0317	0.0403	0.4112	-0.0311	0.1686	0.4141
$0.25y_1$,	ρ_D	0.0189	-0.1342	0.3608	-0.0592	0.2178	0.3596
0.5	Maximum	1.0127	1.0088	1.6875	1.0257	1.0494	1.6921
	Minimum	0.9921	0.9938	0.0113	0.9709	0.9832	0.0114

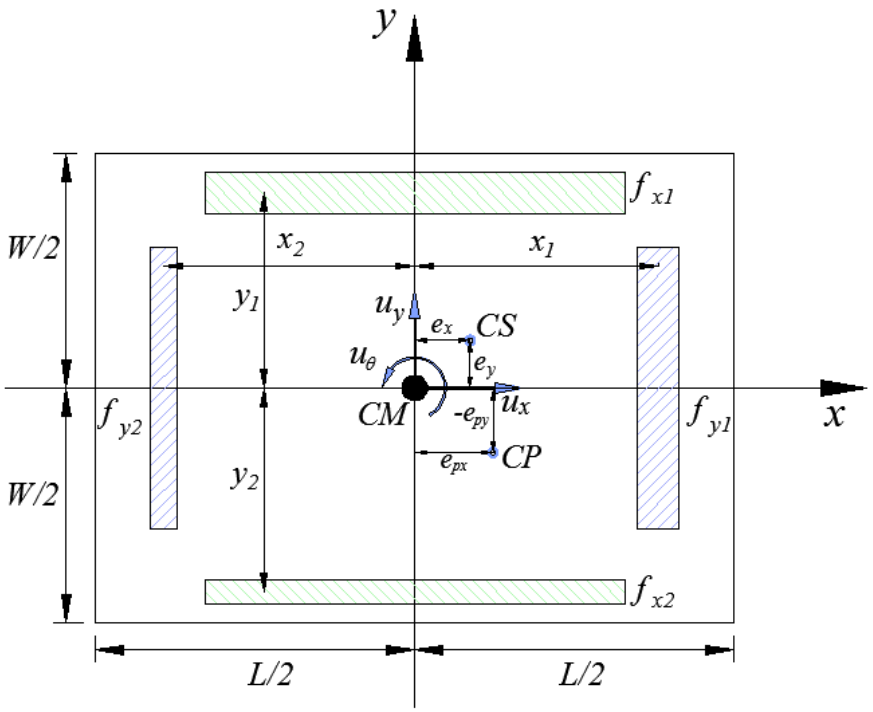

Figure 2.1 Schematic plan view of the idealized one-story building.

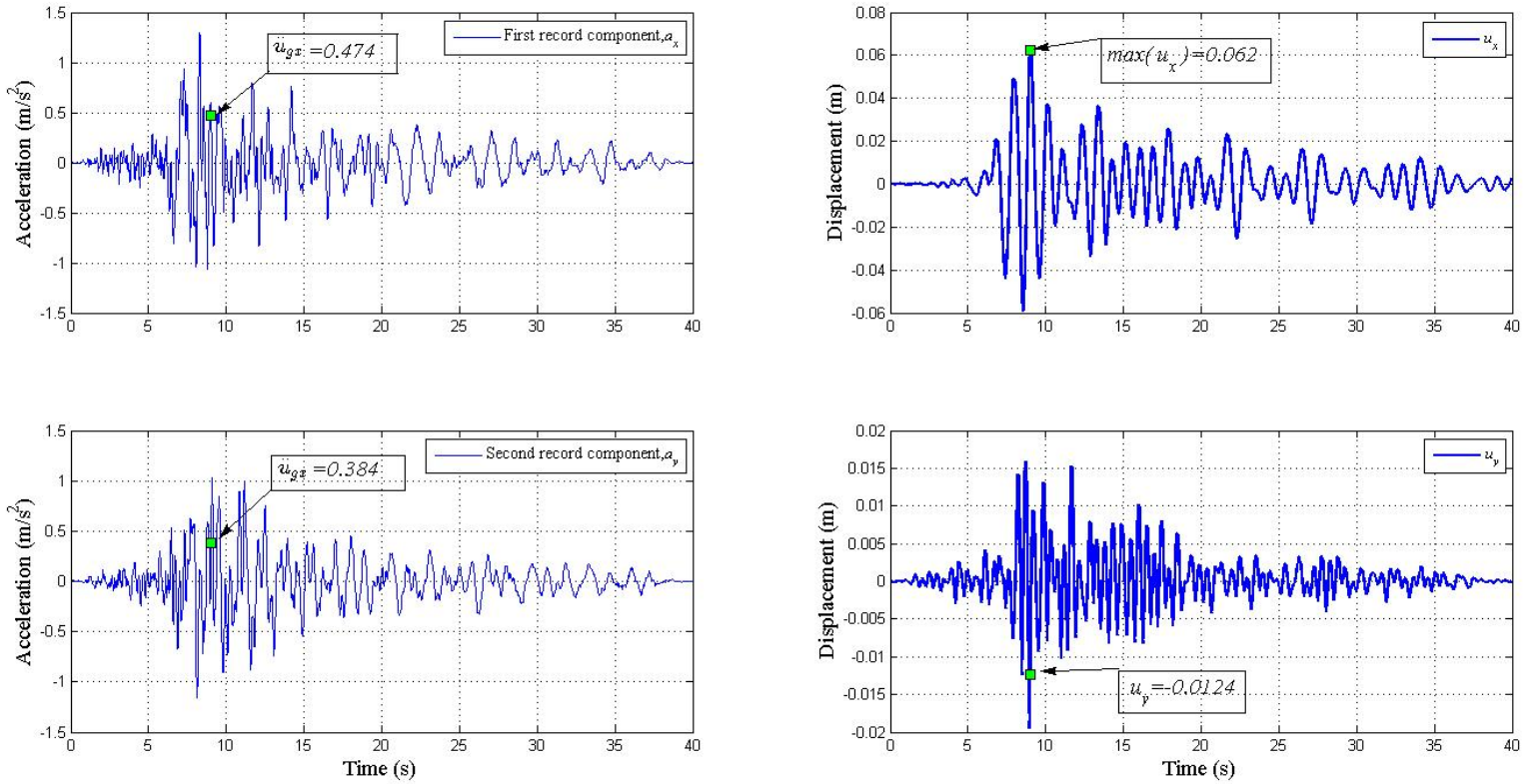

Figure 2.2 Components of an arbitrarily selected record (COALINGA 05/02/83, PARKFIELD - GOLD HILL) scaled by the same factor such that the PSA at *Tx* = 1.0 (s) -(for the first record component) equals 0.25 (g), and linear elastic responses of two-way symmetric system

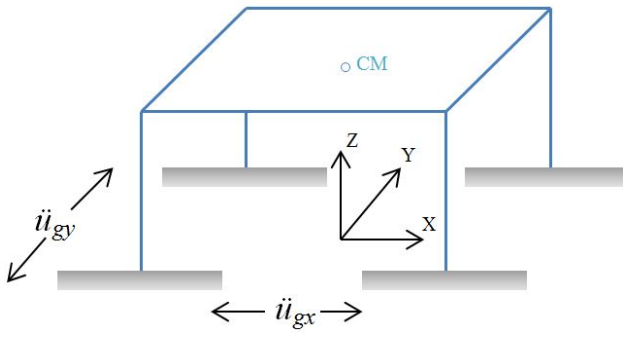

(a) Three-dimensional structure under seismic excitations

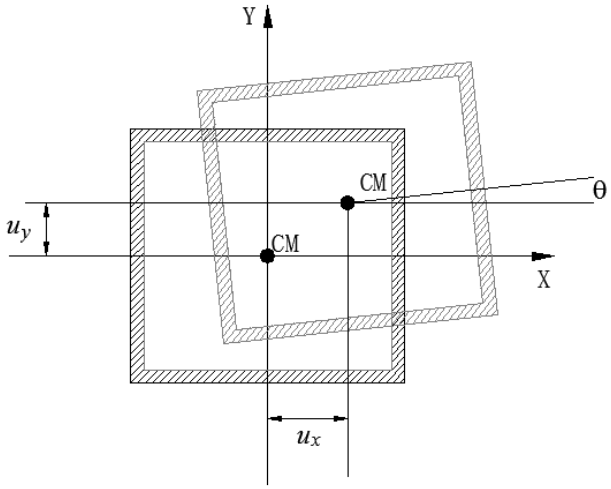

(b) Plan view

Figure 2.3 Illustration of the lateral load resisting elements by assuming all the elements are located at the edges of the slab.

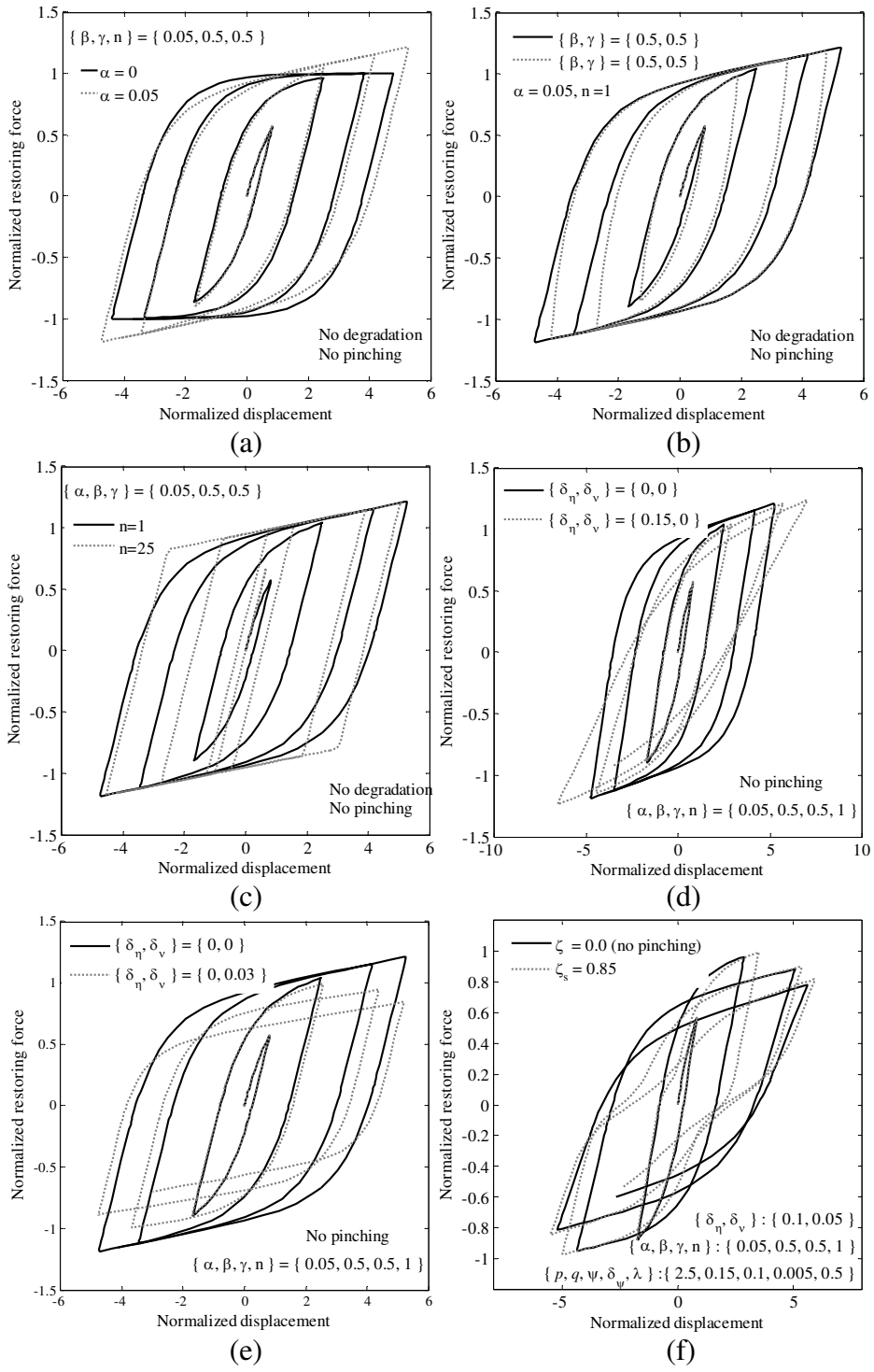

Figure 2.4 Effect of Bouc-Wen model parameters on hysteresis loop of inelastic SDOF system

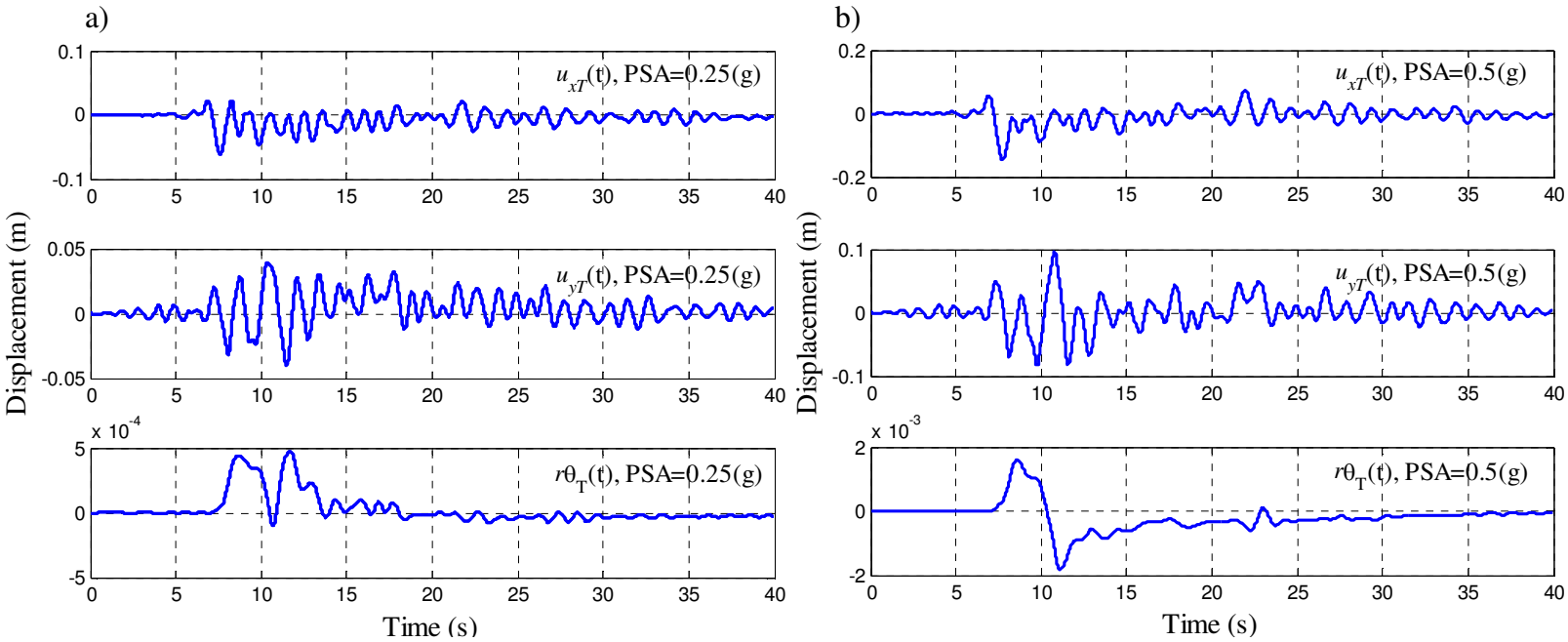

Figure 2.5 Responses of two-way symmetric system considering the *A*-Δ effect: a) Responses for the record components that are scaled by the same factor such that the PSA at T_x = 1.0 (s) equal to 0.25 (g), b) Responses for the record components that are scaled by the same factor such that the PSA at T_x = 1.0 (s) equal to 0.5 (g).

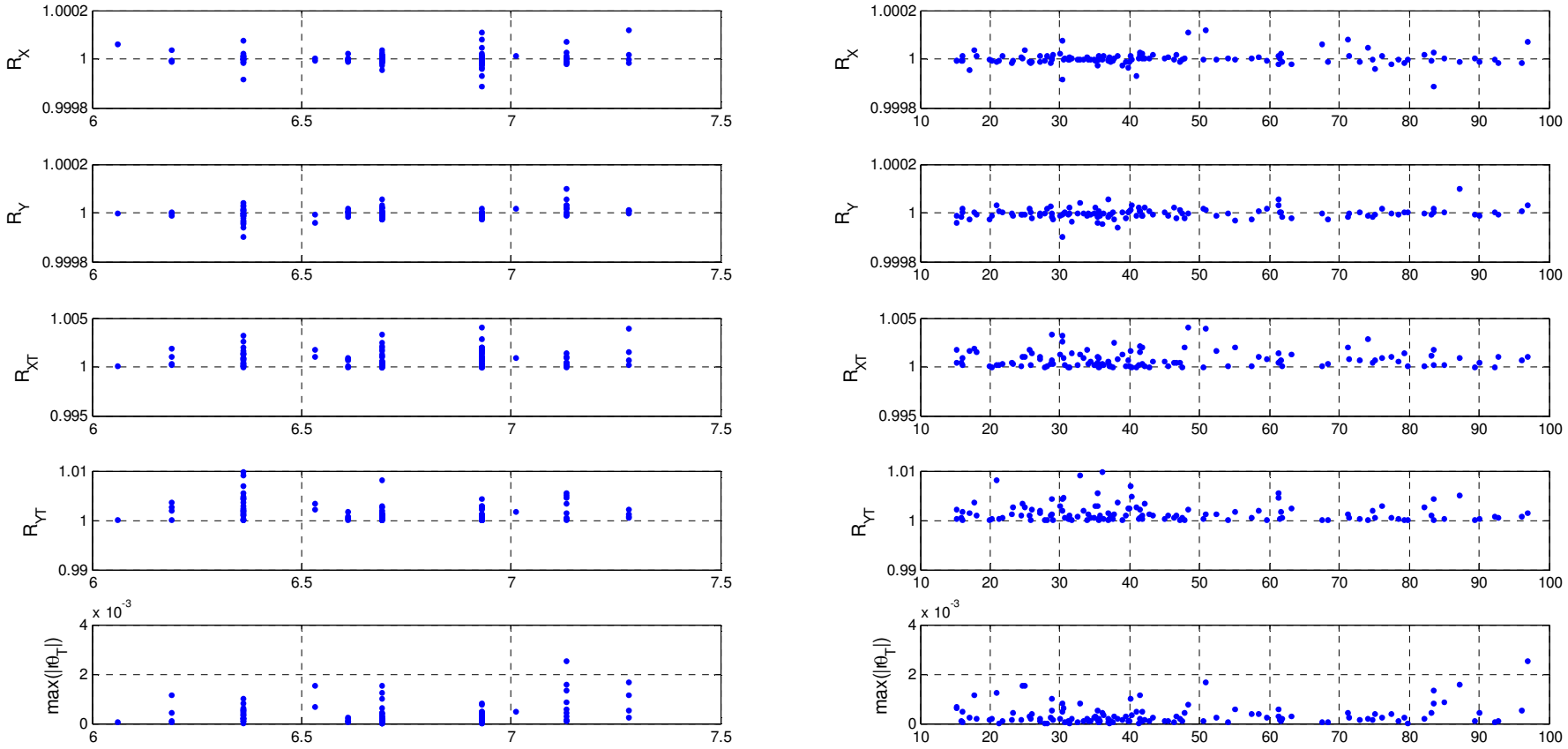

Figure 2.6 Samples of ratios and rotational response versus magnitude and site-to-source distance for the second two-way symmetric system shown in Table 2.2

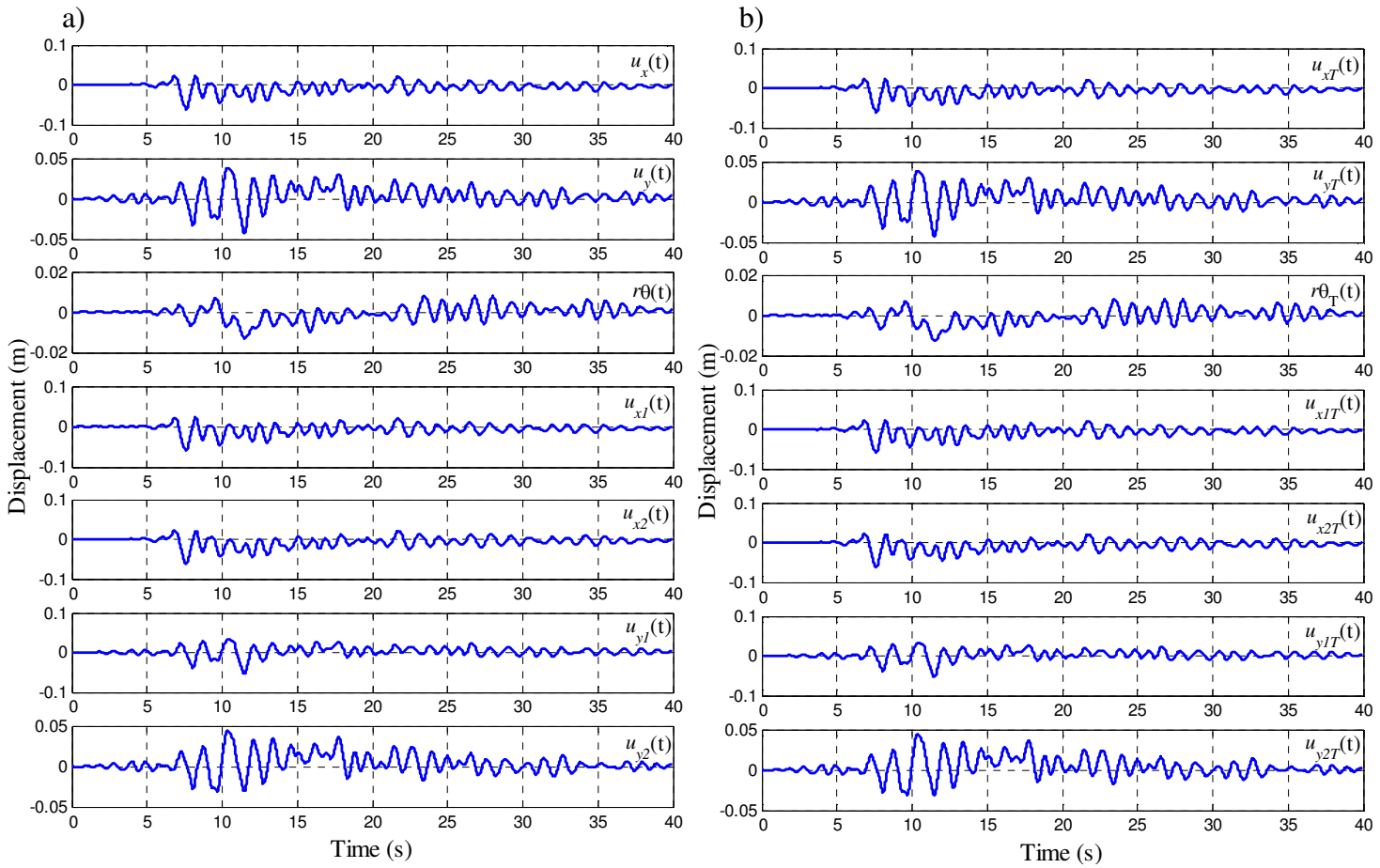

Figure 2.7 Responses by ignoring and considering the *A*-Δ effect for the second one-way asymmetric system listed in Table 2.3 and the scaled record shown in Figure 2.2: a) Responses without considering the *A*-Δ effect, b) Responses considering the *A*-Δ effect.

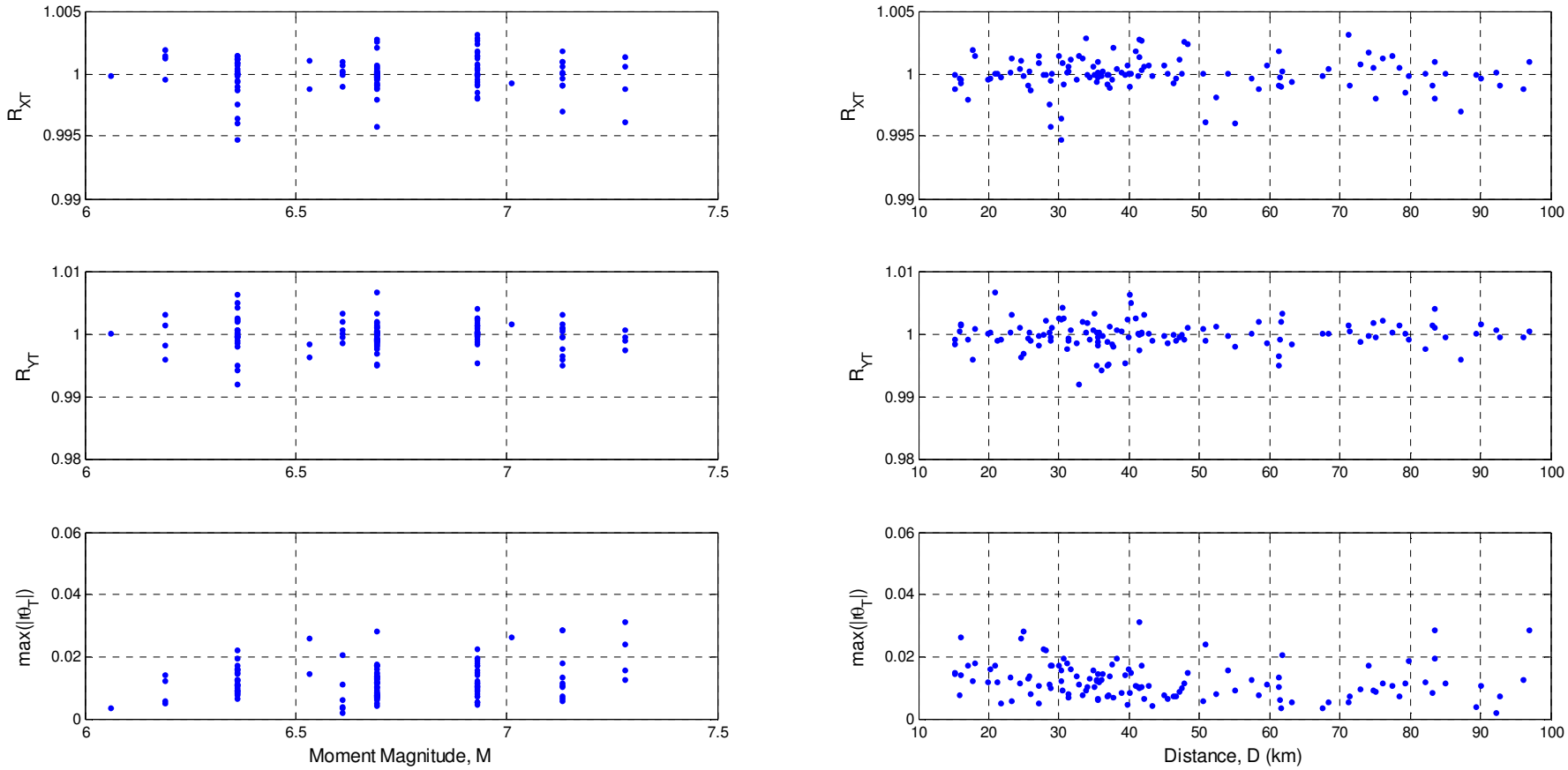

Figure 2.8 Samples of ratios and rotational response versus magnitude and site-to-source distance for the second one-way symmetric system shown in Table 2.3

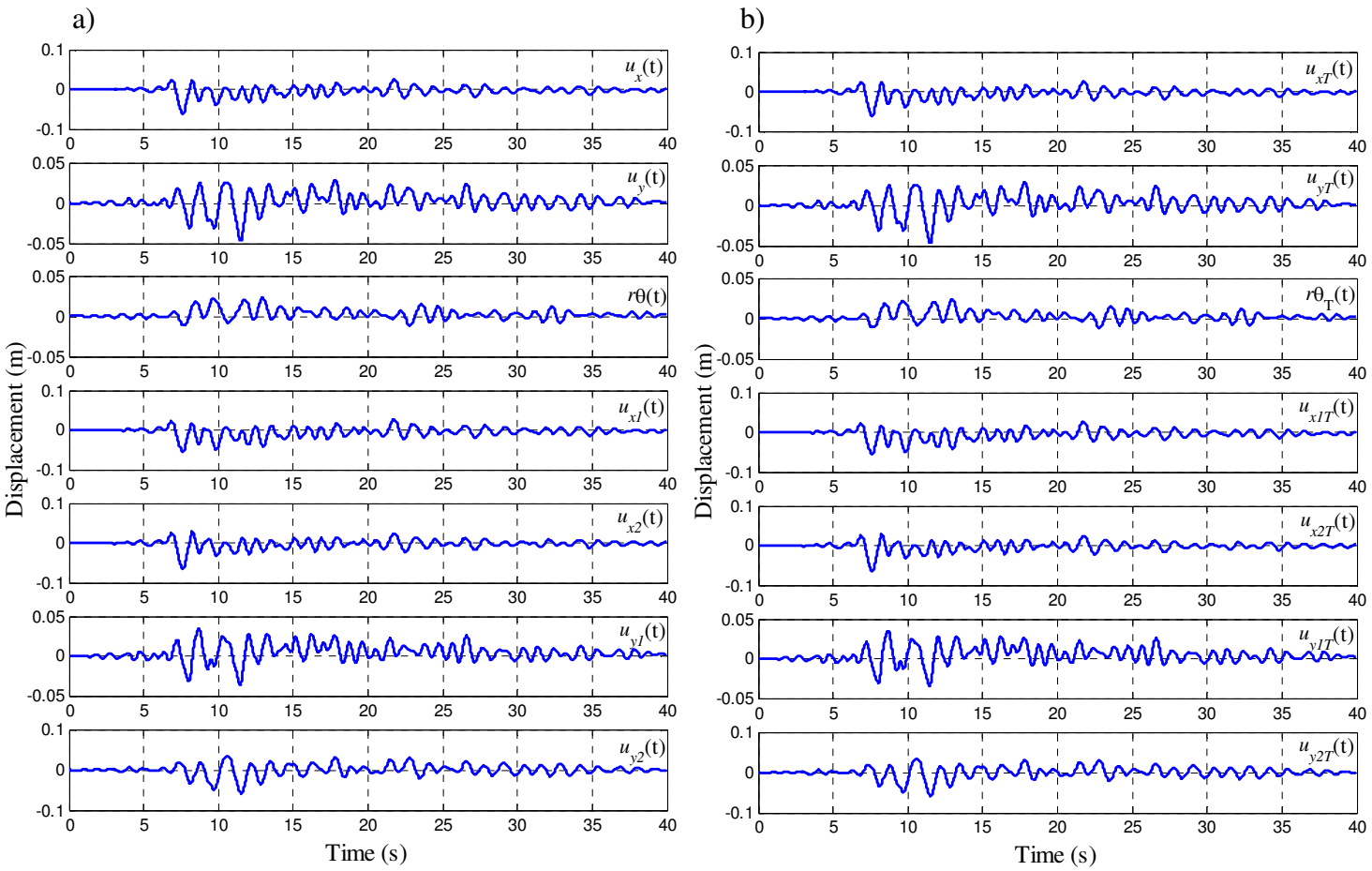

Figure 2.9 Responses by ignoring and considering the *A*-Δ effect for the second two-way asymmetric system listed in Table 2.4 and the scaled record shown in Figure 2.3: a) Responses without considering the *A*-Δ effect, b) Responses considering the *A*-Δ effect.

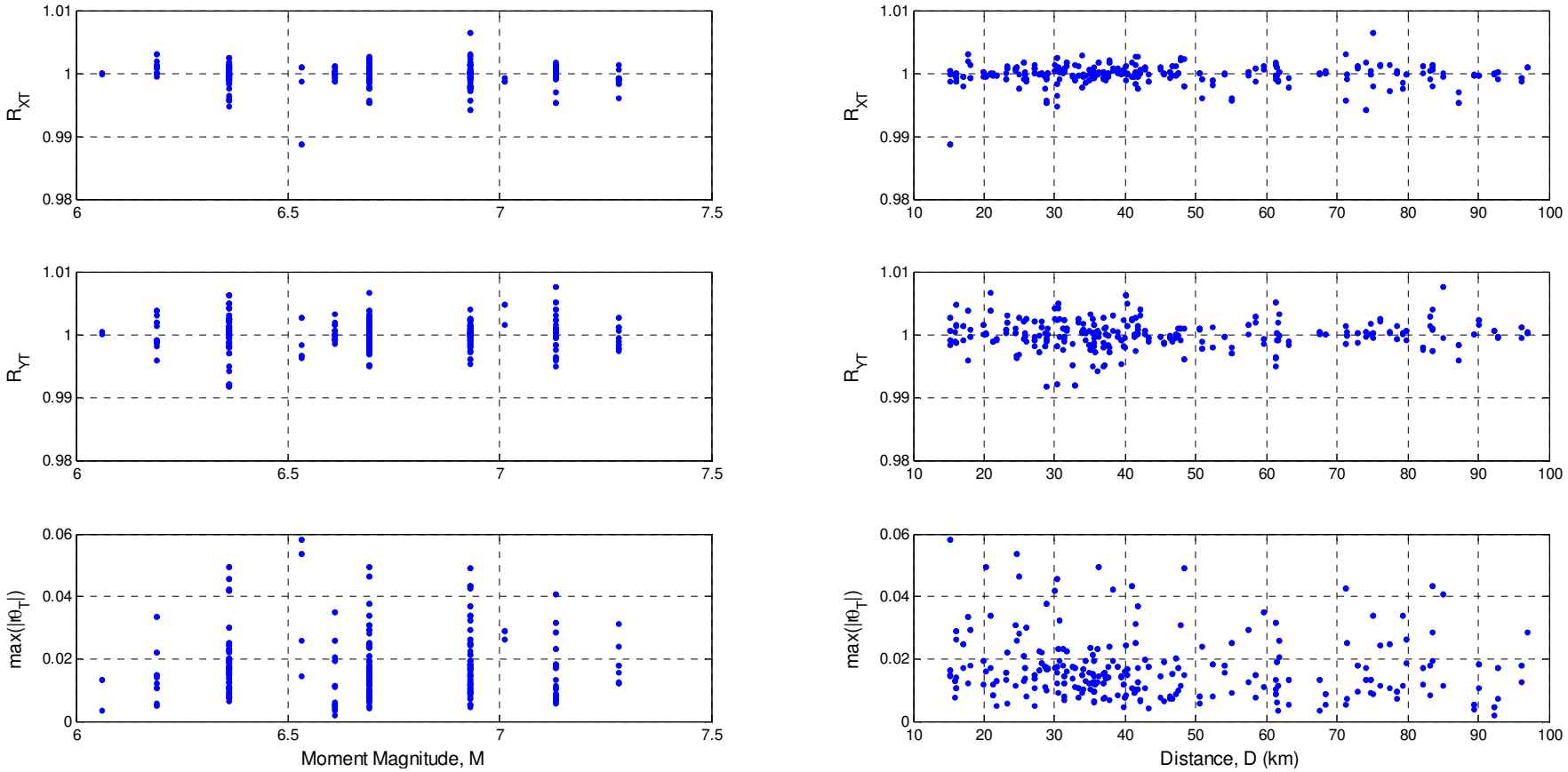

Figure 2.10 Samples of ratios and rotational response versus magnitude and site-to-source distance for the second asymmetric system shown in Table 2.4.

CHAPTER 3. INEALSTIC TORSIONAL RESPONSE WITH *P*-Δ AND INSTANTANOUS LOAD ECCENTRICITIES EFFECT

3.1 Introduction

Field observations of earthquake damage have shown that many building failures during earthquakes are associated with torsional load effects (Esteva 1987). However, because the linear and nonlinear torsional responses are controlled by many parameters, literature reviews indicate (Rutenberg 2002; De Stefano and Pintucchi 2008) that conclusions from various research and investigations are not consistent.

The torsional responses can be induced when the center of stiffness (CS) and center of strength (CP) does not coincide with the center of mass (CM). Even for two-way symmetric structures, torsion could occur because the so called accidental load eccentricity and accidental torsional motion. The accidental torsional motion is mainly attributed to two factors: the first one is symmetric-plan structure is usually not perfectly symmetric due to uncertainty in the physical property (e.g. modulus of elasticity) of the structure and/or the inaccuracy in the geometry of the structural member as compared to the design dimension; the other factor is ground rotational motion about the vertical axis (Chopra 2001). Furthermore, torsional responses could also occur because the instantaneous load eccentricity discussed in Hong (2013). This instantaneous load eccentricity is due to that the CM moves with respect to its original position or to the supports or the CS when a structure responds to seismic ground motions. This motion results in the instantaneous load eccentricities under

seismic horizontal excitations, thereby cause additional torsional load effect. This is a second-order effect was termed A-Δ effect (Hong 2013).

Another second-order effect, which has significant implication in structural design, is known as *P*-Δ effect. This *P*-Δ effect basically described the increased overturning moment caused by the action of vertical loads acting through structural lateral deformations. The *P*-Δ effect decreases the capacity of buildings to resist the seismic loading and could cause structural instability. For parametric investigation, simple one-story and multi-story models represented by simplified single- and/or multi-degree-of-freedom (SDOF and/or MDOF) systems have been widely used to evaluate the *P*-Δ effect by several studies, including those given by Bernal (1987), MacRae (1994), Tremblay et al. (1999), Gupta and Krawinkler (2000), Vian and Bruneau (2003). Bernal (1987) suggested that amplification factors could be used to take into account the *P*-Δ effect in elastic and inelastic systems. MacRae (1994) used the concept "hysteresis center curve" (HCC) (MacRea and Kawashima 1993) in dealing with *P*-Δ effect for assessing the structural instability, and concluded that the *P*-Δ effect decreases both elastic and inelastic stiffness of structures. Tremblay et al. (1999) investigated the use of three different amplification factors accounting for *P*-Δ effect for multistory structures under earthquake excitations, typical of eastern and western Canada. By analyzing a 20-storey steel moment resisting frame (MRF), they concluded that the increased strength could result in the ductility demand within the level computed without *P*-Δ effect, but the lateral displacements in the structure using the approximate methods were generally larger than those obtained by neglecting the action of gravity loads. In Gupta and Krawinkler (2000), various structural models including 3-, 9- and 20-story frame structures located in Seattle and Los Angles were

investigated by considering P-Δ effects. They concluded that when accounting for large P-Δ effects, the seismic responses become sensitive to modeling assumptions and ground motion characteristics; furthermore, they indicated that the elastic analysis cannot be used to replicate P-Δ effects on the inelastic system response. Vian and Bruneau (2003) examined the P-Δ effect using shaking table test results, confirming that the stability factor is the most important factor for the structural stability and collapse. Furthermore, analysis results presented by Tremblay et al. (1999), Gupta and Krawinkler (2000), and Humar et al. (2006) indicate that an increase in strength or stiffness, according to some of the suggested methods to compensate the P-Δ effect, does not ensure the structural stability. The conclusions from these studies indicate that there is no commonly accepted simple approximate method to estimate P-Δ effect considering seismic excitations and nonlinear inelastic responses.

As the consideration of the A-Δ effect for seismic responses is a relatively new adventure, its effect together with the P-Δ effect in bui1dings subjected to earthquakes are unknown and should be investigated. The assessment of the statistical characterizations of the inelastic torsional behavior under bidirectional seismic excitations by considering the A-Δ and/or P-Δ effects forms the main objective of this Chapter. For the assessment, two-way symmetric, one-way and two-way asymmetric single-story systems with different lateral uncoupled frequency ratio, stability factor, and load eccentricities are considered. Since the ground motions are stochastic, the uncertainty due to record-to-record variability on the inelastic torsional responses is investigated by using a set of 123 California records from 11 seismic events selected from the Next Generation Attenuation Database (PEER Center, 2006).

3.2 Single-story model and solution procedure

Consider the idealized one-story building shown in Figure 3.1. The system has a rigid horizontal slab with uniformly distributed mass. The lateral load resisting elements (frames or walls) are denoted as A, B, C and D. The elements B and C are oriented and only resist force in the x-direction, while the elements A and D are oriented and only resist force in the y-direction. The distances from the CM to the elements (A, D and B, C) denoted by x_i and y_i, and the center of the stiffness (CS) located at (e_x, e_y) are also shown in the figure.

By using u_x, u_y and θ denoting the displacement along *X*-axis, displacement along *Y*-axis and rotation of the rigid slab with respect to the CM, the equations of motion (see Appendix A) of the considered system with *P*-Δ effect, can be rewritten as:

$$m\ddot{u}_x + c_x\dot{u}_x + \sum f_{xi} = -m\ddot{u}_{gx} - m\ddot{u}_{gv}\,u_x/h + mg\,u_x/h \tag{3.1a}$$

$$m\ddot{u}_y + c_y\dot{u}_y + \sum f_{yi} = -m\ddot{u}_{gy} - m\ddot{u}_{gv}\,u_y/h + mg\,u_y/h \tag{3.1b}$$

$$mr^2\ddot{\theta} + c_\theta\dot{\theta} + \sum(-f_{xi}\,y_i + f_{yi}x_i) = 0 \tag{3.1c}$$

where *m* is the mass; *r* is the radius of gyration of the slab about the CM; *c* denotes the damping coefficient; *f* denotes the resisting force of the elements, an overdot on a variable denotes its temporal derivative, the summation Σ is over applicable lateral load resisting elements; *h* is the height of the structure. Symbols *c* and $\ddot{u}_g$ with an additional subscript *x* and *y* are used to denote the quantities associated with the *X*-axis and *Y*-axis, respectively; while $\ddot{u}_{gv}$ represents the vertical ground accelerations.

$mg\,u_x/h$ and $mg\,u_y/h$ stand for the *P*-Δ effect induced by the gravity load, while $m\ddot{u}_{gv}\,u_x/h$ and $m\ddot{u}_{gv}\,u_y/h$ represent that induced by vertical seismic excitation.

By incorporating the Rayleigh damping and considering that the damping ratio, ζ, for the two translational modes is the same (and assumed to be equal to 5% throughout the study.), the equation of motion with *P*-Δ effect can be expressed as:

$$\ddot{u}_x+\left(a_0+a_1\omega_x^2\right)\dot{u}_x-a_1\omega_x^2\frac{e_y}{r}\dot{u}_\theta+\alpha_x\omega_{x1}^2\left(u_x-\frac{y_1}{r}u_\theta\right)+\left(1-\alpha_x\right)\omega_{x1}^2z_{x1}+\alpha_x\omega_{x2}^2\left(u_x-\frac{y_2}{r}u_\theta\right)+\left(1-\alpha_x\right)\omega_{x2}^2z_{x2}=-\ddot{u}_{gx}-\ddot{u}_{gv}u_x/h+\ddot{u}_{gv}g/h \tag{3.2a}$$

$$\ddot{u}_y+\left(a_0+a_1\omega_y^2\right)\dot{u}_y+a_1\omega_y^2\frac{e_x}{r}\dot{u}_\theta+\alpha_y\omega_{y1}^2\left(u_y+\frac{x_1}{r}u_\theta\right)+\left(1-\alpha_y\right)\omega_{y1}^2z_{y1}+\alpha_y\omega_{y2}^2\left(u_y+\frac{x_2}{r}u_\theta\right)+\left(1-\alpha_y\right)\omega_{y2}^2z_{y2}=-\ddot{u}_{gy}-\ddot{u}_{gv}u_y/h+\ddot{u}_{gv}g/h \tag{3.2b}$$

$$\ddot{u}_\theta+\left(a_0+a_1\omega_\theta^2\right)\dot{u}_\theta-a_1\omega_x^2\frac{e_y}{r}\dot{u}_x+a_1\omega_y^2\frac{e_x}{r}\dot{u}_y+\frac{y_1}{r}\left[-\alpha_x\omega_{x1}^2\left(u_x-\frac{y_1}{r}u_\theta\right)-\left(1-\alpha_x\right)\omega_{x1}^2z_{x1}\right]+\frac{y_2}{r}\left[-\alpha_x\omega_{x2}^2\left(u_x-\frac{y_2}{r}u_\theta\right)-\left(1-\alpha_x\right)\omega_{x2}^2z_{x2}\right]+\frac{x_1}{r}\left[\alpha_y\omega_{y1}^2\left(u_y+\frac{x_1}{r}u_\theta\right)+\left(1-\alpha_y\right)\omega_{y1}^2z_{y1}\right]+\frac{x_2}{r}\left[\alpha_y\omega_{y2}^2\left(u_y+\frac{x_2}{r}u_\theta\right)+\left(1-\alpha_y\right)\omega_{y2}^2z_{y2}\right]=0 \tag{3.2c}$$

where $\omega_x=\sqrt{\omega_{x1}^2+\omega_{x2}^2}$, $\omega_y=\sqrt{\omega_{y1}^2+\omega_{y2}^2}$ and $\omega_\theta=\sqrt{\sum\omega_{xi}^2\left(y_i/r\right)^2+\sum\omega_{yi}^2\left(x_i/r\right)^2}$ represent the vibration frequency along the *X*-axis, *Y*-axis, and the rotational vibration frequency, respectively□ in which ω_{xi} and ω_{yi} are the vibration frequencies of *i*-th resisting element oriented along the *X*- and *Y*-direction; $u_\theta = r\theta$; α_x and α_y are the ratio of the post-yield to initial stiffness along the *X*- and *Y*-axis;

$a_0 = 2\zeta\omega_x\omega_y/(\omega_x+\omega_y); a_1 = 2\zeta/(\omega_x+\omega_y)$; z_{xi} and z_{yi} are the hysteretic displacement for each element governed by the Bouc-Wen hysteretic model (see Appendix B).

Since the CM moves with respect to its original position or to the supports or the CS when a structure responds to seismic ground motions (see Figure 3.2), this resulted in the instantaneous load eccentricities under seismic horizontal excitations that are functions of the time-varying relative position of the instantaneous CM (Hong 2013). By taking into account this second order effect, which was termed *A*-Δ effect, Eq. (3.1c) becomes,

$$mr^2\ddot{\theta} + c_\theta\dot{\theta} + \sum\left(-f_{xi}\left(y_i - u_y\right) + f_{yi}\left(x_i - u_x\right)\right) = 0 \tag{3.3}$$

and the displacement of the *i*-th element placed parallel *X*- and *Y*-axis (u_{xi} and u_{yi}) becomes

$$u_{xiT}(t) = u_{xT}(t) - \left(y_i - u_{yT}(t)\right)\theta_T(t) \tag{3.4a}$$

and

$$u_{yiT}(t) = u_{yT}(t) + \left(x_i - u_{xT}(t)\right)\theta_T(t) \tag{3.4b}$$

where the symbols $u_x(t), u_y(t), u_{xi}(t), u_{yi}(t),$ and $\theta(t)$ with an additional subscript T (i.e., $u_{xT}(t), u_{yT}(t), u_{xiT}(t), u_{yiT}(t),$ and $\theta_T(t)$) are used to emphasize that these quantities referred to those when both the *A*-Δ and *P*-Δ effects are considered. This resulted in the (time-dependent) stiffness matrix **K** (by considering *A*-Δ effect) becomes (Hong 2013),

$$\mathbf{K}=\begin{bmatrix} K_{XX} & 0 & K_{\theta X}+K_{XX}u_{yT} \\ 0 & K_{YY} & K_{\theta Y}-K_{YY}u_{xT} \\ K_{\theta X}+K_{XX}u_{yT} & K_{\theta Y}-K_{YY}u_{xT} & K_{\theta\theta}+2K_{\theta X}u_{yT}-2K_{\theta Y}u_{xT}+K_{XX}u_{yT}^2+K_{YY}u_{xT}^2 \end{bmatrix} \quad (3.5)$$

where K_{XX}, K_{YY}, $K_{\theta\theta}$, $K_{\theta X}$ and $K_{\theta Y}$ denote the elements of the stiffness matrix **K;** and **K** is time-dependent since u_{xT} and u_{yT} vary in time. In other words, the *A*-Δ effect affects the stiffness that couples the translational and rotational displacements. Based on these considerations, the displacements under bidirectional seismic excitations accounting for *A*-Δ and *P*-Δ effects are governed by

$$\ddot{u}_{xT}+\left(a_0+a_1\omega_x^2\right)\dot{u}_{xT}-a_1\omega_x^2\frac{e_y}{r}\dot{u}_{\theta T}+\alpha_x\omega_{x1}^2\left[u_{xT}-\frac{\left(y_1-u_{yT}\right)}{r}u_{\theta T}\right]+\left(1-\alpha_x\right)\omega_{x1}^2 z_{x1}+$$
$$\alpha_x\omega_{x2}^2\left[u_{xT}-\frac{\left(y_2-u_{yT}\right)}{r}u_{\theta T}\right]+\left(1-\alpha_x\right)\omega_{x2}^2 z_{x2}=-\ddot{u}_{gx}-\ddot{u}_{gv}u_{xT}/h+\ddot{u}_{gv}g/h \quad (3.6a)$$

$$\ddot{u}_{yT}+\left(a_0+a_1\omega_y^2\right)\dot{u}_{yT}+a_1\omega_y^2\frac{e_x}{r}\dot{u}_{\theta T}+\alpha_y\omega_{y1}^2\left[u_{yT}+\frac{\left(x_1-u_{xT}\right)}{r}u_{\theta T}\right]+\left(1-\alpha_y\right)\omega_{y1}^2 z_{y1}+$$
$$\alpha_y\omega_{y2}^2\left[u_{yT}+\frac{\left(x_2-u_{xT}\right)}{r}u_{\theta T}\right]+\left(1-\alpha_y\right)\omega_{y2}^2 z_{y2}=-\ddot{u}_{gy}-\ddot{u}_{gv}u_{yT}/h+\ddot{u}_{gv}g/h \quad (3.6b)$$

$$\ddot{u}_{\theta T}+\left(a_0+a_1\omega_\theta^2\right)\dot{u}_{\theta T}-a_1\omega_x^2\frac{e_y}{r}\dot{u}_{xT}+a_1\omega_y^2\frac{e_x}{r}\dot{u}_{yT}+$$
$$\frac{\left(y_1-u_{yT}\right)}{r}\left[-\alpha_x\omega_{x1}^2\left(u_{xT}-\frac{\left(y_1-u_{yT}\right)}{r}u_{\theta T}\right)-\left(1-\alpha_x\right)\omega_{x1}^2 z_{x1}\right]+$$
$$\frac{\left(y_2-u_{yT}\right)}{r}\left[-\alpha_x\omega_{x2}^2\left(u_{xT}-\frac{\left(y_2-u_{yT}\right)}{r}u_{\theta T}\right)-\left(1-\alpha_x\right)\omega_{x2}^2 z_{x2}\right]+ \quad (3.6c)$$
$$\frac{\left(x_1-u_{xT}\right)}{r}\left[\alpha_y\omega_{y1}^2\left(u_{yT}+\frac{\left(x_1-u_{xT}\right)}{r}u_{\theta T}\right)+\left(1-\alpha_y\right)\omega_{y1}^2 z_{y1}\right]+$$
$$\frac{\left(x_1-u_{xT}\right)}{r}\left[\alpha_y\omega_{y2}^2\left(u_{yT}+\frac{\left(x_2-u_{xT}\right)}{r}u_{\theta T}\right)+\left(1-\alpha_y\right)\omega_{y2}^2 z_{y2}\right]=0$$

To simplify the parametric study of inelastic system, rather than estimating the displacement responses, the normalized displacements defined by,

$$\mu_x = \frac{u_{xT}}{\Delta_x},\ \tilde{\mu}_y = \frac{u_{yT}}{\Delta_x},\ \mu_\theta = \frac{u_{\theta T}}{\Delta_x},\ \mu_{zxi} = \frac{z_{xi}}{\Delta_{xi}},\ \mu_{zyi} = \frac{z_{yi}}{\Delta_{yi}} \tag{3.7}$$

are used, where Δ_{xi} and Δ_{yi} are the yield displacements of the *i*-th element parallel to the *X*- and *Y*-axis, respectively; $\Delta_x = \min(\Delta_{xi})$ denotes the initial yield displacement (capacity) of the structure along *X*-axis; the normalized displacements μ_x and μ_y ($u_y = \tilde{\mu}_y \Delta_{x/y}$ and $\Delta_{x/y} = \Delta_x / \Delta_y$) represent the ductility demands of CM along the *X*- and *Y*-axis, while μ_{xi} (or μ_{yi}) represents the ductility demand for the *i*-th lateral load resisting element.

The formulation above shows that the responses of the system are characterized by ω_x, ω_y, Ω_θ, the eccentricity ratios e_x/r and e_y/r. The normalized responses (see Eq.(3.7)) are expressed as fractions of Δ_{xi}, Δ_{yi}, Δ_x and Δ_y, and Δ_x / r value defined according to the physical property of the structure. To facilitate parametric studies of the responses of the system described above, the normalized yield strength ϕ_x and ϕ_y are introduced, which are defined by (Chopra 2001),

$$\phi_x = \Delta_x / d_{0x} \text{ and } \phi_y = \Delta_y / d_{0y} \tag{3.8}$$

where d_{0x} and d_{0y} are the peak linear elastic displacement responses along the *X*-axis and *Y*-axis. d_{0x} equals $S_x/(\omega_x)^2$, where S_x is the pseudo-spectral acceleration (PSA) for the first record component, while d_y equals $S_y/(\omega_y)^2$, where S_y is the PSA for the second record component. By using and defining the above normalized variables, Eq (3.6) can be expressed as,

$$\ddot{\mu}_x+\left(a_0+a_1\omega_x^2\right)\dot{\mu}_x-a_1\omega_x^2\frac{e_y}{r}\dot{\mu}_\theta+a_x\omega_{x1}^2\left[\mu_x-\frac{(y_1-\tilde{\mu}_y\Delta_x)}{r}\mu_\theta\right]+\left(1-\alpha_x\right)\omega_{x1}^2\mu_{zx1}+$$
$$a_x\omega_{x2}^2\left[\mu_x-\frac{(y_2-\tilde{\mu}_y\Delta_x)}{r}\mu_\theta\right]+\left(1-\alpha_x\right)\omega_{x2}^2\mu_{zx2}\delta_x-\left(1-\ddot{u}_{gv}/g\right)\theta_x\omega_x^2\mu_x=-\frac{1}{\Delta_x}\ddot{u}_{gx}$$

(3.9a)

$$\ddot{\tilde{\mu}}_y+\left(a_0+a_1\omega_y^2\right)\dot{\tilde{\mu}}_y+a_1\omega_y^2\frac{e_x}{r}\dot{\mu}_\theta+a_y\omega_{y1}^2\left[\tilde{\mu}_y+\frac{(x_1-\mu_x\Delta_x)}{r}\mu_\theta\right]+\left(1-\alpha_y\right)\omega_{y1}^2\mu_{zy1}\frac{\Delta_y}{\Delta_x}+$$
$$a_y\omega_{y2}^2\left[\tilde{\mu}_y+\frac{(x_2-\mu_x\Delta_x)}{r}\mu_\theta\right]+\left(1-\alpha_y\right)\omega_{y2}^2\mu_{zy2}\frac{\Delta_y}{\Delta_x}\delta_y-\left(1-\ddot{u}_{gv}/g\right)\theta_y\omega_y^2\mu_y=-\frac{1}{\Delta_x}\ddot{u}_{gy}$$

(3.9b)

$$\ddot{\mu}_\theta+\left(a_0+a_1\omega_\theta^2\right)\dot{\mu}_\theta-a_1\omega_x^2\frac{e_y}{r}\dot{\mu}_x+a_1\omega_y^2\frac{e_x}{r}\dot{\mu}_y+$$
$$\frac{(y_1-\tilde{\mu}_y\Delta_x)}{r}\left[-\alpha_x\omega_{x1}^2\left(\mu_x-\frac{(y_1-\tilde{\mu}_y\Delta_x)}{r}\mu_\theta\right)-\left(1-\alpha_x\right)\omega_{x1}^2\mu_{zx1}\right]+$$
$$\frac{(y_2-\tilde{\mu}_y\Delta_x)}{r}\left[-\alpha_x\omega_{x2}^2\left(\mu_x-\frac{(y_2-\tilde{\mu}_y\Delta_x)}{r}\mu_\theta\right)-\left(1-\alpha_x\right)\omega_{x2}^2\mu_{zx2}\delta_x\right]+ \qquad (3.9c)$$
$$\frac{(x_1-\mu_x\Delta_x)}{r}\left[\alpha_y\omega_{y1}^2\left(\tilde{\mu}_y+\frac{(x_1-\mu_x\Delta_x)}{r}\mu_\theta\right)+\left(1-\alpha_y\right)\omega_{y1}^2\mu_{zy1}\frac{\Delta_y}{\Delta_x}\right]+$$
$$\frac{(x_1-\mu_x\Delta_x)}{r}\left[\alpha_y\omega_{y2}^2\left(\tilde{\mu}_y+\frac{(x_2-\mu_x\Delta_x)}{r}\mu_\theta\right)+\left(1-\alpha_y\right)\omega_{y2}^2\mu_{zy2}\frac{\Delta_y}{\Delta_x}\delta_y\right]=0$$

$$\dot{\mu}_{zxi}=\left(\dot{\mu}_x-\left(\frac{(y_i-\tilde{\mu}_y\Delta_x)}{r}\dot{\mu}_\theta-\frac{\dot{\tilde{\mu}}_y\Delta_x}{r}\mu_\theta\right)\right)-$$
$$\mu_{zxi}\left|\dot{\mu}_x-\left(\frac{(y_i-\tilde{\mu}_y\Delta_x)}{r}\dot{\mu}_\theta-\frac{\dot{\tilde{\mu}}_y\Delta_x}{r}\mu_\theta\right)\right|\left|\dot{\mu}_{zxi}\right|^{n-1}\left[\beta+\gamma\,\mathrm{sgn}\left(\left(\begin{array}{l}\dot{\mu}_x-(\frac{(y_i-\tilde{\mu}_y\Delta_x)}{r}\dot{\mu}_\theta-\\ \frac{\tilde{\mu}_y\Delta_x}{r}\mu_\theta)\end{array}\right)\mu_{zxi}\right)\right] \qquad (3.9d)$$

$$\dot{\mu}_{zyi} = \left(\dot{\mu}_y + \left(\frac{(x_i - \mu_x \Delta_x)}{r} \dot{\mu}_\theta - \frac{\dot{\mu}_x \Delta_x}{r} \mu_\theta \right) \right) -$$

$$\mu_{zyi} \left| \dot{\mu}_y + \left(\frac{(x_i - \mu_x \Delta_x)}{r} \dot{\mu}_\theta - \frac{\dot{\mu}_x \Delta_x}{r} \mu_\theta \right) \right| \left| \dot{\mu}_{zyi} \right|^{n-1} \left[\beta + \gamma \cdot \mathrm{sgn} \left(\left(\dot{\mu}_y + (\frac{(x_i - \mu_x \Delta_x)}{r} \dot{\mu}_\theta - \frac{\dot{\mu}_x \Delta_x}{r} \mu_\theta) \right) \mu_{zyi} \right) \right] \tag{3.9e}$$

where $\delta_x = \Delta_{x2} / \Delta_{x1}$ and $\delta_y = \Delta_{y2} / \Delta_{y1}$ represent the ratios between yield displacements of different load resisting elements along *X*- and *Y*-axis; $\theta_i = mg / K_{ii} h$ is the stability factor of the structure (MacRae 1994), where K_{ii} representing K_{XX} or K_{YY} is the initial linear elastic stiffness.

By introducing the following vector,

$$\{M_1 \; M_2 \; M_3 \; M_4 \; M_5 \; M_6 \; M_7 \; M_8 \; M_9 \; M_{10}\} = \{\mu_x \; \dot{\mu}_x \; \tilde{\mu}_y \; \dot{\tilde{\mu}}_y \; \mu_\theta \; \dot{\mu}_\theta \; \mu_{zx1} \; \mu_{zx2} \; \mu_{zy1} \; \mu_{zy2}\}$$

Eq. (3.9) can be expressed as a series of first-order differential equations, and solved by Gear's method (Shampine and Reichelt, 1997),

$$\dot{M}_1 = M_2 \tag{3.10a}$$

$$\dot{M}_2 = -\left(a_0 + a_1 \omega_x^2\right) M_2 + a_1 \omega_x^2 \frac{e_y}{r} M_6 - \alpha_x \omega_{x1}^2 \left[M_1 - \frac{\left(y_1 - \Delta_y M_3\right)}{r} M_5 \right] -$$
$$\left(1 - \alpha_x\right) \omega_{x1}^2 M_7 - \alpha_x \omega_{x2}^2 \left[M_2 - \frac{\left(y_2 - \Delta_y M_3\right)}{r} M_5 \right] - \tag{3.10b}$$
$$\left(1 - \alpha_x\right) \omega_{x2}^2 M_8 \delta_x + \left(1 - \ddot{u}_{gv} / g\right) \theta_x \omega_x^2 M_{10} - \frac{\ddot{u}_{gx}}{\Delta_x}$$

$$\dot{M}_3 = M_4 \tag{3.10c}$$

$$\dot{M}_4 = -\left(a_0 + a_1\omega_y^2\right)M_4 - \alpha_1\omega_y^2\frac{e_x}{r}M_6 - \alpha_y\omega_{y1}^2\left[M_3 + \frac{\left(x_1 - \Delta_x M_1\right)}{r}M_5\right] -$$
$$\left(1-\alpha_y\right)\omega_{y1}^2 M_9\frac{\Delta_y}{\Delta_x} - \alpha_y\omega_{y2}^2\left[M_3 + \frac{\left(x_2 - \Delta_x M_1\right)}{r}M_5\right] - \tag{3.10d}$$
$$\left(1-\alpha_y\right)\omega_{y2}^2 M_{10}\frac{\Delta_y}{\Delta_x}\delta_y + \left(1-\ddot{u}_{gv}/g\right)\theta_y\omega_y^2 M_3 - \frac{\ddot{u}_{gy}}{\Delta_x}$$

$$\dot{M}_5 = M_6 \tag{3.10e}$$

$$\dot{M}_6 = -\left(a_0 + a_1\omega_\theta^2\right)M_6 + a_1\omega_x^2\frac{e_y}{r}M_2 - a_1\omega_y^2\frac{e_x}{r}M_4 -$$
$$\frac{\left(y_1 - \Delta_x M_3\right)}{r}\left[-\alpha_x\omega_{x1}^2\left[M_1 - \frac{\left(y_1 - \Delta_x M_3\right)}{r}M_5\right] - \left(1-\alpha_x\right)\omega_{x1}^2 M_7\right] -$$
$$\frac{\left(y_2 - \Delta_x M_3\right)}{r}\left[-\alpha_x\omega_{x2}^2\left[M_1 - \frac{\left(y_2 - \Delta_x M_3\right)}{r}M_5\right] - \left(1-\alpha_x\right)\omega_{x2}^2 M_8\delta_x\right] - \tag{3.10f}$$
$$\frac{\left(x_1 - \Delta_x M_1\right)}{r}\left[\alpha_y\omega_{y1}^2\left[M_3 + \frac{\left(x_1 - \Delta_x M_1\right)}{r}M_5\right] + \left(1-\alpha_y\right)\omega_{y1}^2 M_9\frac{\Delta_y}{\Delta_x}\right] -$$
$$\frac{\left(x_2 - \Delta_x M_1\right)}{r}\left[\alpha_y\omega_{y2}^2\left[M_3 + \frac{\left(x_2 - \Delta_x M_1\right)}{r}M_5\right] + \left(1-\alpha_y\right)\omega_{y2}^2 M_{10}\frac{\Delta_y}{\Delta_x}\delta_y\right]$$

$$\dot{M}_7 = \left(M_2 - \left(\frac{\left(y_1 - M_3\Delta_x\right)}{r}M_6 - \frac{M_4\Delta_x}{r}M_5\right)\right) -$$
$$M_7\left|\begin{matrix} M_2 - (\frac{\left(y_1 - M_3\Delta_x\right)}{r}M_6 - \\ \frac{M_4\Delta_x}{r}M_5) \end{matrix}\right|\left|M_7\right|^{n-1}\left[\beta + \gamma\,sgn\left(\begin{matrix} (M_2 - (\frac{\left(d_{y1} - M_3\Delta_x\right)}{r}M_6 - \\ \frac{M_4\Delta_x}{r}M_5))M_7 \end{matrix}\right)\right]$$

(3.10g)

$$\dot{M}_8 = \frac{1}{\delta_x}\left(M_2 - \left(\frac{\left(y_2 - M_3\Delta_x\right)}{r} M_6 - \frac{M_4\Delta_x}{r} M_5 \right)\right) -$$

$$M_8 \left| \frac{1}{\delta_x} \left[\begin{array}{l} M_2 - (\frac{\left(y_2 - M_3\Delta_x\right)}{r} M_6 - \\ \frac{M_4\Delta_x}{r} M_5) \end{array} \right] \right| \left|M_8\right|^{n-1} \left[\beta + \gamma \square sgn \left(\begin{array}{l} \frac{1}{\delta_x}(M_2 - \\ (\frac{\left(y_2 - M_3\Delta_x\right)}{r} M_6 - \\ \frac{M_4\Delta_x}{r} M_5))M_8 \end{array} \right) \right] \quad (3.10h)$$

$$\dot{M}_9 = \frac{\Delta_x}{\Delta_y}\left(M_4 + \left(\frac{\left(x_1 - M_1\Delta_x\right)}{r} M_6 - \frac{M_2\Delta_x}{r} M_5 \right)\right) -$$

$$M_9 \left| \frac{\Delta_x}{\Delta_y} \left[\begin{array}{l} M_4 + (\frac{\left(x_1 - M_1\Delta_x\right)}{r} M_6 - \\ \frac{M_2\Delta_x}{r} M_5) \end{array} \right] \right| \left|M_9\right|^{n-1} \left[\beta + \gamma \square sgn \left(\begin{array}{l} \frac{\Delta_x}{\Delta_y}(M_4 + \\ (\frac{\left(x_1 - M_1\Delta_x\right)}{r} M_6 - \\ \frac{M_2\Delta_x}{r} M_5))M_9 \end{array} \right) \right] \quad (3.10i)$$

$$\dot{M}_{10} = \frac{\Delta_x}{\Delta_y\delta_y}\left(M_4 + \left(\frac{\left(x_2 - M_1\Delta_x\right)}{r} M_6 - \frac{M_2\Delta_x}{r} M_5 \right)\right) -$$

$$M_{10} \left| \frac{\Delta_x}{\Delta_y\delta_y} \left[\begin{array}{l} M_4 + (\frac{\left(x_2 - M_1\Delta_x\right)}{r} M_6 - \\ \frac{M_2\Delta_x}{r} M_5) \end{array} \right] \right| \left|M_{10}\right|^{n-1} \left[\beta + \gamma \square sgn \left(\begin{array}{l} \frac{\Delta_x}{\Delta_y\delta_y}(M_4 + \\ (\frac{\left(x_2 - M_1\Delta_x\right)}{r} M_6 - \\ \frac{M_6\Delta_x}{r} \mu_\theta))M_5 \end{array} \right) \right] \quad (3.10j)$$

For a given structural system with an assumed stability factor, the solution of Eq. (3.10) is obtained as below:

1) For a given record, determine the peak linear elastic responses d_{0x} and d_{0y} for the corresponding linear elastic SDOF systems;

2) The record components are scaled with the same factor such that its first record component (*X*-direction) leads to the PSA at T_x=1.0 (s) equal to 0.25 (g) or 0.5(g);

3) Compute the yield displacement $\Delta_x = \phi_x d_{0x}$ and $\Delta_y = \phi_y d_{0y}$;

4) Solve Eq. (3.2) to find u_x, u_y, u_θ, u_{xi}, u_{yi};

5) Radius of gyration *r* for the considered geometry is given by $r = \sqrt{\left(L^2 + W^2\right)/12}$. Throughout this study the aspect ratio (L/W) was considered to be equal to be equal to 2. By considering that the structure has the height over width ratio equal to 1 (i.e., h_n/W = 1), and that the height of structure can be assigned based the following approximate relation $T_n = 0.075\left(h_n\right)^{3/4}$, where T_n = T_x = T_y, it is concluded that *r* = 10 m. This value can be used to calculate the ratio of Δ_x / r;

6) For given values ϕ_x and ϕ_y, solve Eq. (3.10) to find μ_x, μ_y, μ_θ;

7) The displacements of the lateral load resisting elements μ_{xi} and $\mu_{yi.}$ can be solved using $u_{xiT}(t) = \mu_x \Delta_x - \left(\frac{y_i}{r} - \tilde{\mu}_y \frac{\Delta_x}{r}\right)\mu_\theta \Delta_x$ and $u_{yiT}(t) = \tilde{\mu}_y \Delta_x + \left(\frac{x_i}{r} - \mu_x \frac{\Delta_x}{r}\right)\mu_\theta \Delta_x$;

8) Compare u_x, u_y, u_θ, u_{xi}, u_{yi} (considering only *P*-Δ effect) and u_{xT}, u_{yT}, $u_{\theta T}$, u_{xiT}, u_{yiT} (considering both *A*-Δ and *P*-Δ effects) to determine the potential differences between the obtained torsional effects;

9) Repeat Steps 1) through 7) for each of the 123 records and estimate the statistics of torsional effects;

10) Repeat step 3) through 8) with varying stability factors to investigate the impact of the stability factors on inelastic torsional response.

3.3 Statistical assessment of the normalized responses

3.3.1 Ground motion records

Nonlinear inelastic responses of a structure can be sensitive to both the structural dynamic properties (e.g., the natural vibration period and damping ratio) and the characteristics of the individual ground motion used as seismic input (e.g., intensity, duration and frequency) (Williamson 2003; Kalkan and Graizer 2007). Because of the uncertainty in ground motions, the responses should be quantified using statistics and, the selection of real earthquake records should consider the severity, intensity, and magnitude of earthquake, and the site condition. To evaluate the inelastic response of structures considering A-Δ and P-Δ effects, a set of 123 California records assembled from 11 seismic events are selected in this study. These records are a subset of 592 records that are extracted from the Next Generation Attenuation (NGA) database (PEER, 2006) with selection criteria detailed in Hong and Goda (2007). Since nonlinear inelastic responses are of concern, the following more stringent criteria are used to select the 123 records:

(1) The low-cut filter corner frequency in processing raw data equals 0.2 Hz or less;

(2) The moment magnitude of the event is greater than 6;

(3) The distance D (i.e., closest horizontal distance to the projected faults on the earth or the epicentral distance if the former is not available) is greater than 15 km;

(4) The shear wave velocity *Vs30* in the uppermost 30 m is greater than 360 (m/s), representing NEHRP's site class A, B and C (i.e, Hard rock, Rock and very dense soil and soft rock) (BSSC 2001).

The 123 records, each with three components, employed in this study are those satisfied the criteria. In Table 3.1, the records are identified by the event ID, earthquake name and record ID. For the analysis, it is assumed that the orientation of the first record component parallels the *X*-axis, second component parallels the *Y*-axis, and the third vertical record component parallels the *Z*-axis.

3.3.2 Numerical results

3.3.2.1 General consideration

There are many parameters that could affect the torsional responses, including ω_x, Ω_y, Ω_θ, load eccentricities, normalized yield strength and nonlinear hysteretic model (De Stefano and Pintucchi 2008). In this study, symmetric, one-way asymmetric and two-way asymmetric systems are considered to evaluate the responses and to investigate the influence of the *A*-Δ and *P*-Δ effect on the seismic responses. For the numerical analysis, in the subsequent sections (i.e. section 3.3.2.2 and 3.3.2.3), the uncoupled lateral frequencies along *X*-axis and *Y*-axis are assumed to be the same ($\omega_x = \omega_y = 2\pi$ or 4π); the normalized yield strengths ϕ_x and ϕ_y are considered to be the same and equal to 0.5; and the stability factor $\theta_x = \theta_y = 0.045$. The uncoupled torsional-to-lateral frequency ratio Ω_θ is considered to vary from 0.8 to 2.0 (Goel and Chopra 1991). A large Ω_θ value represents torsionally stiff system with resisting elements near the perimeter of the building plan, and a small Ω_θ value indicates a torsionally flexible system with a stiff central core (De la Llera and Chopra 1995).

The Bouc-Wen hysteretic model (see Appendix B) has 12 parameters: four shape parameters $\{\alpha, \beta, \gamma, n\}$, two degradation parameters $\{\delta_\eta, \delta_\nu\}$ and six pinching

parameters $\{\zeta_s, p, q, \psi, \delta_\psi, \lambda\}$ (Foliente, 1995; Ma et al., 2004). The shape parameter α controls the post-yield tangent stiffness of hysteresis loop; shape parameters β and γ control the loading and unloading path, and n controls smoothness of hysteretic model that changing smoothness of transition between pre-yielding and post-yielding state. For the numerical analysis to be carried out, the strength and stiffness degradations are neglected by considering $\delta_\eta = 0$ and $\delta_\nu = 0$. The shape parameters selected for the numerical analysis to be carried out are $\{\alpha, \beta, \gamma, n\} = \{0.05, 0.5, 0.5, 2\}$. The remaining parameters for the Bouc-Wen model [α, $\beta_{\mu xi}$, $\beta_{\mu yi}$, $\gamma_{\mu xi}$, $\gamma_{\mu yi}$, n_{xi}, n_{yi}] = [0, 0.5, 0.5, 0.5, 0.5, 2, 2] are considered for each lateral load resisting element.

To reduce the number of the parameters that need to be considered for the parametric investigation, it is assumed that the distances from the CM to each lateral load resisting element along each direction are equal (i.e. $|x_1| = |x_2|$ and $|y_1| = |y_2|$), and the ratio $|x_i|/L$ equals $|y_i|/W$, which is denoted using the symbol χ. Based on these assumptions, and the relation $\Omega_\theta = \sqrt{\omega_\theta / \omega_x}$ it can be shown that $\chi = \Omega_\theta \Big/ \sqrt{(W/r)^2 + K_{YY}/K_{XX}\,(L/r)^2}$. In other words, under these assumptions, the value of the ratio can be calculated based on other structural characteristics. The calculated value of χ can readily be used to define the locations of the lateral load resisting elements: two lateral load resisting elements that parallel the *X*-axis are placed at *y* equal to χW and $-\chi W$ while the two elements that parallel the *Y*-axis are placed at *x* equal to χL and $-\chi L$. For the structure systems to be analysis, the eccentricity ratios defined as e_x/r and e_x/r are considered to be equal to 0 and

$0.25|y_i|/r$ for one-way asymmetric system, and $0.25|x_i|/r$ and $0.25|y_i|/r$ for two-way asymmetric systems.

3.3.2.2 Two-way symmetric system

Consider an arbitrary earthquake record selected from Table 3.1 for a symmetric system. To illustrate that the responses of A-Δ and P-Δ effects are not linear proportional to the intensity of the excitation, consider a structure with T_X = 1 and T_Y = 1. The record components of a selected record are scaled with the same factor such that its first record component leads to a PSA at T_X =1.0s equal to 0.25g and 0.5g. For example, the record of the Coalinga earthquake (Moment Magnitude M = 6.36) recorded at the Parkfield - Gold Hill 2 West (Record ID: 350, epicentral distance D = 47.41 km and the shear wave velocity in the uppermost 30m, V_{s30} = 376.1 m/s) is depicted in the Figure 3.3. Nonlinear inelastic seismic responses for Case 6 defined in Table 3.2, including A-Δ and P-Δ effects, are calculated by solving Eq. (3.10); the obtained time histories of the responses are shown in Figure 3.4. The figure shows a visible rotational response $r\theta_T(t)$ that is caused by A-Δ and P-Δ effect for symmetric system. To analyze the response affected by A-Δ and P-Δ effect, the ratios defined as $R_X = \max(|u_{xT}(t)|)/\max(|u_x(t)|)$, and $R_Y = \max(|u_{yT}(t)|)/\max(|u_y(t)|)$ are calculated. Furthermore, the maximum of the ratios for the displacements of the lateral load resisting elements defined as $R_{XT} = \max(|u_{x1T}(t)|, |u_{x2T}(t)|)/\max(|u_{x1}(t)|, |u_{x2}(t)|)$ and $R_{YT} = \max(|u_{y1T}(t)|, |u_{y2T}(t)|)/\max(|u_{y1}(t)|, |u_{y2}(t)|)$ are also calculated.

By repeating the above analysis for all the considered records, samples of R_X, R_Y, R_{XT}, R_{YT} and $\max(r\theta_T)$ for each of the cases listed in Table 3.2 are obtained. To

illustrate the variability of the ratios versus M and D, samples for Case 2 defined in Table 3.2 are illustrated in Figure 3.5. The results shown in Figure 3.5 indicate that the correlation coefficients calculated from the samples are small, suggesting that that R_X, R_Y, R_{XT}, R_{YT} and max($r\theta_T$) could be reasonably assumed to be independent of M and D. Since plots for other cases are similar to those shown in Figure 3.5, they are not included.

By adopting this assumption, statistics of the ratios are calculated and included in Table 3.2 for the considered structural systems shown in the same table. The results indicate that the means of R_X, R_Y, R_{XT} and R_{YT} are near unity and the coefficient of variation (COV) values of R_X and R_Y are small, implying that the influence of combining A-Δ and P-Δ on the nonlinear response of the CM is negligible. Comparison of the statistics of the ratios R_X, R_Y, R_{XT} and R_{YT} shown in Table 3.2 indicates that there are differences among these ratios, suggesting that the displacements on the lateral load-resisting elements are affected by considering and ignoring the A-Δ effect. Statistics of max($r\theta_T$) shown in Table 3.2 also indicate that the additional torsional responses are considerably large in two-way symmetric system (e.g. the Case 8 listed in Table 3.2, the mean value of torsional displacement, $r\theta_T$, equals to 0.052m) and sensitive to the natural vibration periods.

Since torsional flexibility is controlled by the uncoupled torsional-to-lateral frequency ratio Ω_θ which ranges from 0.8 to 2.0 for the systems shown in Table 3.2. The results shown in table 3.2 indicates that the increase in Ω_θ leads to a decreased rotational response. The COV of torsional response ranges from 0.8 to 1.1 for all

systems, which indicates that there is a large uncertainty in torsional response for two-way symmetric system by considering the *A*-Δ and *P*-Δ effects.

3.3.2.3 One-way asymmetric system and Two-way asymmetric system

For one-way asymmetric system and two-way asymmetric system, the analysis similar to that presented in the previous section was carried out. The results obtained for a few systems defined in Tables 3.3 and 3.4 are also presented in these tables. For illustration purpose, the time histories of the displacements for Case 6 ($\Omega_\theta = 1$, PSA = 0.5g) shown in Table 3.3 and for Case 6 shown in Table 3.4 are depicted in Figures 3.6 and 3.7 by ignoring and considering the *A*-Δ effect. Moreover, samples of R_{XT}, R_{YT} and max($r\theta_T$) versus *M* and *D* are shown in Figures 3.8 for Case 2 defined in Table 3.3 and in Figure 3.9 for Case 2 defined in Table 3.4. The figures shows that the calculated correlation coefficients are small, indicating that these ratios and responses may be considering to be independent of M or D. Similar plots for other cases defined in Tables 3.3 and 3.4 are not presented because they exhibit similar trends.

By considering the ratios are independent of *M* and *D*, the calculated statistics of R_X, R_Y, max$(r\theta)$, R_{XT}, R_{YT} and max($r\theta_T$) for each considered structural model of one-way symmetric or two-way asymmetric systems are presented in Tables 3.3 and 3.4. For asymmetric systems, since the means R_X, R_Y and R_{XT}, R_{YT} are near unity, the influence of the *A*-Δ effect on the displacements of the CM is again negligible. In other words, the addition of the instantaneous load eccentricities does not affect significantly the inelastic responses as compared to the symmetrical systems. This

may be explained by noting that that the torsional responses are already present for unsymmetrical system even without A-Δ effect.

3.3.2.4 Influence of stability factor

The P-Δ effect is considering in Eq. (3.1) through the stability factor θ. To investigate the impact of θ on the estimated seismic ductility demand and torsional behavior by considering A-Δ and P-Δ effects, the analysis is carried out for θ from 0.03 to 0.09 for two-way symmetric and one-way asymmetric system but considering Case 2 shown in Table 3.2 and Case 2 shown in Table 3.3 only.

Statistics of R_X, R_Y, max(u_x), max(u_y), R_{XT} , R_{YT}, max(u_{xT}), max(u_{yT}) and max($r\theta_T$) for two-way symmetric and one-way asymmetric systems considering A-Δ and P-Δ effects are listed in Table 3.5 and Table 3.6. The results show that by varying θ, the mean values of R_X, R_Y, max(u_x), max(u_y), R_{XT} , R_{YT}, max(u_{xT}), max(u_{yT}) and max($r\theta_T$) are almost the same by including or excluding the A-Δ effect for θ ranging from 0.03 to 0.07. However, significant differences on the maximum lateral displacements along X-axis and Y-axis are indicated in the table when θ equals 0.09. For example, the mean values of max(u_x) and max(u_y) are 4.9349 (m) and 0.0321(m) if only P-Δ effect is considered; while the mean values of max(u_{xT}) and max(u_{yT}) are 5.2700(m) and 0.0394(m) if both A-Δ and P-Δ effects are considered. On average, the increase is about 7% and 22% of the lateral displacements along X-axis and Y-axis. Similar trends are also observed for one-way asymmetric system. However, the obtained samples of max($r\theta$) and max($r\theta_T$) in Table 3.6 indicate that with increasing θ, A-Δ effect tends to reduce the torsional displacements. For example, for $\theta = 0.09$ Table

3.6 shows that the mean value of max($r\theta$) is 0.0396 while that of max($r\theta_T$) is 0.0130, resulting in a reduction of 60%. It shows that with varying stability factor θ, A-Δ effect can introduce significant changes on the lateral and torsional displacements, especially when θ is large.

It must be emphasized that the definition of the stability coefficient θ ($\theta_i = mg/K_i h$) is different from that defined in code. In Appendix J in the NBCC 2005 User's Guide, stability factor θ_{NBCC} is determined by the following equation:

$$\theta_{NBCC} = \frac{\sum_{i=x}^{n} W_i}{R_o \sum_{i=x}^{n} F_i} \frac{\Delta_{mx}}{h_s} \tag{3.11}$$

where, $\sum_{i=x}^{n} F_i$ is the seismic design shear force at the level under consideration, which is equal to the sum of the design lateral forces acting at and above the story; $\sum_{i=x}^{n} W_i$ is that portion of the factored dead plus live load above the story; Δ_{mx} is the maximum inelastic interstory deflection; h_s is the interstory height; R_o is the overstrength-related force modification factor; $R_o \sum_{i=x}^{n} F_i$ is a measure of the capacity at the level under consideration.

For a single-story building, Eq. (11) can be expressed,

$$\theta_{NBCC} = \frac{W}{R_o V} \frac{\Delta_m}{h_s} = \frac{W}{h_s R_o V / \Delta_y} \frac{\Delta_m}{\Delta_y} = \frac{W}{h_s R_o V / \phi d_0} \mu = \frac{W \phi}{R_o K h_s} \mu \tag{3.12a}$$

where μ is the ductility displacement demand $\mu = \Delta_m / \Delta_y$. This equation re-written as,

$$\theta_{NBCC} = \frac{1}{R_o}\theta \tag{3.12b}$$

showing the relation between θ_{NBCC} and θ defined in this study.

3.4 Discussion and Conclusions

In this chapter, investigation of the inelastic seismic responses under bi-directional excitations and considering the A-Δ and P-Δ effects are carried out. The analysis considered a set of 123 California seismic records; the two-way symmetric, one-way asymmetric and two-way asymmetric systems are considered. The nonlinear behaviour of lateral load resisting element is modeled using the Bouc-Wen model. The statistics of the responses or response ratios are summarized. The main conclusions that can be drawn from the numerical results are:

(1) The responses affected by the A-Δ and P-Δ effects are sensitive to the natural vibration periods and the stability factor.

(2) The A-Δ effect can introduce significant changes on the lateral and torsional displacements, if θ is large.

(3) Significant changes on the maximum lateral displacements along X-axis and Y-axis and torsional displacement are observed by including and excluding A-Δ if θ is large and the P-Δ effect is considered. The consideration of the A-Δ effect does not always increase the seismic demand.

It must be emphasized that the number of cases considered is very limited, and the CP is considered to coincide with the CS. In reality this may not be the case. Furthermore, only single-story building model is considered although in reality the buildings are much more complex; the rotational components of ground motion (coupled tilt and Translational Ground Motion Response Spectra) which may affect the maximum seismic demand was not included. All these deserve further investigation and are beyond the scope of chapter.

References

Bernal D. (1987). Amplification factors for inelastic dynamic *P*-Δ effects in earthquake analysis. Earthquake Engineering and Structural Dynamics; 15:635–651.

Building Seismic Safety Council (BSSC) (1995). NEHRP Recommended Provisions for Seismic Regulations for New Buildings, FEMA 222A/223A, Vol. 1 (Provisions) and Vol. 2 (Commentary), developed for the Federal Emergency Management Agency, Washington, D.C.

Chopra, A.K. (2001) Dynamics of structures: theory and applications to earthquake engineering (2nd ed.). Prentice Hall, N.J.

De La Llera J.C. and Chopra, A. K. (1995a). Understanding the inelastic seismic behaviour of asymmetric-plan buildings. Earthquake Engineering and Structural Dynamics; 24(4):549 – 572.

De la Llera, J. C. and Chopra, A. K. (1995b). Estimation of accidental torsion effects for seismic design of buildings. Journal of Structural Engineering, ASCE; 121(1):102–114.

De Stefano, M. and Pintucchi, B. (2008). A review of research on seismic behaviour of irregular building structures since 2002. Bull. Earthquake Eng.; 6:285–308

De-La-Colina, J. (1999). Effects of torsion factors on simple non-linear systems using fully-bidirectional analyses. Earthquake Engineering and Structural Dynamics 1999; 28(7):691–706.

Foliente, G.C. (1995). Hysteresis modeling of wood joints and structural systems. Journal of Structural Engineering; 121(6):1013–1022.

Goel, R. K. and Chopra, A. K. (1991). Inelastic seismic response of one-storey, asymmetric-plan systems: Effects of system parameters and yielding. Earthquake Engineering & Structural Dynamics; 20(3): 201-222.

Goda, K., Hong, H.P. and Lee, C.S. (2009). Probabilistic characteristics of seismic ductility demand of SDOF systems with Bouc-Wen hysteretic behavior. Journal of Earthquake Engineering; 13:600–622.

Gupta, A., and Krawinkler, H. (2000). Dynamic P–Δ effects for flexible inelastic steel structures. ASCE Journal of Structural Engineering; 126: 145–154.

Hong, H. P., and Goda, K. (2007). Orientation-dependent ground motion measure for seismic hazard assessment. Bulletin of the Seismological Society of America; 97(5):1525-1538.

Hong, H. P., Goda, K. and Davenport, A. G. (2006). eismic hazard analysis: a comparative study. Canadian J. Civil Eng; 33(9): 1156–1171.

Hong, H. P. and Hong, P. (2007). Assessment of ductility demand and reliability of bilinear single-degree-of-freedom systems under earthquake loading. Canadian J. Civil Eng; 34(12): 1606–1615

Humar, J. L. and Kumar, P. (1998). Torsional motion of buildings during earthquakes II Inelastic response. Canadian Journal of Civil Engineering; 25(5)**:**917–934.

Lee, C.S. (2011). Inelastic seismic displacement demand of simplified equivalent nonlinear structural systems. Ph.D. diss., The University of Western Ontario(Canada).

Lee, C.S., and Hong, H.P. (2010). Inelastic Responses of Hysteretic Systems under Biaxial Seismic Excitations, Engineering Structures;

Lucchini, A. Monti, G. and Kunnath, S. (2009). Seismic behavior of single-story asymmetric-plan buildings under uniaxial excitation. Earthquake Engineering and Structural Dynamics; 38:1053–1070

Ma, F., Zhang, H., Bockstedte, A., Foliente, G.C. and Paevere, P. (2004). Parameter analysis of the differential model of hysteresis. Transactions of the ASME; 71(3): 342–349.

MacRae GA. (1994). *P*-Δ effects on single-degree-of-freedom structures in earthquakes. Earthquake Spectra; 10:539–568.

Pacific Earthquake Engineering Research (PEER) Center Next Generation Attenuation database. http://peer.berkeley.edu/nga/index.html.

Paulay, T. (1997). Are existing seismic torsion provisions achieving the design aims? Earthquake spectra; 13(2):259–279.

Peruš I., Fajfar P. (2005). On the inelastic torsional response of single-storey structures under bi-axial excitation. Earthquake Engineering and Structural Dynamics; 34(8):931–941.

Rutenberg A. (1998). AEE Task Group (TG) 8: behaviour and irregular and complex structures–progress since 1998. Proceedings of the 12th European conference on earthquake engineering, CD ROM. London; 2002.

Ryan, K.L. and Chopra, A.K. (2004). Estimation of seismic demands on isolators in asymmetric buildings using non-linear analysis. Earthquake Engineering and Structural Dynamics; 33(3):395–418.

Tremblay, R., Cote, B. and Leger, P. (1999). An Evaluation of *P*-Δ Amplification Factors in Multistorey Steel Moment Resisting Frames. Canadian Journal of Civil Engineering; 26: 535-548.

Tso, W.K. and Wong, C. M. (1995). Seismic displacements of torsionally unbalanced buildings. Earthquake Engineering and Structural Dynamics; 24:1371–1387.

Tso, W.K. and Myslimaj, B. (2002). Effect of strength distribution on the inelastic torsional response of asymmetric structural systems. Proceedings of the 12th European Conference on Earthquake Engineering, Paper No. 081, London, U.K.

Vian D, Bruneau M. (2003). Tests to structural collapse of single degree of freedom frames subjected to earthquake excitation. Journal of Structural Engineering; 129:1676 1685.

Wen Y.K. (1976). Method for random vibration of hysteretic systems. Journal of Engineering Mechanics; 102(2):249–263.

Table 3.1 Selected records from the NGA database (PEER, 2006)

Event ID	Earthquake name	Number of records	Record ID
25	Parkfield	2	28, 33
30	San Fernando	6	58, 59, 64, 81, 89, 94
50	Imperial Valley-06	2	164, 190
76	Coaling*A*-01	23	323, 327, 330, 335, 336, 339, 342, 344, 345, 346, 347, 350, 351, 352, 353, 354, 355, 356, 357, 358, 364, 366, 369
90	Morgan Hill	2	450,470
101	N. Palm Springs	1	531
118	Loma Prieta	29	731, 734, 735, 736, 739, 745, 747, 749, 750, 751, 762, 769, 771, 773, 776, 781, 782, 787, 788, 789, 791, 794, 795, 796, 797, 804, 807, 812, 813
123	Cape Mendocino	1	827
125	Landers	4	838, 887, 891, 897
127	Northridge-01	42	942, 945, 946, 957, 963, 965, 974, 980, 990, 991, 993, 994, 1005, 1007, 1008, 1011, 1015, 1017, 1019, 1020, 1021, 1022, 1023, 1026, 1027, 1028, 1029, 1030, 1031, 1033, 1038, 1039, 1041, 1046, 1047, 1053, 1057, 1065, 1070, 1074, 1079, 1091
158	Hector Mine	11	1763, 1767, 1768, 1786, 1794, 1795, 1812, 1824, 1831, 1832, 1836

Table 3.2 Statistics of R_X, R_Y, R_{XT}, R_{YT}, and max$(r\theta_T)$ for two-way symmetric systems considering A-Δ and P-Δ effects.

System and loading condition		Variable				
T_x, T_y, Ω, PSA (g)	Statistics	R_X	R_Y	R_{XT}	R_{YT}	max$(r\theta_T)$
Case 1	Mean	1.0000	1.0000	1.0007	1.0012	0.0005
	COV	0.0001	0.0001	0.0008	0.0012	1.0381
1.0, 1.0, 0.8,	ρ_M	0.0888	0.1338	0.0139	-0.0494	0.1533
0.25	ρ_D	0.0759	0.2134	0.0271	-0.0296	0.0878
	Maximum	1.0004	1.0004	1.0036	1.0063	0.0029
	Minimum	0.9993	0.9998	0.9998	1.0000	0.0000
Case 2	Mean	1.0000	1.0000	1.0008	1.0015	0.0004
	COV	0.0001	0.0001	0.0008	0.0013	0.9611
1.0, 1.0, 1.0,	ρ_M	0.0773	0.1810	0.0533	-0.1019	0.1374
0.25	ρ_D	0.0871	0.1824	0.0389	-0.0685	0.0886
	Maximum	1.0003	1.0004	1.0033	1.0060	0.0020
	Minimum	0.9992	0.9997	0.9999	1.0001	0.0000
Case 3	Mean	1.0000	1.0000	1.0009	1.0016	0.0003
	COV	0.0001	0.0001	0.0010	0.0015	0.9958
1.0, 0.5, 1.25,	ρ_M	0.0313	0.2457	0.1208	-0.1291	0.1493
0.25	ρ_D	0.1149	0.0834	0.0882	-0.1789	0.0736
	Maximum	1.0002	1.0003	1.0063	1.0074	0.0019
	Minimum	0.9996	0.9997	1.0000	1.0000	0.0000
Case 4	Mean	1.0000	1.0000	1.0008	1.0015	0.0002
	COV	0.0000	0.0001	0.0009	0.0016	0.9882
1.0, 1.0, 1.6,	ρ_M	-0.0425	0.1588	0.1880	-0.0697	0.1530
0.25	ρ_D	0.0148	0.0040	0.1158	-0.2581	0.0590
	Maximum	1.0002	1.0004	1.0046	1.0080	0.0012
	Minimum	0.9997	0.9997	1.0000	1.0000	0.0000
Case 5	Mean	1.0000	1.0000	1.0007	1.0013	0.0002
	COV	0.0000	0.0000	0.0008	0.0015	1.0532
1.0, 1.0, 2.0,	ρ_M	-0.0742	0.0616	0.1774	-0.0083	0.1531
0.25	ρ_D	0.0415	0.0243	0.1784	-0.2039	0.0894
	Maximum	1.0001	1.0003	1.0046	1.0081	0.0011
	Minimum	0.9998	0.9999	1.0000	1.0000	0.0000
Case 6	Mean	1.0000	1.0000	1.0015	1.0027	0.0015
	COV	0.0002	0.0001	0.0017	0.0026	0.8045
1.0, 1.0, 1.0,	ρ_M	0.1120	0.1046	-0.0300	-0.0930	0.2014
0.5	ρ_D	-0.0179	0.1169	-0.1535	-0.2363	0.0605

	Maximum	1.0008	1.0009	1.0119	1.0129	0.0053
	Minimum	0.9988	0.9994	0.9992	0.9999	0.0002
Case 7	Mean	1.0000	1.0000	1.0010	1.0018	0.0021
	COV	0.0001	0.0001	0.0011	0.0020	1.0193
2.0, 2.0, 1.0,	ρ_M	-0.1271	0.0782	0.1383	0.1520	0.4511
0.25	ρ_D	0.1478	0.0658	-0.1193	0.0059	0.0970
	Maximum	1.0002	1.0003	1.0067	1.0142	0.0156
	Minimum	0.9991	0.9994	1.0000	0.9999	0.0001
Case 8	Mean	1.0000	1.0000	1.0012	1.0030	0.0052
	COV	0.0001	0.0003	0.0014	0.0031	1.1660
2.0, 2.0, 1.0,	ρ_M	0.1871	0.0027	0.0806	0.1143	0.4533
0.5	ρ_D	0.0560	0.0329	-0.0284	-0.0926	0.0677
	Maximum	1.0003	1.0012	1.0071	1.0160	0.0544
	Minimum	0.9995	0.9985	0.9996	1.0000	0.0003

Table 3.3 Statistics of R_X, R_Y, max($r\theta$), R_{XT}, R_{YT} , and max($r\theta_T$) for one-way asymmetric systems considering *A*-Δ and *P*-Δ effects.

System and loading condition		Variable					
T_X, T_Y, Ω, e_x, e_y, *PSA (g)*	Statistics	R_X	R_Y	max($r\theta$)	R_{XT}	R_{YT}	max($r\theta_T$)
Case 1	Mean	1.0001	0.9998	0.0113	1.0001	0.9998	0.0113
	COV	0.0019	0.0031	0.8337	0.0019	0.0025	0.8394
1.0, 1.0, 0.8,	ρ_M	0.1210	-0.0286	0.2740	0.0014	0.1119	0.2698
0, 0.25y_1,	ρ_D	0.1173	-0.0379	0.1769	0.0592	0.0023	0.1765
0.25	Maximum	1.0106	1.0178	0.0908	1.0099	1.0129	0.0917
	Minimum	0.9960	0.9739	0.0025	0.9953	0.9879	0.0025
Case 2	Mean	1.0002	0.9999	0.0136	1.0001	0.9999	0.0136
	COV	0.0022	0.0032	0.7101	0.0020	0.0025	0.7123
1.0, 1.0, 1.0,	ρ_M	0.1044	-0.0375	0.2865	0.0459	0.0369	0.2830
0, 0.25y_1,	ρ_D	0.0741	-0.0388	0.1368	0.0205	0.0403	0.1383
0.25	Maximum	1.0143	1.0170	0.0893	1.0132	1.0118	0.0904
	Minimum	0.9954	0.9731	0.0027	0.9956	0.9886	0.0027
Case 3	Mean	1.0000	0.9998	0.0130	1.0000	0.9999	0.0130
	COV	0.0019	0.0029	0.6180	0.0017	0.0025	0.6191
1.0, 1.0, 1.25,	ρ_M	0.0484	-0.0432	0.3051	-0.0171	0.1041	0.3056
0, 0.25y_1,	ρ_D	0.0863	-0.0369	0.1758	0.0554	0.0820	0.1832
0.25	Maximum	1.0094	1.0136	0.0682	1.0092	1.0088	0.0690
	Minimum	0.9929	0.9765	0.0030	0.9955	0.9900	0.0030
Case 4	Mean	1.0000	0.9999	0.0107	1.0001	0.9999	0.0107
	COV	0.0015	0.0020	0.5772	0.0015	0.0023	0.5752
1.0, 1.0, 1.6,	ρ_M	0.0069	-0.0567	0.3258	-0.0820	0.0306	0.3253
0, 0.25y_1,	ρ_D	0.0917	-0.0375	0.2416	0.0528	0.1334	0.2434
0.25	Maximum	1.0070	1.0064	0.0508	1.0066	1.0062	0.0506
	Minimum	0.9915	0.9843	0.0030	0.9968	0.9908	0.0030
Case 5	Mean	1.0000	0.9999	0.0089	1.0000	0.9998	0.0089
	COV	0.0014	0.0018	0.5502	0.0017	0.0022	0.5497
1.0, 1.0, 2.0,	ρ_M	0.0638	-0.2633	0.3338	0.0023	-0.0472	0.3351
0, 0.25y_1,	ρ_D	0.1148	-0.1838	0.3176	0.0902	0.0689	0.3176
0.25	Maximum	1.0058	1.0070	0.0403	1.0101	1.0057	0.0401
	Minimum	0.9904	0.9878	0.0028	0.9906	0.9905	0.0027
Case 6	Mean	1.0004	0.9993	0.0245	1.0000	0.9996	0.0244
	COV	0.0049	0.0077	1.0654	0.0041	0.0056	1.0567
1.0, 1.0, 1.0,	ρ_M	0.3686	-0.0898	0.3070	0.2510	0.0044	0.3099
0, 0.25y_1,	ρ_D	0.2753	-0.1057	0.2349	0.2357	-0.0363	0.2352

0.5	Maximum	1.0293	1.0238	0.2299	1.0169	1.0259	0.2288
	Minimum	0.9859	0.9220	0.0044	0.9835	0.9623	0.0044
Case 7	Mean	1.0001	1.0004	0.0363	1.0002	1.0007	0.0365
	COV	0.0015	0.0031	0.8894	0.0022	0.0033	0.8961
2.0, 2.0, 1.0,	ρ_M	0.1136	0.0981	0.4764	0.1687	0.0943	0.4764
0, 0.25y_1,	ρ_D	0.0213	-0.0300	0.2273	0.1225	0.0157	0.2300
0.25	Maximum	1.0062	1.0173	0.2731	1.0071	1.0175	0.2792
	Minimum	0.9923	0.9874	0.0038	0.9923	0.9878	0.0038
Case 8	Mean	1.0002	1.0004	0.0651	1.0005	1.0006	0.0664
	COV	0.0015	0.0081	1.1535	0.0025	0.0066	1.1551
2.0, 2.0, 1.0,	ρ_M	0.2731	0.0598	0.4826	0.2363	-0.0348	0.4881
0, 0.25y_1,	ρ_D	0.0491	-0.0060	0.2835	0.1376	-0.0637	0.2812
0.5	Maximum	1.0054	1.0683	0.5943	1.0107	1.0464	0.6049
	Minimum	0.9969	0.9616	0.0050	0.9956	0.9746	0.0049

Table 3.4 Statistics of R_X, R_Y, max($r\theta$), R_{XT}, R_{YT} , and max($r\theta_T$) for two-way asymmetric systems considering A-Δ and P-Δ effects.

System and loading condition		Variable					
T_x, T_y, Ω, e_x, e_y, PSA(g)	Statistics	R_X	R_Y	max($r\theta$)	R_{XT}	R_{YT}	max($r\theta_T$)
Case 1	Mean	1.0007	0.9993	0.0241	1.0006	0.9998	0.0241
1.0, 1.0, 0.8,	COV	0.0051	0.0054	1.0109	0.0045	0.0037	1.0089
0.25x_1,	ρ_M	-0.0291	-0.1296	0.2648	0.0406	-0.0806	0.2650
0.25y_1,	ρ_D	0.1005	-0.1845	0.2370	0.1992	-0.2081	0.2357
0.25	Maximum	1.0377	1.0080	0.1865	1.0249	1.0086	0.1846
	Minimum	0.9790	0.9447	0.0074	0.9846	0.9739	0.0074
Case 2	Mean	1.0007	0.9996	0.0273	1.0005	1.0000	0.0273
1.0, 1.0, 1.0,	COV	0.0061	0.0058	0.8851	0.0044	0.0034	0.8821
0.25x_1,	ρ_M	0.0172	-0.1409	0.2606	0.0605	-0.0979	0.2611
0.25y_1,	ρ_D	0.1209	-0.2007	0.2184	0.1983	-0.1881	0.2176
0.25	Maximum	1.0380	1.0092	0.1853	1.0258	1.0094	0.1835
	Minimum	0.9695	0.9413	0.0080	0.9879	0.9773	0.0080
Case 3	Mean	1.0003	0.9996	0.0259	1.0003	1.0000	0.0259
1.0,1.0, 1.25,	COV	0.0051	0.0059	0.8201	0.0033	0.0035	0.8196
0.25x_1,	ρ_M	0.0309	-0.0961	0.2710	0.0406	-0.0588	0.2699
0.25y_1,	ρ_D	0.1857	-0.1525	0.2333	0.2442	-0.1904	0.2320
0.25	Maximum	1.0240	1.0076	0.1573	1.0151	1.0097	0.1571
	Minimum	0.9686	0.9390	0.0068	0.9890	0.9747	0.0067
Case 4	Mean	1.0001	0.9997	0.0228	0.9999	0.9999	0.0228
1.0, 1.0, 1.6,	COV	0.0036	0.0049	0.7467	0.0025	0.0030	0.7463
0.25x_1,	ρ_M	0.1025	-0.0754	0.2775	-0.0968	-0.1388	0.2766
0.25y_1,	ρ_D	0.2228	-0.1001	0.2753	0.1174	-0.0914	0.2749
0.25	Maximum	1.0189	1.0065	0.1148	1.0084	1.0064	0.1144
	Minimum	0.9900	0.9500	0.0056	0.9879	0.9758	0.0056
Case 5	Mean	0.9999	1.0000	0.0196	0.9999	1.0000	0.0196
1.0, 1.0, 2.0,	COV	0.0026	0.0033	0.7025	0.0023	0.0023	0.7027
0.25x_1,	ρ_M	0.0691	-0.1179	0.2361	-0.0260	-0.1235	0.2351
0.25y_1,	ρ_D	0.1571	-0.1815	0.2283	0.0552	-0.0958	0.2273
0.25	Maximum	1.0104	1.0058	0.0911	1.0089	1.0057	0.0906
	Minimum	0.9913	0.9699	0.0034	0.9923	0.9860	0.0034
Case 6	Mean	1.0002	0.9991	0.0525	0.9999	0.9996	0.0524
1.0, 1.0, 1.0,	COV	0.0144	0.0111	1.1310	0.0127	0.0093	1.1228
0.25x_1,	ρ_M	0.1012	-0.0726	0.3241	0.0744	-0.1471	0.3254
0.25y_1,	ρ_D	0.2777	-0.1210	0.2630	0.2679	-0.1848	0.2626

0.5	Maximum	1.0694	1.0232	0.4513	1.0593	1.0199	0.4359
	Minimum	0.9306	0.8901	0.0112	0.9274	0.9101	0.0111
Case 7	Mean	0.9996	0.9997	0.0741	0.9997	1.0000	0.0742
2.0, 2.0, 1.0,	COV	0.0026	0.0046	0.9187	0.0033	0.0041	0.9114
$0.25x_1$,	ρ_M	0.0350	0.0487	0.4209	0.0932	0.0673	0.4212
$0.25y_1$,	ρ_D	0.0030	-0.1001	0.3170	0.1766	-0.0710	0.3219
0.25	Maximum	1.0118	1.0090	0.5921	1.0114	1.0128	0.5806
	Minimum	0.9927	0.9689	0.0078	0.9861	0.9867	0.0076
Case 8	Mean	0.9997	1.0013	0.1335	1.0004	1.0005	0.1329
2.0, 2.0, 1.0,	COV	0.0043	0.0061	1.1518	0.0071	0.0070	1.1140
$0.25x_1$,	ρ_M	-0.0308	0.2184	0.4123	0.1035	0.0054	0.4161
$0.25y_1$,	ρ_D	-0.0480	0.0007	0.3330	0.1536	-0.0706	0.3350
0.5	Maximum	1.0128	1.0291	1.2698	1.0488	1.0252	1.2015
	Minimum	0.9827	0.9826	0.0144	0.9798	0.9753	0.0146

Table 3.5 Statistics of R_X, R_Y, max(u_x), max(u_y), max($r\theta$), R_{XT}, R_{YT}, max(u_{xT}), max(u_{yT}) and max($r\theta_T$) for Case 2 shown in Table 3.2 (two-way symmetric system considering A-Δ and P-Δ effects).

stability factor		Variable								
θ	Statistics	R_X	R_Y	max(u_x)	max(u_y)	R_{XT}	R_{YT}	max(u_{xT})	max(u_{yT})	max($r\theta_T$)
0.03	Mean	1.0000	1.0000	0.0281	0.0273	1.0003	1.0006	0.0281	0.0273	0.0001
	COV	0.0000	0.0000	0.8426	0.9081	0.0005	0.0010	0.8426	0.9081	1.8432
	ρ_M	-0.0687	-0.0660	-0.0263	-0.0300	-0.0904	-0.1839	-0.0263	-0.0300	-0.0354
	ρ_D	-0.0211	0.0861	-0.3453	-0.2929	-0.1687	-0.3036	-0.3453	-0.2929	-0.2882
	Maximum	1.0001	1.0001	0.1743	0.2101	1.0030	1.0067	0.1743	0.2101	0.0015
	Minimum	1.0000	0.9996	0.0014	0.0011	1.0000	1.0000	0.0014	0.0011	0.0000
0.05	Mean	1.0000	1.0000	0.0287	0.0280	1.0003	1.0007	0.0287	0.0280	0.0001
	COV	0.0000	0.0000	0.8390	0.9023	0.0005	0.0010	0.8390	0.9023	1.7640
	ρ_M	-0.0405	-0.0545	-0.0314	-0.0394	-0.0844	-0.2273	-0.0314	-0.0394	-0.0530
	ρ_D	0.0376	0.0806	-0.3480	-0.2949	-0.1249	-0.3327	-0.3480	-0.2949	-0.2988
	Maximum	1.0001	1.0001	0.1746	0.2128	1.0030	1.0061	0.1746	0.2128	0.0015
	Minimum	0.9999	0.9995	0.0014	0.0011	1.0000	1.0000	0.0014	0.0011	0.0000
0.07	Mean	1.0000	1.0000	0.0299	0.0291	1.0004	1.0008	0.0299	0.0291	0.0001
	COV	0.0000	0.0000	0.8417	0.8854	0.0005	0.0015	0.8417	0.8854	1.6511
	ρ_M	0.0399	-0.0760	-0.0500	-0.0604	-0.0495	-0.1629	-0.0500	-0.0604	-0.0760
	ρ_D	0.1134	0.1135	-0.3674	-0.2958	-0.1287	-0.2418	-0.3674	-0.2958	-0.3234
	Maximum	1.0001	1.0001	0.1750	0.2155	1.0040	1.0146	0.1750	0.2155	0.0016
	Minimum	0.9996	0.9996	0.0015	0.0011	1.0000	1.0000	0.0015	0.0011	0.0000
0.09	Mean	1.0005	1.0853	4.9349	0.0321	1.0010	1.0204	5.2700	0.0394	0.0003
	COV	0.0062	0.8716	11.0191	0.8732	0.0062	0.2110	11.0237	2.2730	4.6376

ρ_M	-0.0607	-0.0623	-0.0623	-0.1243	-0.0673	-0.0631	-0.0623	-0.0949	-0.0826
ρ_D	-0.1269	-0.1276	-0.1278	-0.2976	-0.1443	-0.1296	-0.1278	-0.2078	-0.1897
Maximum	1.0683	11.4914	603.1171	0.2184	1.0684	3.3894	644.3358	0.9758	0.0154
Minimum	0.9993	0.9993	0.0015	0.0011	1.0000	1.0000	0.0015	0.0011	0.0000

Table 3.6 Statistics of R_X, R_Y, max(u_x), max(u_y), max($r\theta$), R_{XT} , R_{YT}, max(u_{xT}), max(u_{yT}) and max($r\theta_T$) for Case 2 shown in Table 3.3. (for one-way asymmetric systems considering *A*-Δ and *P*-Δ effects).

stability factor		Variable									
θ	Statistics	R_X	R_Y	max(u_x)	max(u_y)	max($r\theta$)	R_{XT}	R_{YT}	max(u_{xT})	max(u_{yT})	max($r\theta_T$)
0.03	Mean	1.0000	1.0000	0.0275	0.0267	0.0081	1.0000	1.0000	0.0275	0.0267	0.0081
	COV	0.0006	0.0007	0.8502	0.9206	0.8341	0.0008	0.0009	0.8502	0.9205	0.8310
	ρ_M	0.1230	0.0570	-0.0237	-0.0311	-0.0135	0.0541	-0.0640	-0.0235	-0.0311	-0.0157
	ρ_D	0.1195	0.0733	-0.3441	-0.2911	-0.3346	-0.0419	-0.0515	-0.3440	-0.2911	-0.3377
	Maximum	1.0024	1.0025	0.1706	0.2093	0.0495	1.0039	1.0022	0.1706	0.2093	0.0487
	Minimum	0.9976	0.9972	0.0014	0.0011	0.0004	0.9976	0.9971	0.0014	0.0011	0.0004
0.05	Mean	1.0000	1.0000	0.0280	0.0273	0.0082	1.0000	1.0000	0.0280	0.0273	0.0082
	COV	0.0008	0.0009	0.8485	0.9150	0.8299	0.0008	0.0011	0.8485	0.9149	0.8267
	ρ_M	0.0964	0.0333	-0.0284	-0.0413	-0.0138	0.0624	-0.0508	-0.0282	-0.0414	-0.0165
	ρ_D	0.0572	0.0645	-0.3474	-0.2923	-0.3347	-0.0170	-0.0232	-0.3473	-0.2923	-0.3380
	Maximum	1.0031	1.0030	0.1708	0.2120	0.0504	1.0033	1.0036	0.1709	0.2120	0.0496
	Minimum	0.9969	0.9966	0.0015	0.0011	0.0004	0.9971	0.9956	0.0015	0.0011	0.0004
0.07	Mean	1.0000	1.0000	0.0290	0.0285	0.0084	1.0000	1.0000	0.0290	0.0285	0.0084
	COV	0.0012	0.0011	0.8546	0.8969	0.8247	0.0013	0.0013	0.8549	0.8968	0.8216
	ρ_M	0.0689	-0.0371	-0.0439	-0.0652	-0.0178	-0.0057	-0.0856	-0.0437	-0.0654	-0.0214
	ρ_D	-0.0003	0.0148	-0.3629	-0.2941	-0.3422	-0.0871	-0.0010	-0.3629	-0.2941	-0.3457
	Maximum	1.0089	1.0052	0.1712	0.2147	0.0511	1.0107	1.0049	0.1713	0.2147	0.0503
	Minimum	0.9959	0.9954	0.0015	0.0011	0.0004	0.9973	0.9951	0.0015	0.0011	0.0004
0.09	Mean	1.0046	1.2873	2.2726	0.0396	0.1650	1.0042	1.0077	3.5359	0.3380	0.0130
	COV	0.0506	2.4742	10.9419	2.3965	10.5044	0.0464	0.0844	10.9950	10.0580	3.6934
	ρ_M	-0.0592	-0.0623	-0.0624	-0.0962	-0.0625	-0.0610	-0.0639	-0.0624	-0.0633	-0.0683

ρ_D	-0.1272	-0.1276	-0.1280	-0.2042	-0.1291	-0.1283	-0.1276	-0.1279	-0.1299	-0.1789
Maximum	1.5633	36.3235	275.8194	1.0387	19.2255	1.5169	1.9432	431.2006	37.7291	0.5354
Minimum	0.9945	0.9950	0.0015	0.0012	0.0004	0.9943	0.9820	0.0015	0.0012	0.0004

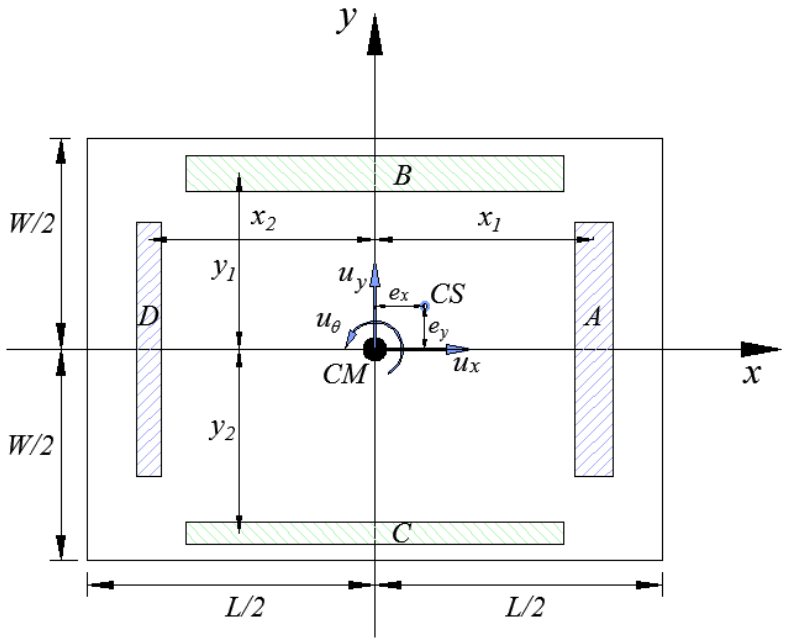

Figure 3.1 Schematic plan view of the idealized one-story building.

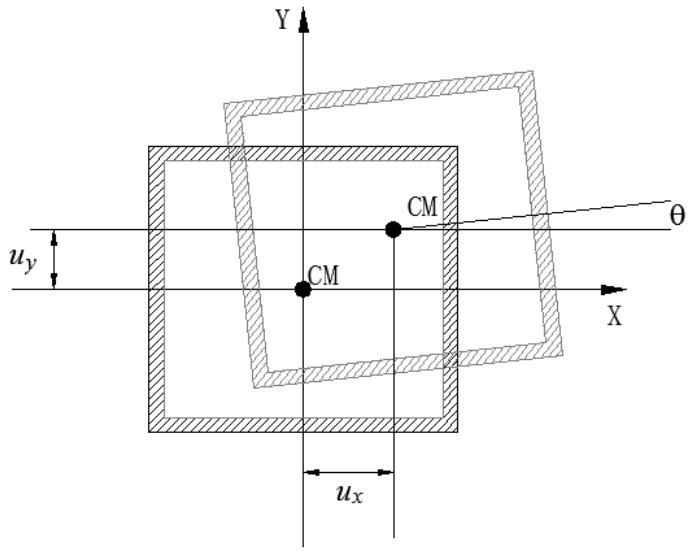

Figure 3.2 Illustration of the lateral load resisting elements by assuming all the elements are located at the edges of the slab.

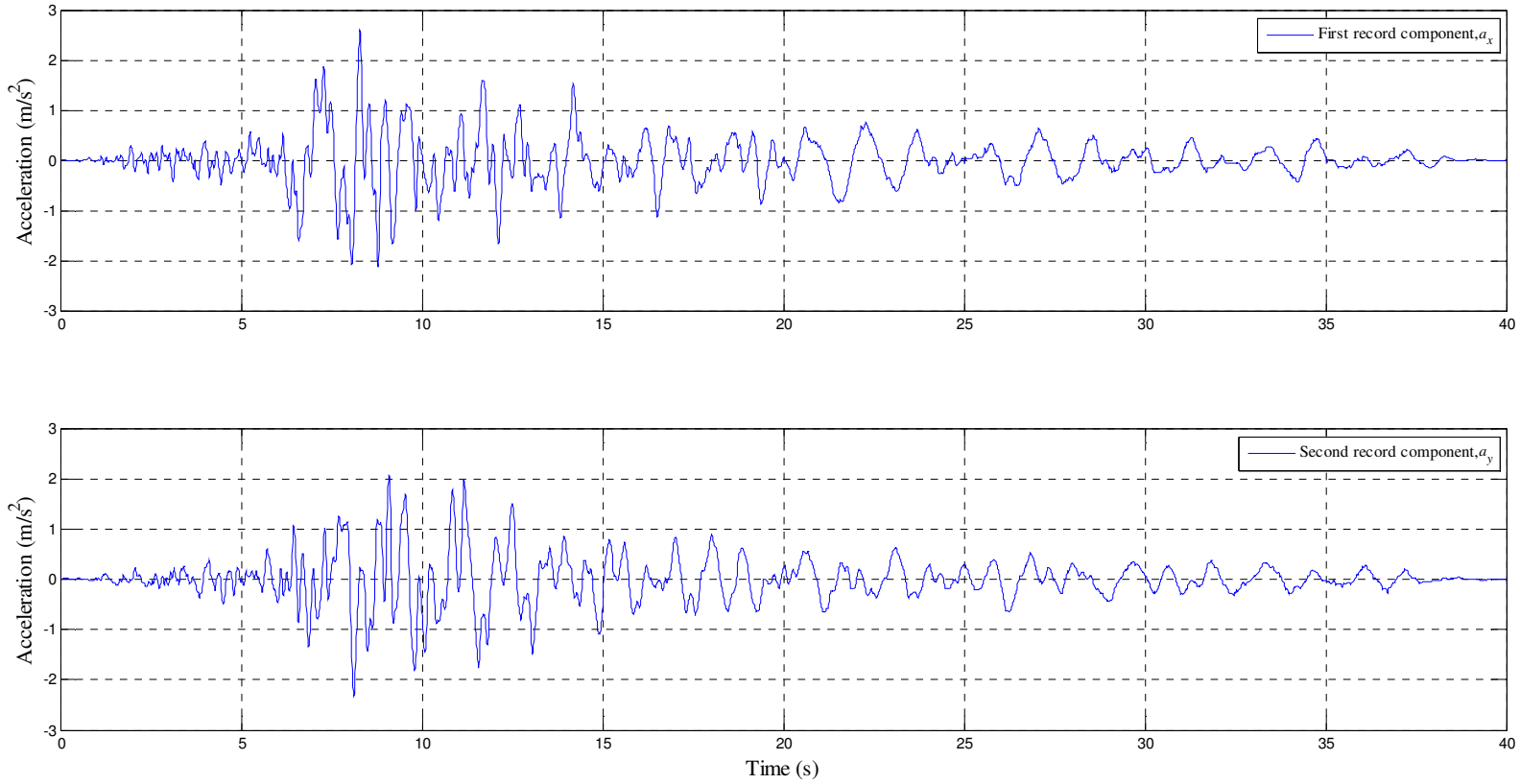

Figure 3.3 Components of an arbitrarily selected record (COALINGA 05/02/83, PARKFIELD - GOLD HILL) scaled by the same factor such that the PSA at *Tx* = 1.0 (s) (for the first record component) equals 0.5 (g)

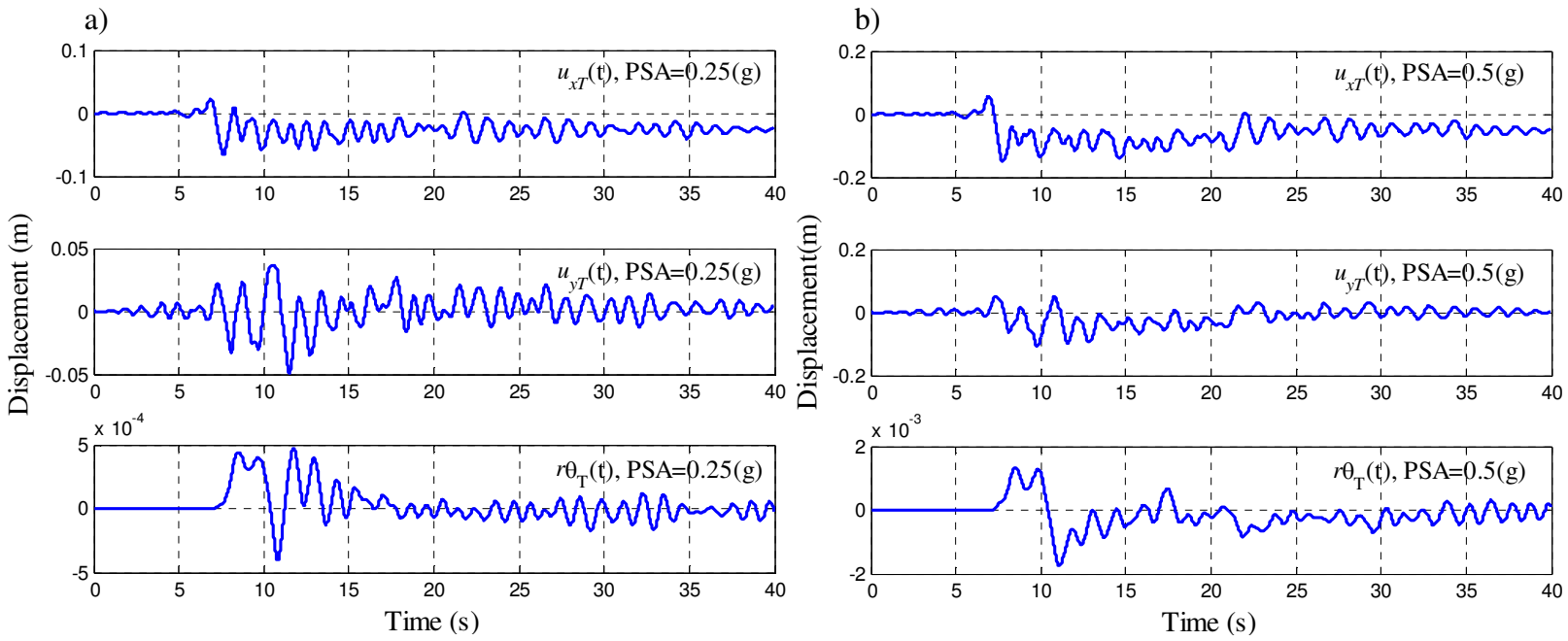

Figure 3.4 Responses of two-way symmetric system considering the *A*-Δ and *P*-Δ effects: a) Responses for the record components that are scaled by the same factor such that the PSA at T_x = 1.0 (s) equal to 0.25 (g), b) Responses for the record components that are scaled by the same factor such that the PSA at T_x = 1.0 (s) equal to 0.5 (g).

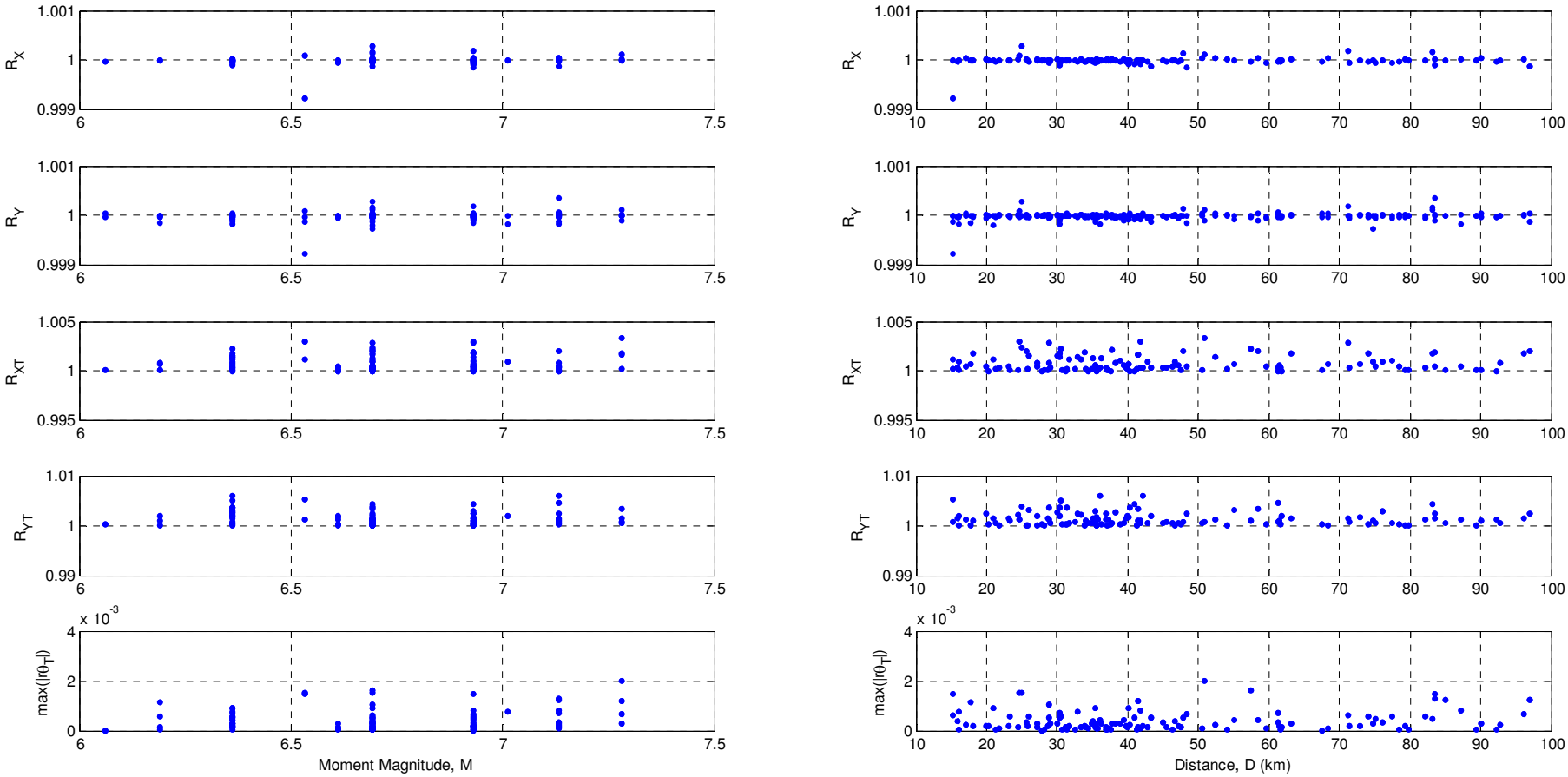

Figure 3.5 Samples of ratios and rotational response versus magnitude and distance for the Case 2 of two-way symmetric system shown in Table 3.2

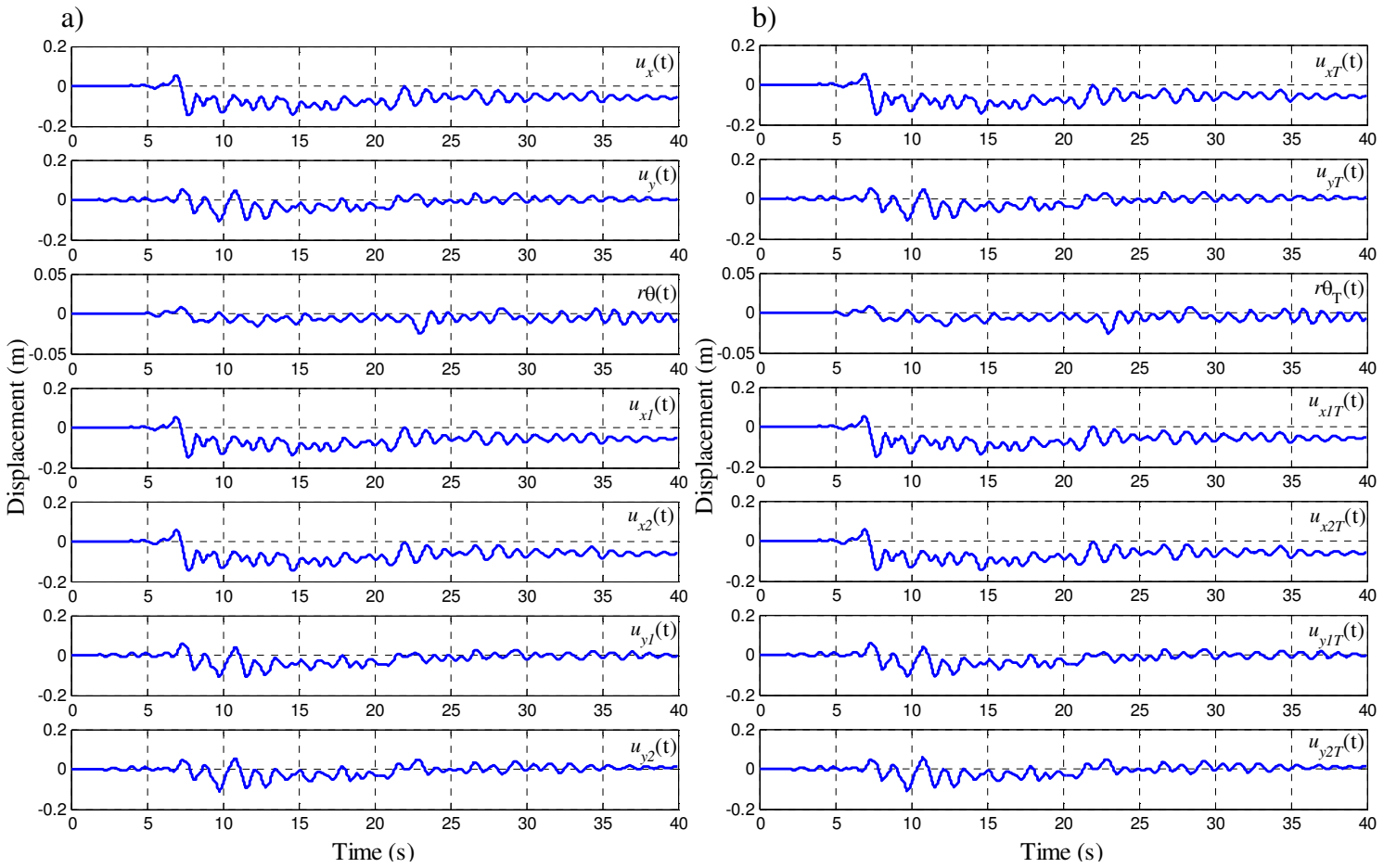

Figure 3.6 Responses by ignoring and considering the *A*-Δ effect for Case 6 of one-way asymmetric system listed in Table 3.3 and the scaled record shown in Figure 3.3: a) Responses considering the *P*-Δ effect, but without the *A*-Δ effect, b) Responses considering both *A*-Δ and *P*-Δ effect.

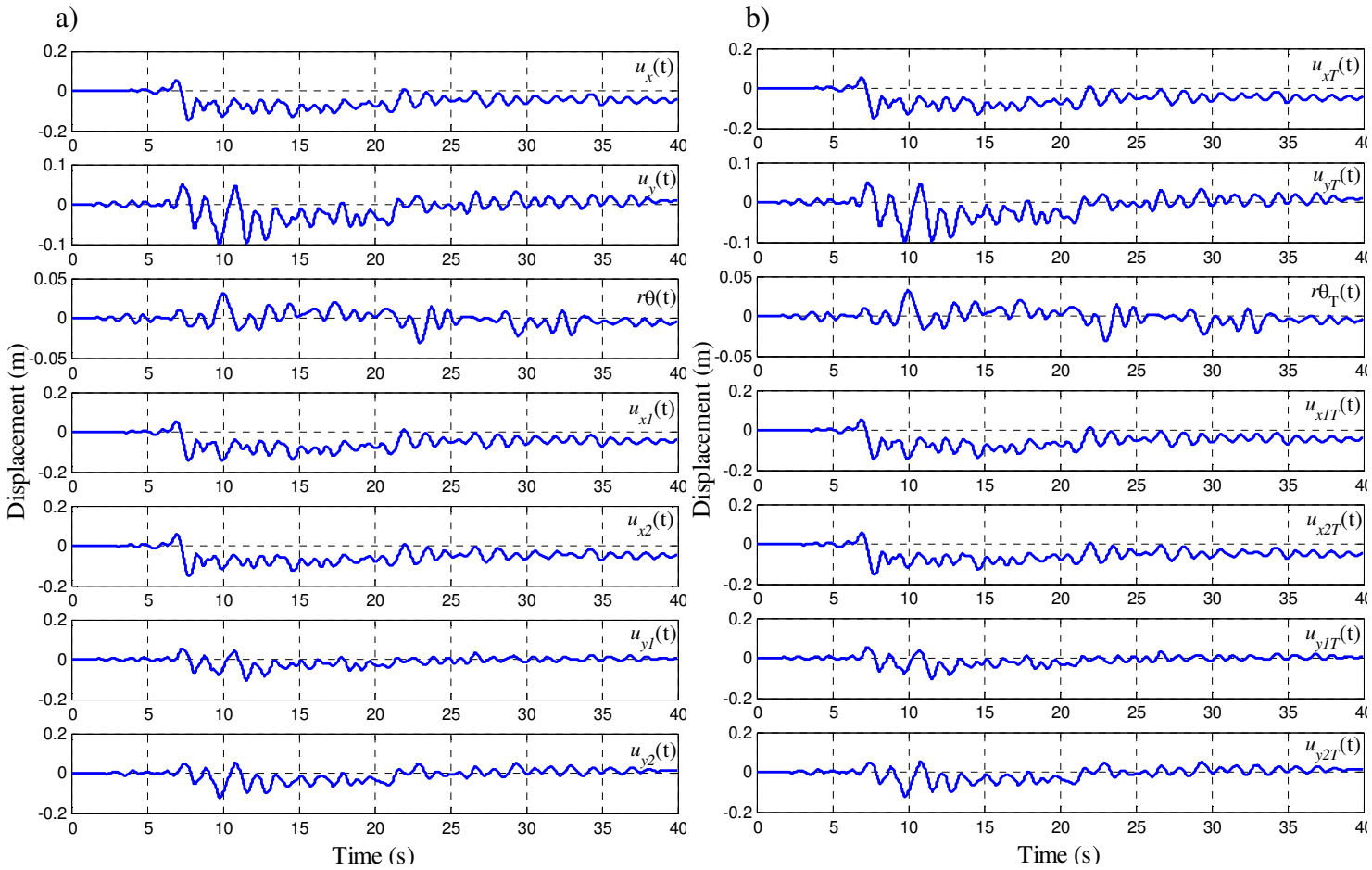

Figure 3.7 Responses by ignoring and considering the *A*-Δ effect for Case 6 two-way asymmetric system listed in Table 3.4 and the scaled record shown in Figure 3: a) Responses considering the *P*-Δ effect, but without the *A*-Δ effect, b) Responses considering both *A*-Δ and *P*-Δ effect.

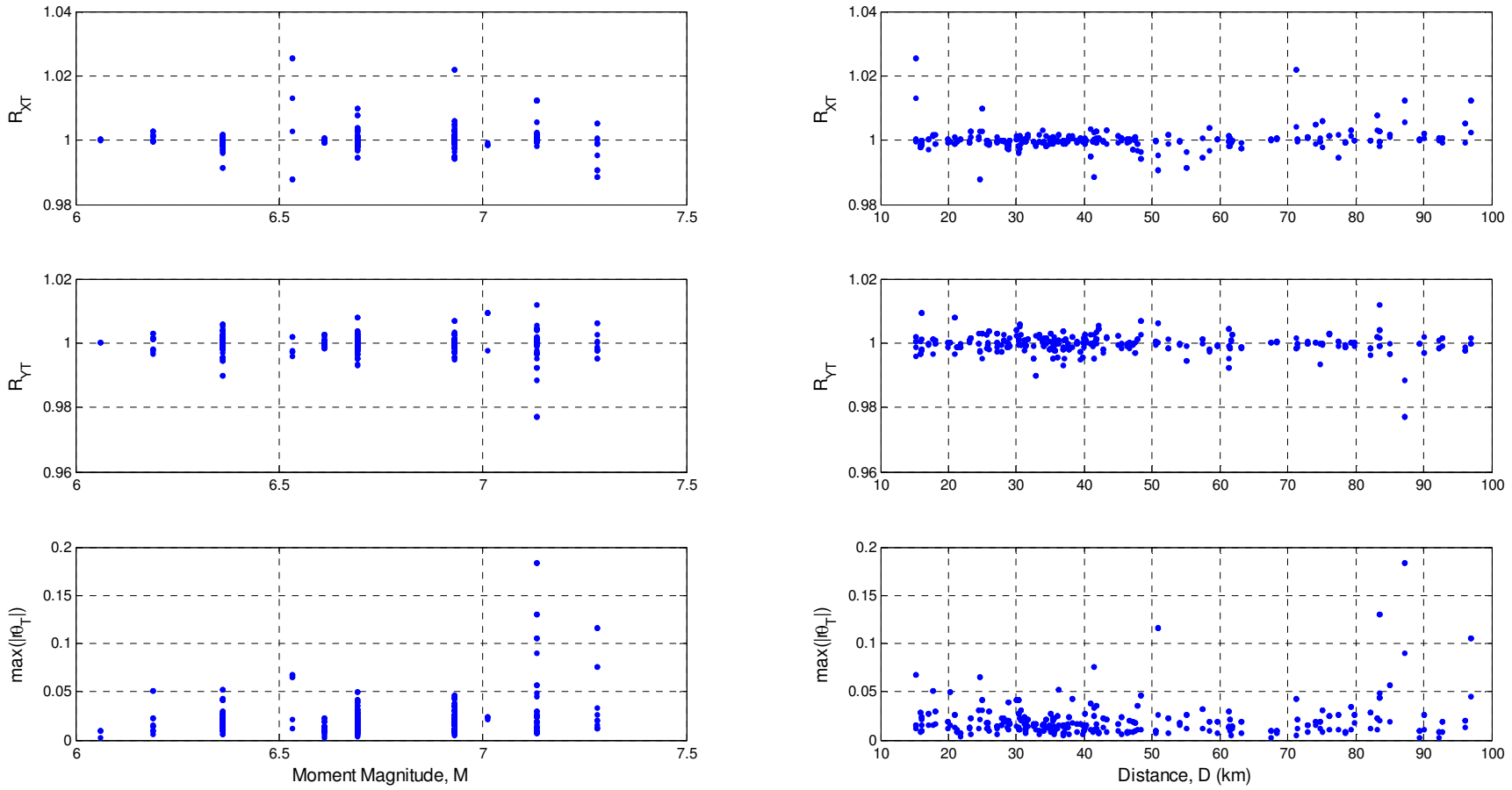

Figure 3.8 Samples of ratios and rotational response versus magnitude and distance for Case 2 of the one-way symmetric system shown in Table 3.3

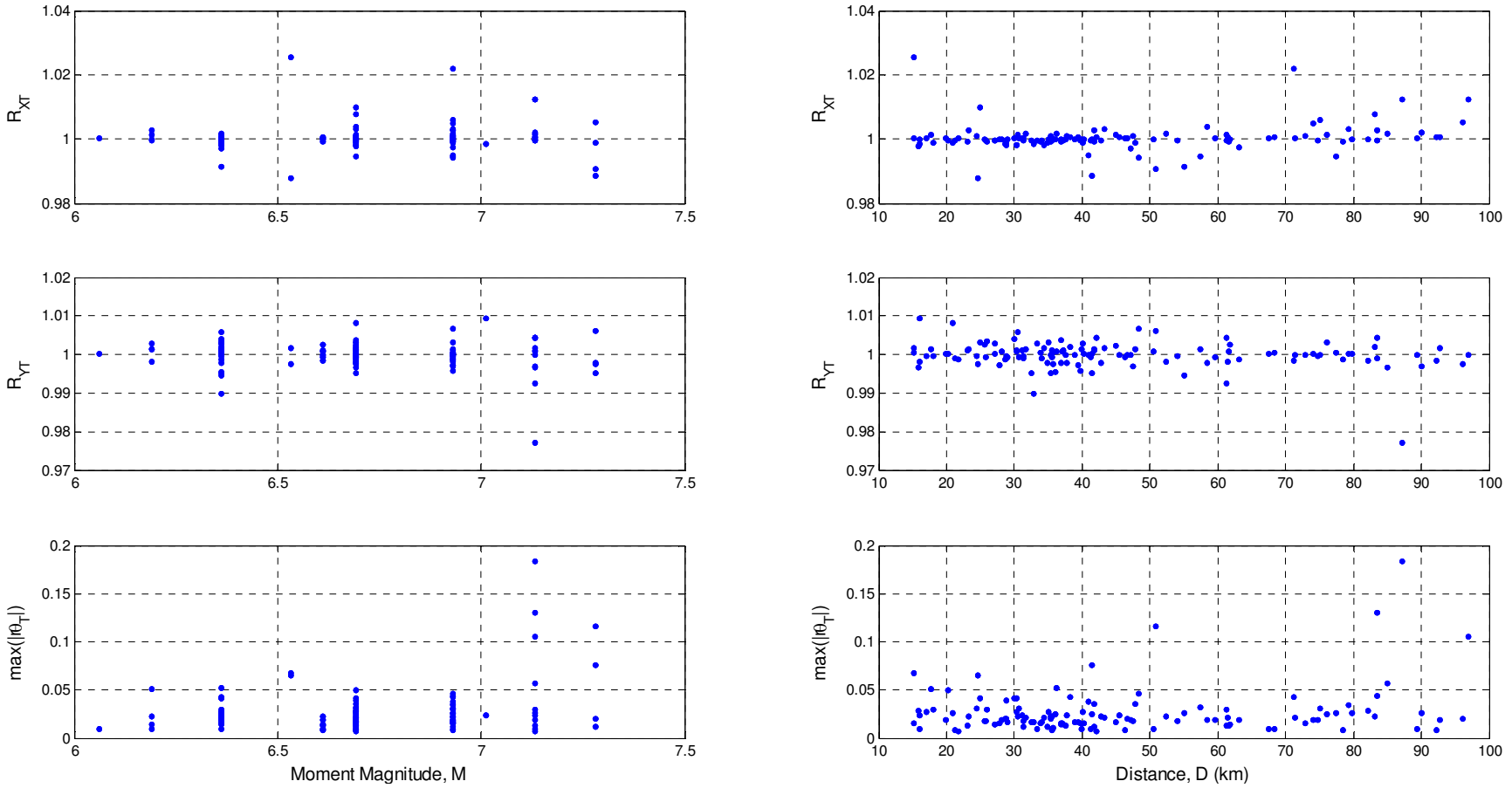

Figure 3.9 Samples of ratios and rotational response versus magnitude and distance for Case 2 of the asymmetric system shown in Table 3.4.

CHAPTER 4. CONCLUSIONS AND FUTURE WORK

4.1 Summary and conclusions

This study is focused on the evaluation of the torsional responses considering the instantabeous load eccentricity. For the assessment of inelastic seismic displacement demand and inelastic torsional response of buildings, the structural is represented using idealized one-story model and each lateral load resisting element is modeled using the Bouc-Wen hysteretic model. The governing equations of motion were developed by considering these effects and the structures that are subjected to biaxial excitations. The numerical analyses were carried out by implementing the governing equations in MATLAB®. Since the ground motion is uncertain and varies from record-to-record, 123 ground motion records from 11 California seismic events were considered to take into account this record-to-record variability.

Chapter 2 investigates the impact of instantaneous load eccentricities on torsional responses by ignoring and considering A-Δ effect. It is concluded that the responses affecting by the A-Δ effect are sensitive to the natural vibration periods; On average, a slight underestimation of seismic displacement demand occurs if the A-Δ effect is ignored, especially for two-way symmetrical systems; however, the observations also indicate that the consideration of the A-Δ effect is not necessary since in most considered cases, on average, the A-Δ effect does not affect the inelastic responses to a large degree.

In Chapter 3, the assessment of the statistical characterizations of the inelastic torsional behavior under bidirectional seismic excitations by considering the A-Δ and/or

P-Δ effects was carried out. The analyses show that the responses affected by the *A*-Δ and *P*-Δ effects are sensitive to the natural vibration periods and the stability factor; significant changes on the maximum lateral displacements along *X*-axis and *Y*-axis and torsional displacement are observed by including and excluding *A*-Δ if θ is large and the *P*-Δ effect is considered; and the consideration of the *A*-Δ effect do not always increase the seismic demand.

4.2 Future Work

The investigation of inelastic seismic response of structures is a specialized and complex task as many uncertainties involved. The evaluations and conclusions of the inelastic analyses carried out in this thesis showed that many factors related to structural modeling and loading condition would have a significant impact on inelastic responses. The current study focused only on a small part of those factors. The recommendations for further research are listed below:

(1) Only single-story building model is considered in this study, although buildings are much more complex. The evaluation of the impact of the *A*-Δ effect on multi-story buildings could be valuable for practical applications and seismic risk assessment;

(2) The rotational components of ground motion (coupled tilt and Translational Ground Motion Response Spectra) which may affect the maximum seismic demand was not included;

(3) The investigation of inelastic seismic dynamic responses (i.e translational and torsional response) with pinching effect, strength degradation and stiffness deterioration and *A*-Δ effect deserves further consideration.

APPENDIX A: RESULTS FOR CASES WITH THE CENTER OF STRENGTH DIFFERING FROM THE CENTER OF STIFFNESS

In the main text, the analysis results are presented for the cases where the CP coincides with the CS. For completeness, the analysis for the cases with the location of the CP differs from the location of the CS are presented. For the evaluation, let $\Delta_x = \min(\Delta_{xi}) = \Delta_{x1}$ denote the initial yield displacement (capacity) of the structure along *X*-axis, and $\Delta_y = \min(\Delta_{yi}) = \Delta_{y1}$ denote the initial yield displacement (capacity) of the structure along *Y*-axis. The ratios of Δ_{x2}/Δ_{x1} and Δ_{y2}/Δ_{y1} are assumed equal ($\Delta_{x2}/\Delta_{x1}=\Delta_{y2}/\Delta_{y1}=1.1$).

Results show that by considering the differences in the locations of the centers, torsional responses caused with and without by A-Δ effect are increased. Detail of the cases and results are presented in Tables A1 to A3 for selected two-way symmetric systems, one-way asymmetric systems, and two-way asymmetric systems.

Since the conclusions that can be drawn from the results are similar to those that can be drawn from the results discussed in the main text (Chapter 2), no further explanation and discussion are given.

Table A.1. Statistics of R_X, R_Y, max($r\theta$), R_{XT} , R_{YT} , and max($r\theta_T$) for two-way symmetric systems considering A-Δ effect.

System and loading condition		Variable					
T_x, T_y, Ω, PSA(g)	Statistics	R_X	R_Y	max($r\theta$)	R_{XT}	R_{YT}	max($r\theta_T$)
1.0, 1.0, 0.8, 0.25	Mean	1.0000	1.0000	0.0025	1.0001	1.0004	0.0026
	COV	0.0002	0.0002	0.7758	0.0011	0.0020	0.8136
	ρ_M	-0.0021	0.0544	0.2430	-0.0078	-0.1262	0.2585
	ρ_D	0.0328	0.2204	0.3780	0.1210	-0.0369	0.3974
	Maximum	1.0007	1.0008	0.0147	1.0042	1.0076	0.0175
	Minimum	0.9992	0.9995	0.0003	0.9959	0.9951	0.0003
1.0, 1.0, 1.0, 0.25	Mean	1.0000	1.0000	0.0028	1.0002	1.0002	0.0028
	COV	0.0002	0.0002	0.8023	0.0011	0.0020	0.7684
	ρ_M	0.0183	0.0903	0.2361	0.0539	-0.0296	0.2426
	ρ_D	0.0977	0.1963	0.3718	0.1386	-0.0951	0.3650
	Maximum	1.0011	1.0009	0.0177	1.0034	1.0088	0.0169
	Minimum	0.9992	0.9994	0.0004	0.9959	0.9946	0.0004
1.0,1.0,1.25, 0.25	Mean	1.0000	1.0000	0.0032	1.0002	1.0004	0.0032
	COV	0.0003	0.0002	0.7318	0.0012	0.0022	0.7135
	ρ_M	0.0380	0.0219	0.1906	0.1011	-0.0909	0.1926
	ρ_D	0.0913	0.1244	0.3000	0.1780	-0.1584	0.2956
	Maximum	1.0014	1.0010	0.0165	1.0038	1.0094	0.0159
	Minimum	0.9990	0.9993	0.0003	0.9960	0.9948	0.0003
1.0, 1.0, 1.6, 0.25	Mean	1.0000	1.0000	0.0034	1.0000	1.0004	0.0034
	COV	0.0004	0.0003	0.7045	0.0011	0.0022	0.7035
	ρ_M	0.0158	-0.0716	0.1717	0.1467	-0.0313	0.1779
	ρ_D	0.0818	-0.0039	0.2717	0.1760	-0.0207	0.2827
	Maximum	1.0018	1.0012	0.0137	1.0030	1.0094	0.0138
	Minimum	0.9987	0.9991	0.0001	0.9963	0.9934	0.0001
1.0, 1.0, 2.0, 0.25	Mean	1.0000	1.0000	0.0032	1.0000	1.0003	0.0032
	COV	0.0003	0.0002	0.6951	0.0009	0.0024	0.6972
	ρ_M	0.0090	-0.1149	0.1534	0.0568	0.0861	0.1592
	ρ_D	0.0404	-0.1053	0.2972	0.1240	0.0881	0.3036
	Maximum	1.0015	1.0010	0.0116	1.0025	1.0108	0.0116
	Minimum	0.9983	0.9994	0.0001	0.9968	0.9921	0.0001
1.0, 1.0, 1.0, 0.5	Mean	1.0000	1.0000	0.0050	1.0000	1.0002	0.0052
	COV	0.0003	0.0005	0.5954	0.0020	0.0039	0.5930
	ρ_M	0.0808	0.0590	0.2564	0.0720	0.1776	0.2551

	ρ_D	-0.0028	0.0972	0.2715	0.1228	0.0471	0.2341
	Maximum	1.0007	1.0014	0.0210	1.0082	1.0203	0.0186
	Minimum	0.9981	0.9975	0.0009	0.9919	0.9882	0.0010
2.0, 2.0, 1.0, 0.25	Mean	1.0000	1.0000	0.0089	1.0002	1.0003	0.0093
	COV	0.0003	0.0002	0.8786	0.0019	0.0024	0.9043
	ρ_M	0.1261	-0.0157	0.4477	-0.0662	-0.0345	0.4623
	ρ_D	0.1749	-0.0663	0.4333	0.0102	0.0038	0.4446
	Maximum	1.0030	1.0014	0.0505	1.0073	1.0075	0.0563
	Minimum	0.9996	0.9987	0.0010	0.9910	0.9943	0.0011
2.0, 2.0, 1.0, 0.5	Mean	1.0000	1.0000	0.0123	1.0003	1.0007	0.0139
	COV	0.0003	0.0003	0.8544	0.0025	0.0040	0.8658
	ρ_M	0.1253	-0.0581	0.4669	0.0852	0.0951	0.5237
	ρ_D	0.1852	0.0067	0.3943	0.0249	-0.0125	0.4451
	Maximum	1.0020	1.0007	0.0615	1.0107	1.0123	0.0697
	Minimum	0.9987	0.9984	0.0011	0.9909	0.9902	0.0013

Table A.2. Statistics of R_X, R_Y , max($r\theta$), R_{XT} , R_{YT} , and max($r\theta_T$) for one-way asymmetric systems considering A-Δ effect.

System and loading condition		Variable					
T_x, T_y, Ω, e_x, e_y, PSA(g)	Statistics	R_X	R_Y	max($r\theta$)	R_{XT}	R_{YT}	max($r\theta_T$)
1.0, 1.0, 0.8,	Mean	1.0000	1.0000	0.0098	1.0000	0.9999	0.0098
0, 0.25y_1,	COV	0.0007	0.0006	0.7234	0.0012	0.0023	0.7071
0.25	ρ_M	-0.0644	-0.0427	0.2679	-0.0437	0.0380	0.2685
	ρ_D	-0.0296	-0.0722	0.1798	0.0294	0.0720	0.1709
	Maximum	1.0021	1.0024	0.0656	1.0041	1.0066	0.0641
	Minimum	0.9959	0.9976	0.0016	0.9957	0.9902	0.0016
1.0, 1.0, 1.0,	Mean	1.0000	1.0000	0.0124	1.0001	1.0001	0.0125
0, 0.25y_1,	COV	0.0008	0.0008	0.6538	0.0012	0.0024	0.6542
0.25	ρ_M	-0.0278	-0.0678	0.2755	-0.0030	-0.0136	0.2755
	ρ_D	-0.0194	-0.0642	0.0868	0.0046	0.0672	0.0888
	Maximum	1.0028	1.0036	0.0732	1.0041	1.0093	0.0730
	Minimum	0.9956	0.9974	0.0017	0.9952	0.9920	0.0017
1.0, 0.5, 1.25,	Mean	1.0001	1.0000	0.0124	1.0000	1.0001	0.0124
0, 0.25y_1,	COV	0.0009	0.0008	0.6118	0.0012	0.0021	0.6128
0.25	ρ_M	-0.0190	0.0059	0.2858	-0.0113	-0.0457	0.2846
	ρ_D	-0.0613	-0.0021	0.1542	-0.0133	-0.0102	0.1574
	Maximum	1.0032	1.0030	0.0641	1.0039	1.0061	0.0643
	Minimum	0.9960	0.9971	0.0016	0.9951	0.9917	0.0016
1.0, 1.0, 1.6,	Mean	1.0001	0.9999	0.0105	1.0000	1.0001	0.0105
0, 0.25y_1,	COV	0.0008	0.0007	0.5825	0.0011	0.0019	0.5839
0.25	ρ_M	0.0089	-0.0029	0.3141	0.0516	-0.1543	0.3122
	ρ_D	-0.0497	0.0574	0.2240	-0.0164	-0.1442	0.2231
	Maximum	1.0034	1.0018	0.0456	1.0042	1.0053	0.0457
	Minimum	0.9957	0.9975	0.0016	0.9958	0.9923	0.0016
1.0, 1.0, 2.0,	Mean	1.0001	1.0000	0.0087	1.0001	1.0000	0.0087
0, 0.25y_1,	COV	0.0008	0.0006	0.5843	0.0012	0.0022	0.5847
0.25	ρ_M	0.0794	-0.1687	0.3344	0.0747	-0.1993	0.3338
	ρ_D	-0.0035	-0.0598	0.2675	0.0141	-0.2085	0.2683

	Maximum	1.0037	1.0019	0.0317	1.0066	1.0066	0.0315
	Minimum	0.9973	0.9973	0.0020	0.9963	0.9891	0.0020
1.0, 1.0, 1.0,	Mean	0.9999	0.9998	0.0219	0.9998	1.0001	0.0220
0, 0.25y_1,	COV	0.0011	0.0014	1.0277	0.0024	0.0042	1.0369
0.5	ρ_M	-0.0251	0.0166	0.2756	0.0367	-0.0124	0.2794
	ρ_D	-0.0475	-0.0834	0.2827	-0.0665	-0.0072	0.2874
	Maximum	1.0054	1.0045	0.1766	1.0066	1.0166	0.1746
	Minimum	0.9949	0.9900	0.0036	0.9915	0.9869	0.0036
2.0, 2.0, 1.0,	Mean	1.0000	1.0001	0.0333	1.0000	1.0005	0.0334
0, 0.25y_1,	COV	0.0008	0.0007	1.4175	0.0020	0.0045	1.3954
0.25	ρ_M	0.0251	-0.0001	0.3227	-0.0363	0.0751	0.3258
	ρ_D	-0.1645	0.1225	0.3163	0.0026	0.0422	0.3172
	Maximum	1.0034	1.0044	0.4344	1.0069	1.0424	0.4283
	Minimum	0.9951	0.9986	0.0025	0.9929	0.9918	0.0027
2.0, 2.0, 1.0,	Mean	1.0000	1.0001	0.0675	1.0000	1.0008	0.0685
0, 0.25y_1,	COV	0.0009	0.0011	1.6707	0.0031	0.0077	1.6187
0.5	ρ_M	-0.0007	0.0356	0.3683	0.0290	0.0632	0.3774
	ρ_D	-0.2197	0.0650	0.4551	0.0341	0.1313	0.4609
	Maximum	1.0038	1.0081	0.9135	1.0138	1.0701	0.8835
	Minimum	0.9954	0.9969	0.0052	0.9900	0.9888	0.0056

Table A. 3. Statistics of R_X, R_Y, max($r\theta$), R_{XT} , R_{YT}, and max($r\theta_T$) for two-way asymmetric systems considering A-Δ effect.

System and loading condition		Variable					
T_x, T_y, Ω, e_x, e_y, PSA(g)	Statistics	R_X	R_Y	max($r\theta$)	R_{XT}	R_{YT}	max($r\theta_T$)
1.0, 1.0, 0.8,	Mean	1.0000	1.0000	0.0197	0.9999	1.0002	0.0197
0.25x_1,	COV	0.0012	0.0010	0.9158	0.0015	0.0024	0.9223
0.25y_1	ρ_M	-0.0899	-0.0773	0.2685	-0.1318	0.0372	0.2669
0.25	ρ_D	-0.0963	-0.1327	0.3089	-0.0734	0.0463	0.3105
	Maximum	1.0039	1.0028	0.1353	1.0054	1.0067	0.1374
	Minimum	0.9932	0.9958	0.0030	0.9955	0.9912	0.0030
1.0, 1.0, 1.0,	Mean	1.0003	1.0000	0.0244	0.9997	1.0001	0.0245
0.25x_1,	COV	0.0012	0.0012	0.8833	0.0017	0.0027	0.8896
0.25y_1	ρ_M	-0.0888	-0.0588	0.2628	-0.1797	0.0415	0.2618
0.25	ρ_D	-0.0746	-0.0236	0.2952	-0.1253	0.0633	0.2981
	Maximum	1.0043	1.0043	0.1642	1.0060	1.0075	0.1672
	Minimum	0.9965	0.9948	0.0039	0.9897	0.9900	0.0039
1.0,1.0, 1.25,	Mean	1.0000	1.0001	0.0246	0.9998	1.0000	0.0246
0.25x_1,	COV	0.0014	0.0010	0.9279	0.0018	0.0022	0.9280
0.25y_1	ρ_M	-0.0008	-0.0106	0.2744	-0.1352	0.0545	0.2745
0.25	ρ_D	0.0329	0.0625	0.3486	-0.1588	0.1219	0.3498
	Maximum	1.0049	1.0031	0.1873	1.0060	1.0074	0.1872
	Minimum	0.9921	0.9964	0.0045	0.9926	0.9925	0.0045
1.0, 1.0, 1.6,	Mean	0.9998	1.0001	0.0220	1.0000	1.0000	0.0220
0.25x_1,	COV	0.0017	0.0010	0.8441	0.0015	0.0019	0.8427
0.25y_1	ρ_M	-0.0351	0.1178	0.2802	-0.0819	0.0812	0.2805
0.25	ρ_D	0.1228	0.1515	0.3760	-0.0418	0.0676	0.3771
	Maximum	1.0043	1.0036	0.1474	1.0075	1.0060	0.1464
	Minimum	0.9881	0.9961	0.0048	0.9945	0.9950	0.0048
1.0, 1.0, 2.0,	Mean	0.9999	1.0000	0.0190	1.0001	0.9999	0.0190
0.25x_1,	COV	0.0012	0.0009	0.7502	0.0015	0.0019	0.7492
0.25y_1	ρ_M	-0.0119	0.1012	0.2418	0.0881	0.1202	0.2423
0.25	ρ_D	0.0830	0.0342	0.3151	0.0488	0.1092	0.3147
	Maximum	1.0035	1.0026	0.0941	1.0077	1.0052	0.0930
	Minimum	0.9949	0.9953	0.0030	0.9951	0.9948	0.0030
1.0, 1.0, 1.0,	Mean	1.0002	0.9998	0.0447	0.9999	1.0006	0.0447
0.25x_1,	COV	0.0021	0.0026	1.2760	0.0037	0.0043	1.2658
0.25y_1	ρ_M	0.0572	-0.0397	0.3106	-0.2107	-0.0623	0.3097

0.5	ρ_D	-0.0244	-0.0509	0.3965	-0.3648	-0.0405	0.3948
	Maximum	1.0149	1.0151	0.4559	1.0103	1.0159	0.4479
	Minimum	0.9918	0.9869	0.0088	0.9772	0.9841	0.0090
2.0, 2.0, 1.0,	Mean	1.0000	0.9997	0.0723	0.9996	1.0002	0.0726
$0.25x_1$,	COV	0.0030	0.0017	1.3869	0.0046	0.0037	1.3902
$0.25y_1$	ρ_M	0.0346	-0.0598	0.4021	-0.0370	0.1717	0.4031
0.25	ρ_D	0.1788	-0.0259	0.5677	0.0870	0.3147	0.5666
	Maximum	1.0214	1.0027	0.8212	1.0320	1.0247	0.8284
	Minimum	0.9912	0.9881	0.0091	0.9721	0.9920	0.0092
2.0, 2.0, 1.0,	Mean	1.0003	1.0002	0.1465	0.9999	1.0016	0.1474
$0.25x_1$,	COV	0.0023	0.0019	1.6283	0.0074	0.0072	1.6146
$0.25y_1$	ρ_M	0.1179	0.0863	0.4212	-0.0800	0.1975	0.4235
0.5	ρ_D	0.1173	0.1486	0.6283	-0.0337	0.3355	0.6281
	Maximum	1.0138	1.0103	1.8316	1.0551	1.0548	1.8240
	Minimum	0.9922	0.9939	0.0108	0.9608	0.9889	0.0108

APPENDIX B: EQUATION OF MOTION CONSIDERING BOUC-WEN HYSTERETIC MODEL

For single-story model, the equation of motion without considering *P*-Δ effect can be written as (Chopra 2001),

$$m\ddot{u}_x + c_x\dot{u}_x + \sum f_{xi} = -m\ddot{u}_{gx} \tag{B.1a}$$

$$m\ddot{u}_y + c_y\dot{u}_y + \sum f_{yi} = -m\ddot{u}_{gy} \tag{B.1b}$$

$$mr^2\ddot{\theta} + c_\theta\dot{\theta} + \sum(-f_{xi}y_i + f_{yi}x_i) = 0 \tag{B.1c}$$

where m is the mass; r is the radius of gyration of the slab about the CM; c denotes the damping coefficient, $\ddot{u}_g$ is the ground acceleration, f denote the resisting force of the element, an overdot on a variable denotes its temporal derivative, and the summation Σ is over applicable lateral load resisting elements. Symbols c and $\ddot{u}_g$ with an additional subscript x, y and θ are used to denote the quantities associated with the *X*-axis, *Y*-axis and rotation, respectively. f with subscript xi and yi denotes the resisting force along the *X*-axis and *Y*-axis, respectively, for the i-th lateral loading resisting element. Similarly, f with subscript yi denotes the resisting force along the *Y*-axis for the i-th lateral load resisting element. The displacement of the i-th element placed parallel *X*-axis, u_{xi}, and the displacement of the i-th element placed parallel *Y*-axis, u_{yi} ,are respectively given by

$$u_{xi}(t) = u_x(t) - y_i\theta(t) \tag{B.2a}$$

and

$$u_{yi}(t) = u_y(t) + x_i\theta(t) \tag{B.2b}$$

where x_i and y_i denote the distances from the CM to the elements. The notation $u_{xi}(t)$, $u_x(t)$ and q(t) is used to emphasize that u_{xi}, u_x and θ are time dependent.

If each lateral load resisting element is modeled as linear elastic system, the stiffness matrix **K** of the system is given by

$$\mathbf{K} = \begin{bmatrix} K_{XX} & 0 & K_{\theta X} \\ 0 & K_{YY} & K_{\theta Y} \\ K_{\theta X} & K_{\theta Y} & K_{\theta\theta} \end{bmatrix} \tag{B.3}$$

where K_{XX}, K_{YY}, $K_{\theta\theta}$, $K_{\theta X}$ and $K_{\theta Y}$ denote the elements of the stiffness matrix **K**. The n stiffness can be used to defined the dynamic characteristic of the system.

By incorporating the mass and stiffness proportional damping (i.e., Rayleigh damping), for linear systems, Eqs. (1) and (2) leads to (Chopra 2001),

$$\begin{Bmatrix} \ddot{u}_x \\ \ddot{u}_y \\ \ddot{u}_\theta \end{Bmatrix} + a_1\omega_x^2 \begin{bmatrix} a_0/(a_1\omega_x^2)+1 & 0 & e_y/r \\ 0 & a_0/(a_1\omega_x^2)+\Omega_y^2 & e_x\Omega_y^2/r \\ e_y/r & e_x\Omega_y^2/r & a_0/(a_1\omega_x^2)+\Omega_\theta^2 \end{bmatrix} \begin{Bmatrix} \dot{u}_x \\ \dot{u}_y \\ \dot{u}_\theta \end{Bmatrix} + \omega_x^2 \begin{bmatrix} 1 & 0 & e_y/r \\ 0 & \Omega_y^2 & e_x\Omega_y^2/r \\ e_y/r & e_x\Omega_y^2/r & \Omega_\theta^2 \end{bmatrix} \begin{Bmatrix} u_x \\ u_y \\ u_\theta \end{Bmatrix} = \begin{Bmatrix} -\ddot{u}_{gx} \\ -\ddot{u}_{gy} \\ 0 \end{Bmatrix} \tag{B.4}$$

The equations of motion for nonlinear systems can be written as,

$$\begin{Bmatrix} \ddot{u}_x \\ \ddot{u}_y \\ r\ddot{\theta} \end{Bmatrix} + a_1\omega_x^2 \begin{bmatrix} a_0/(a_1\omega_x^2)+1 & 0 & -e_y/r \\ 0 & a_0/(a_1\omega_x^2) + \Omega_y^2 & e_x\Omega_y^2/r \\ -e_y/r & e_x\Omega_y^2/r & a_0/(a_1\omega_x^2) + \Omega_\theta^2 \end{bmatrix} \begin{Bmatrix} \dot{u}_x \\ \dot{u}_y \\ r\dot{\theta} \end{Bmatrix}$$

$$+\alpha\omega_x^2 \begin{bmatrix} 1 & 0 & -e_y/r \\ 0 & \Omega_y^2 & e_x\Omega_y^2/r \\ -e_y/r & e_x\Omega_y^2/r & \Omega_\theta^2 \end{bmatrix} \begin{Bmatrix} u_x \\ u_y \\ r\theta \end{Bmatrix} + (1-\alpha)\omega_x^2 \begin{Bmatrix} \sum \kappa_{xi} z_{xi} \\ \sum \Omega_y^2 \kappa_{yi} z_{yi} \\ \frac{1}{r}\sum\left(-y_i\kappa_{xi}z_{xi} + \Omega_y^2 x_i \kappa_{yi} z_{yi}\right) \end{Bmatrix} = \begin{Bmatrix} -\ddot{u}_{gx} \\ -\ddot{u}_{gy} \\ 0 \end{Bmatrix} \tag{B.5}$$

where $u_\theta = r\theta$, $\Omega_\theta = \omega_\theta / \omega_x$; $\Omega_y = \omega_y / \omega_x$; $e_x = K_{\theta Y} / K_{YY}$ is known as eccentricity alone the X-axis; $e_y = K_{\theta X} / K_{XX}$ is known as eccentricity alone the Y-axis; $\kappa_{xi} = k_{xi} / K_x$, $\kappa_{yi} = k_{yi} / K_y$; $a_0 = 2\zeta\omega_x\omega_y/(\omega_x + \omega_y)$, and $a_1 = 2\zeta/(\omega_x + \omega_y)$. The damping ratio ζ is considered to be equal to 5% throughout this study. The expressions for a_0 and a_1 are obtained by assuming that the damping ratios for the two translational modes are identical and equal to ζ.

To be more realistically represent the structural behavior under strong earthquake excitations, consider that each lateral load resisting element can be modeled using Bouc-Wen hysteretic model (Wen 1976; Foliente 1995; Ma, Zhang et al. 2004; Lee and Hong 2010). Therefore, f_{xi} for the i-th lateral load resisting element (frame or wall) can be expressed as,

$$f_{xi} = \alpha_{xi} k_{xi} u_{xi} + (1-\alpha_{xi}) k_{xi} z_{xi} \tag{B.6}$$

where k_{xi} is the elastic lateral stiffness; α_{xi} is the ratio of the post-yield to initial stiffness and z_{xi} is the hysteretic displacement. z_{xi}, is governed by (Wen 1976; Foliente 1995; Ma et al. 2004),

$$\dot{z}_{xi} = \frac{1}{\eta_{xi}} \left\{ \dot{u}_{xi} - \nu_{xi} z_{xi} \left| \dot{u}_{xi} \right| \left| z_{xi} \right|^{n_{xi}-1} \left[\beta_{xi} + \gamma_{xi} \operatorname{sgn}(\dot{u}_{xi} z_{xi}) \right] \right\} \tag{B.7}$$

where β_{xi}, γ_{xi}, and n_{xi} are the shape parameters; $\eta_{xi} = 1 + \delta_{\eta xi} E_{nxi}$; the parameter $\delta_{\eta xi}$ controls the stiffness degradation; $\nu_{xi} = 1 + \delta_{\nu xi} E_{nxi}$; the parameter $\delta_{\nu xi}$ controls the strength degradation; and the normalized dissipated hysteretic energy, E_{xi}, is defined by,

$$E_{xi} = \frac{(1-\alpha_{xi})}{Q_{xi}\Delta_{xi}} \int_0^t k_{xi} z_{xi} \dot{u}_{xi} \, dt = (1-\alpha_{xi}) \int_0^t \frac{z_{xi}}{\Delta_{xi}} \frac{\dot{u}_{xi}}{\Delta_{xi}} \, dt \tag{B.8}$$

in which $\Delta_{xi} = \left(\beta_{xi} + \gamma_{xi}\right)^{-1/n_{xi}}$ denotes initial yield displacement and $Q_{xi} = k_{xi}\Delta_{xi}$ is the initial yield force. Similarly, f_{yi} is defined by replace the subscript x with y in Eq. (B.6). Note that if α_{xi} and α_{yi} are considered to be equal to one, the material nonlinearity is neglected in the considered system and $f_{xi} = k_{xi} u_{xi}$ and $f_{yi} = k_{yi} u_{yi}$.

References

Chopra, A.K. (2001). Dynamics of structures: theory and applications to earthquake engineering (2nd ed.). Prentice Hall, N.J.

Foliente, G. C. (1995). Hysteresis modeling of wood joints and structural systems. Journal of Structural Engineering; 121(6):1013–1022.

Lee, C.S., and Hong, H.P. (2010). Inelastic Responses of Hysteretic Systems under Biaxial Seismic Excitations, Engineering Structures; Volume 32, Issue 8: 2074-2086.

Ma, F., Zhang, H., Bockstedte, A., Foliente, G.C. and Paevere, P. (2004). Parameter analysis of the differential model of hysteresis. Transactions of the ASME, 71(3), 342–349.

Wen, Y. K. (1976). Method for random vibration of hysteretic systems. Journal of Engineering Mechanics; 102(2): 249-263.

CURRICULUM VITAE

Name:	Xiaojing Cui
Post-secondary Education and Degrees:	The University of Western Ontario London, Ontario, Canada 2011-2013, M.Sc. (Civil Engineering) Centennial College Toronto, Ontario, Canada 2009-2011, College Diploma. (Environmental Technology) Central South University Changsha, Hunan, China 2005-2009, Bachelor. (Civil Engineering)
Related Work Experience	Teaching Assistant and Research Assistant The University of Western Ontario 2011-2013